EUMETSAT Satellite Application Facility on
Support to Operational Hydrology and Water Management

Product Validation Report (PVR) for product H68 (P-IN-PMW)

Gridded MW instantaneous precipitation rate based on intercalibrated PMW instantaneous precipitation rate estimates

Reference Number:	SAF/HSAF/PVR-68
Issue/Revision Index:	2.0
Last Change:	27 February 2022
About this document	This Document has been prepared by the Product Validation Cluster Leader, with the support of the Project Management Team and of the Validation and Development Teams of the Precipitation Cluster

DOCUMENT CHANGE RECORD

Issue / Revision	Date	Description
	03/09/2021	Draft document
1.0	30/09/2021	Final document
2.0	27/02/2022	Updated document

Index

List of tables

List of figures

1 Introduction to the Product Validation Report

The Product Validation Report (PVR) contains all the useful information for users to acquire more about the limits and potentials of the precipitation product. The document collects all the information and all the results obtained from the Quality and Monitoring Assessment cluster.
The precipitation product under review, during the analyzes carried out by the cluster, is on "in-development" phase. The objective of this report is to determine and quantify both the limits and the potential of the product in order to assess the overall quality and make it available to end users.

The report is structured as follows:

In **Chapter 2** there is a brief description of the product and the precipitation algorithm retrieval. More details about this can be found on the PUM (Product User Manual) and on the ATBD (Algorithm Theoretical Baseline Document) of the products themselves.

The main part of this document is contained in **Chapters 3** and **4**: these are dedicated to the description of the validation results obtained for both case studies and analyses over a long period, respectively.

For more information about the analysis, validation, and quality assessment methodology, compare **Appendix 1**.

All detailed information on the data used to compare the products is contained in **Appendix 2**.

Any further results obtained and not included in chapters 3 and 4, are included from **Appendix 3** onwards.

Finally, the last **Appendix 6** is dedicated to the list of numerous acronyms used in this document.

For any errors, oversights, or requests for updates or changes, please contact us via H SAF project website: **http://h-saf.eumetsat.int**

2 P-IN-PMW (H68) product

H68 (P-IN-PMW) is a Level 3 (gridded) MW-based product providing the instantaneous precipitation rate estimate, exploiting the combination of passive microwave (PMW) Level 2 instantaneous precipitation rate products.

2.1 Sensing principle

With the aim of providing users with gridded, optimal MW-based products at regular time intervals, the H SAF product portfolio has been enlarged to provide H68 (P-IN-PMW), a Level 3 (gridded) MW-based instantaneous precipitation rate estimate, based on the combination of PMW (PMW) Level 2 instantaneous precipitation rate products. H68 is provided every half hour, on a regular grid at 0.25°x0.25° resolution over the extended H SAF area (LAT 60°S – 75°N, LON 60°W – 60°E). It is obtained from the precipitation rate estimates of the PMW (Level 2) operational products H01 (based on CDRD algorithm for SSMIS radiometers, Casella et al., 2013, Sanò et al., 2013, Mugnai et al., 2013 a,b), H02B (based on PNPR algorithm for AMSU/MHS radiometers, Sanò et al., 2015), and H18 (based on PNPR-V2 algorithm for ATMS radiometer, Sanò et al., 2016), and on the auxiliary modules H-AUX-17 (CDRD-V2 algorithm for AMSR2 radiometer, Casella et al., 2017), and H-AUX-20 (PNPR-V3 algorithm for GMI radiometer, Sanò et al., 2018). All the available overpasses at a given grid-box every 30 minutes by DMSP (SSMIS), MetOp/NOAA (AMSU/MHS), GCOM-W1 (AMSR2), SNPP and NOAA-20 (ATMS) and GPM-Core Observatory (GMI) satellites are considered. The product is provided in NRT, but because of the latency of some of the input products (e.g., as high as 3 hours for H01), the timeliness is set at 4 hours. This means that the product will be made available in the worst case (at the latest) 4 hours after sensing. H68 is delivered every half hour (generation frequency) from 00:00 UTC to 23:30 UTC to provide instantaneous precipitation rate in each grid box, where at least one overpass by any of the PMW radiometers cited above is available.
This product will be of interest for applications in hydrology, oceanography, national meteorological services and, in general, for research & development activities by research institutes in Europe and worldwide. The H68 product is mostly aimed at users who need precipitation rate estimates at higher latitudes, where products based on merged MW/IR observations are affected by greater uncertainties related to the slant observations of SEVIRI radiometer. The product is also aimed at users who are interested in MW-based products, and, instead of dealing with the different Level 2 MW precipitation rate products, that might be available at a specific location at a given time (characterized by different orbits, swath sizes, and spatial resolution), prefer or need one “optimal” MW precipitation rate estimate at a given time for a given location. It is worth noting that all international agencies delivering operational PMW precipitation rate products distribute both Level 2 (orbital) and Level 3 (usually daily mean or monthly) products. With H68 product, H-SAF adds a new product very suitable for further processing (e.g., time integration, merging with other observations) to obtain products to be used in hydrological models. The product can be used, for example, to easily derive daily mean (H67) or monthly MW-based precipitation estimates, and to carry out seasonal or inter-annual variability analysis.

For each grid-box at 0.25°x0.25° resolution, every 30 min, H68 provides:

Instantaneous precipitation rate (mm/h), where available.
Indication of the phase of the precipitation.
Quality Index (0-100) of the precipitation rate estimate.
Number and type of conical and cross-track satellites overpassing each grid-box in the considered half hour, and their total number.

2.2 Algorithm principle

The H68 algorithm mainly consists of three modules:

a. remapping module;
b. adjustment module;
c. merging module.

The remapping module makes use of CDO (Climate Data Operator), a collection of command line operators developed to manipulate and analyse Climate and NWP model Data. More information about CDO can be found in [1]. The remapping module performs bilinear interpolation of the instantaneous precipitation rate in the original orbital (irregular) grid to remap them on a regular grid. The target (regular) grid description is given as an external file. The scheme used in CDO considers a local bilinear approximation to interpolate to a point in a quadrilateral grid. For the extended H SAF area at 0.25°x0.25° the grid description file is described below:

gridtype = lon/lat
xsize = 480
ysize = 540
x_rst = -59.875
xinc = 0.25
y_rst = -59.875
yinc = 0.25

The remapping module runs every 30 minutes, looks for files produced by H01, H02, H18, H-AUX-17, and H-AUX-20 in the last 30 minutes and performs remapping of those files.

The adjustment module runs after the remapping module (i.e. every 30 minutes) and adjusts all the data produced by H01, H02, H18, H-AUX-17, and H-AUX-20 in the previous 30 minutes and remapped over the 0.25°x0.25° grid. The adjustment is performed by taking as reference the precipitation rate estimate provided by the GPM GMI-DPR combined product (2B-CMB V05) over the extended H SAF area (LAT 60°S – 75°N, LON 60°W – 60°E) from 2014 to 2018. For each Level 2 PMW product (i.e. H01, H02, H18, H-AUX-17, and H-AUX-20) all grid boxes where coincident observations between each radiometer and the GPM GMI/DPR are available are considered. The GPM 2B-CMB estimates and the Level 2 PMW estimates are compared to derive the coefficients a and b of a power-law fit by considering the five-years long coincidence dataset. The power law fit is described as follows:

$$PR_{adj} = a \bullet PR_b \quad \text{PRadj}=a \cdot \text{PRb}$$

where PRadj is the gridded adjusted precipitation rate and PR is the gridded precipitation rate for each H68 input product (i.e. H01, H02, H18, H-AUX-17, and H-AUX-20.
The results of the comparison between the different Level 2 products and the GPM product, have evidenced that different calibration is needed for all products for the different surface types (e.g. ocean and land/coast), except for H-AUX-17 (AMSR2 product) and H-AUX-20 (GMI product) where the calibration is carried out only over ocean. Furthermore, the adjustment is not applied to the whole range of precipitation intensity estimated by the different products. Table 1 reports for each product (i.e. H01, H02, H18, H-AUX-17, and H-AUX-20) the

coefficient a and b (constant, whenever they are derived) and the precipitation rate range in which the power law is applied.

Product	Surface/Region	a	b	Range (mmh-1)
H01	Ocean/Africa	1.00	0.73	0.1-100
	Land/Africa	1.00	0.69	0.1-100
	Ocean/"Europe"	1.34	0.58	0.1-100
	Land/"Europe"	1.15	0.67	0.1-100
H02B	Ocean/Africa	1.19	0.62	0.1-100
	Land/Africa	1.15	0.56	0.1-100
	Ocean/"Europe"	1.11	0.68	0.1-100
	Land/"Europe"	1.37	0.60	0.1-100
H18	Ocean	1.22	0.73	0.1-100
	Land	1.42	0.66	0.1-100
H-AUX-17	Ocean	0.22	1.62	0.1-100
	Land	/	/	/
H-AUX-20	Ocean	1.28	0.96	0.1-10
	Ocean	0.33	1.43	10-100
	Land	/	/	/

Table 1: coefficients a and b (constant) and range of application of the power law derived for each input's product of H68. The power law fits are derived for different surface type. Only for H01 and H02B they are derived separately above 35°N and below 35°S ("Europe"),and between 35° N and 35° S ("Africa"). Two different power laws (applied to different precipitation rate ranges) are derived over Ocean for H-AUX-20.

The merging module runs after the calibration module (i.e. every 30 minutes) and performs an ensemble mean of all the data produced by H01, H02, H18, H-AUX-17, and H-AUX-20 in the previous 30 minutes and remapped at 0.25°x0.25° and calibrated. The ensemble mean module is organized as follow:

Two separate rankings based on the MW radiometer characteristics, one for the products based on conical scanning radiometers, and one for the products based on cross-track scanning radiometers, are derived. The rankings, which consider the characteristics of the sensors and the pixel-based quality flag associated, are defined as follows:

Conical Satellites	Cross-track Satellites
1. H-AUX-20 (GMI)	1. H18 (ATMS-NPP)
2. H-AUX-17 (AMSR2)	2. H18 (ATMS-NOAA20)
3. H01 (F17)	3. H02B (MHS-MetOp B)
4. H01 (F18)	4. H02B (MHS-NOAA18)**
5. H01 (F16)	6. H02B (MHS-NOAA19)
	7. H02B (MHS-MetOp A)
	8. H02B (MHS MetOp C)

Table 2: conical and cross-track satellite ranking. ** MHS onboard NOAA-18 is no longer available, but it is considered in the Table for possible re-processing.

2.3 Main operational characteristics

The architecture of the H68 product generation chain is shown in Figure 1.

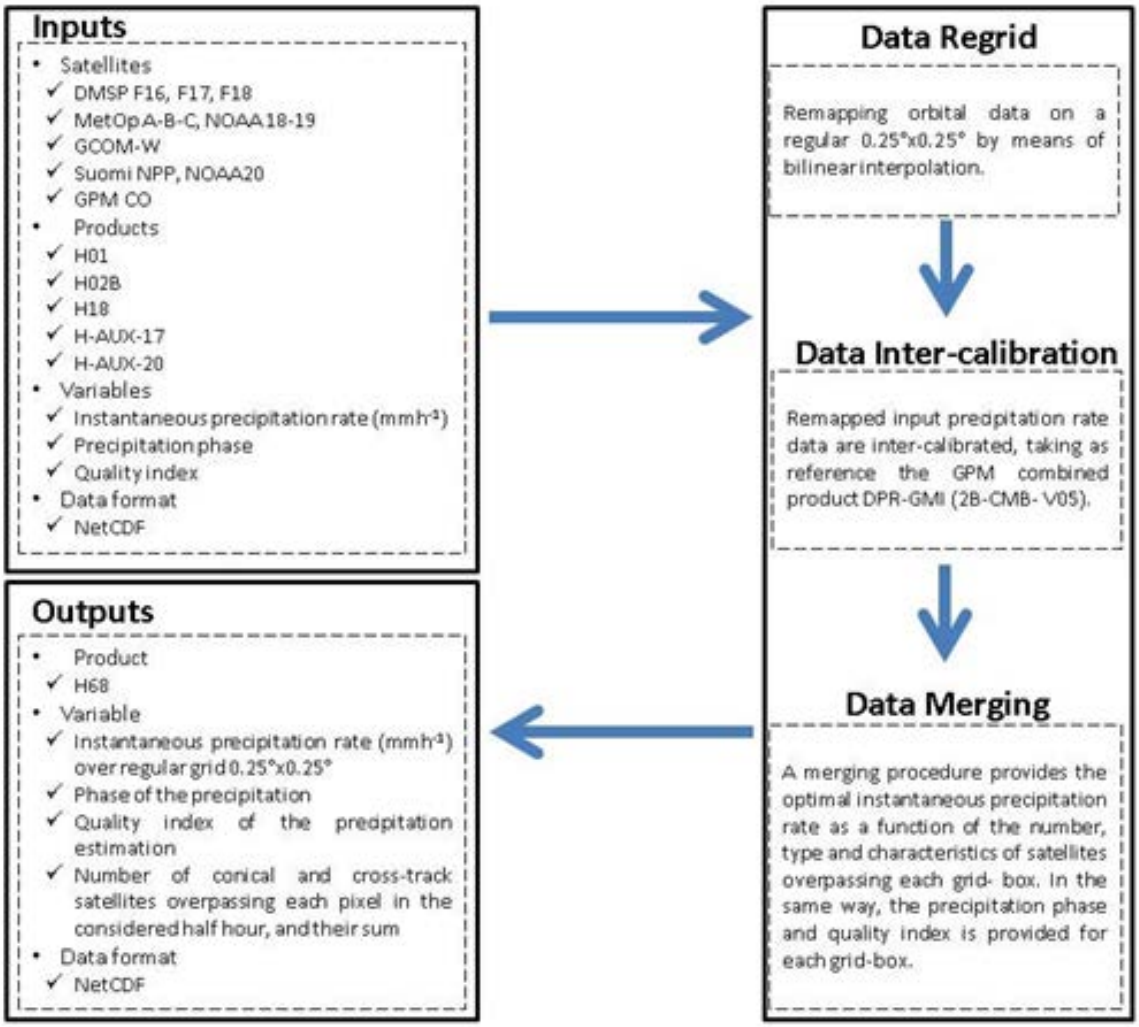

Figure 1: Architecture of H68 product generation chain.

For further and more detailed info on H68 algorithm, please refer to ATBD and/or PUM document available on H SAF website http://h-saf.eumetsat.int

3 Validation results: case study analysis

3.1 Introduction

As reported in the Appendix 1 the common validation methodology is composed of large statistic (multi-categorical and continuous), and case study analysis. Both components (large statistics and case study analysis) are considered complementary in assessing the accuracy of the implemented algorithms. Large statistics helps in identifying existence of pathological behavior, selected case studies are useful in identifying the roots of such behavior, when present.

This Chapter collects the case study analysis performed by PPVG. The Chapter is structured by Country / Team, one section each. The analysis has been conducted to provide information to the User of the product on the variability of the performances with climatological and morphological conditions, as well as with seasonal effects.

Each section presents the case studies analysed giving the following information:

- description of the meteorological event;
- comparison of ground data and satellite products;
- visualization of ancillary data deduced by nowcasting products or lightning network;
- discussion of the satellite product performances;
- indication on the ground data (if requested) availability into the H SAF project.

3.2 Product information

Some main product information are summarized in table.

PRODUCT NAME: **P-IN-PMW (H68)**		
PRODUCT DEVELOPER INSTITUTE: CNR-ISAC	Developers: D'Adderio Leo Pio (Leader), Panegrossi G.	Contact point: leopio.dadderio@artov.isac.cnr.it giulia.panegrossi@artov.isac.cnr.it
OPERATIONAL CHAIN INSTITUTE: COMET	Responsables: Zauli F., Melfi D.	Contact points: francesco.zauli@aeronautica.difesa.it davide.melfi@aeronautica.difesa.it

3.3 Case study analysis in Belgium (RMI)

3.3.1 Case study: 2 October 2019

PRODUCT NAME	H68
CASE STUDY PERIOD	2 October 2019
CASE STUDY AREA	Belgium
METEOROLOGICAL EVENT	Night showers and thunderstorms
VALIDATION INSTITUTE	RMI
PRODUCT DEVELOPER INSTITUTE	CNR-ISAC
OPERATIONAL CHAIN INSTITUTE	COMET

METEOROLOGICAL EVENT DESCRIPTION

Different low pressure systems from England to Scandinavia are moving eastwards influencing the weather over Belgium. As a results, unstable maritime air masses circulate in western Europe. After the passage of an occlusion during the night of 1 to 2 October, a flow of polar air is established between the high pressures in a vast area from the Azores to Greenland and the low pressures in the eastern parts of Europe.
This situation is summarized in the following maps, including fronts and barometric systems:

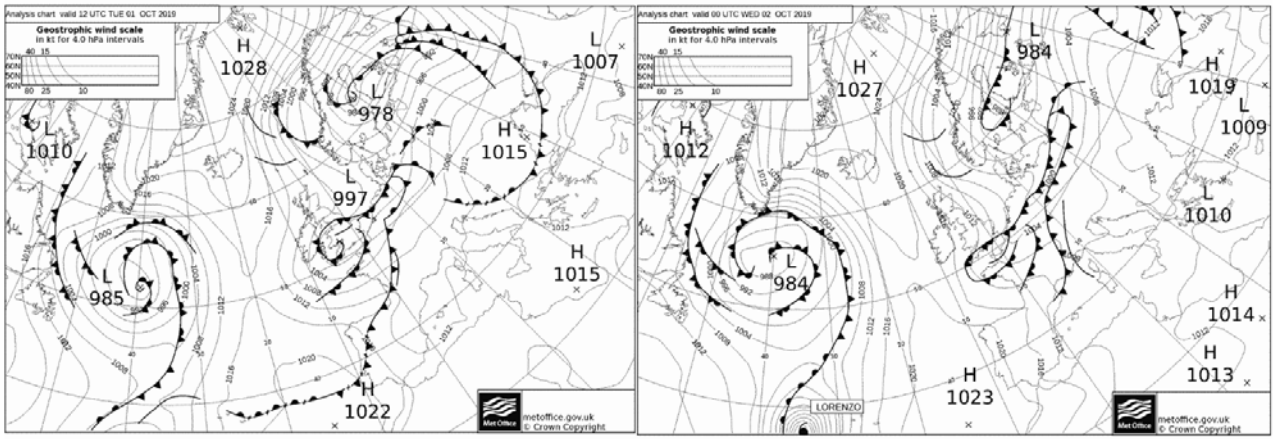

Figure 2: Analysis charts valid for 1 (left) and 2 (right) October 2019 at 12:00 and 00:00 UTC respectively (Contains public sector information licensed under the Open Government Licence v3.0).

DATA/PRODUCTS USED

Reference data: Belgian Radar located at Wideumont, Wallonia (RMI)
Precipitation product H68(H-SAF/EUMETSAT)
Weather charts (MetOffice analyses from Wetterzentrale archive)

RESULTS OF COMPARISON

In Figure 3 and Figure 4 we can see the result of upscaling of radar data to the H68 grid on 2 October 2019 at 02:00 UTC and 04:30 UTC respectively, together with the corresponding H68 data. The upscaled radar data serve as basis for comparison between radar and H68.

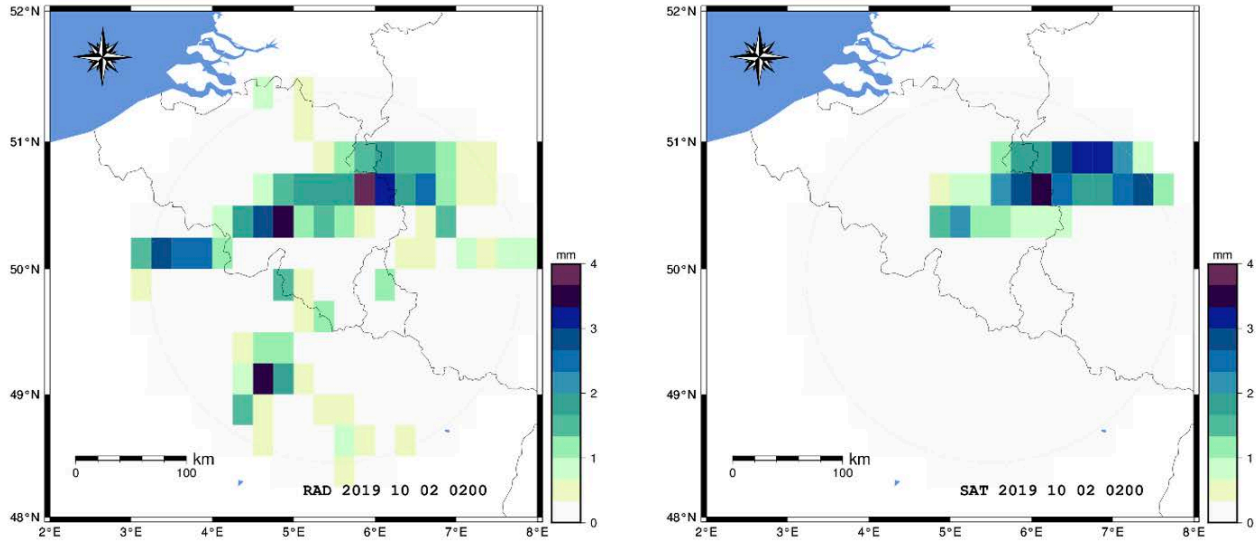

Figure 3: Upscaled radar (left) and H68(right) valid for 2 October 2019 at 02:00 UTC.

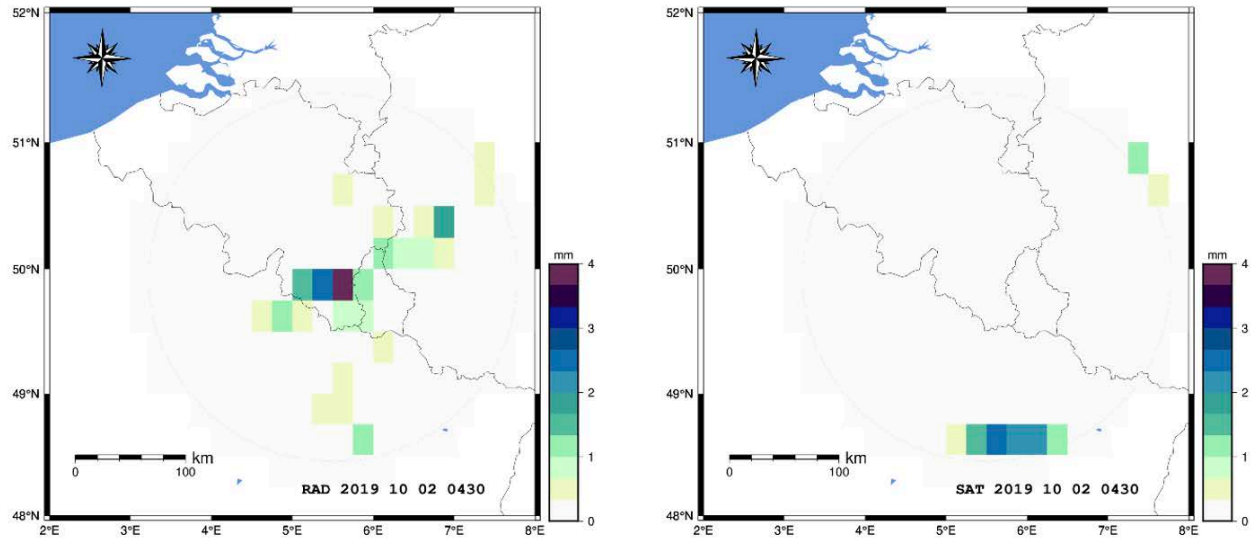

Figure 4: Upscaled radar (left) and H68(right) valid for 2 October 2019 at 04:30 UTC.

The product H68 represents quite well one part of the domain receiving rain in Figure 3, although it misses the western-southwestern parts. In fact, the main difference between radar and the product H68 in Figure 3 is the percentage of grid cells with precipitation exceeding 1 mm/h (17.1% and 9.8% respectively). The bias is fairly low at -0.52 mm/h.

On the other hand, in Figure 4 the product H68 misses the main rain area and it exaggerates the rain in the extreme south of the domain. As a result, the overall bias is still low at -0.52 mm/h as previously.

For the two cases depicted in Figure 3 and Figure 4 we have computed statistical scores shown in the following tables.

H68 vs. RADAR	0.25 mm/h < rr < 1 mm/h	1 mm/h < rr < 10 mm/h	rr > 0.25 mm/h
ME [mm]	-0.27	-0.81	-0.52
STD [mm]	0.68	1.32	1.06
MB [-]	0.45	0.57	0.54
RMSE [mm]	0.73	1.55	1.18
FSE [%]	1.48	0.82	1.04

H68 vs. RADAR	rr > 0.25 mm/h	rr > 1 mm/h
POD [-]	0.32	0.46
FAR [-]	0.14	0.20
CSI [-]	0.30	0.41

Table 3: Statistical scores obtained from the comparison between H68 and radar acquisition, valid for 2 October 2019 at 02:00 UTC.

H68 vs. RADAR	0.25 mm/h < rr < 1 mm/h	1 mm/h < rr < 10 mm/h	rr > 0.25 mm/h
ME [mm]	-0.29	-1.54	-0.52
STD [mm]	0.51	1.39	0.90
MB [-]	0.32	0.16	0.24
RMSE [mm]	0.59	2.07	1.04
FSE [%]	1.39	1.13	1.52

H68 vs. RADAR	rr > 0.25 mm/h	rr > 1 mm/h
POD [-]	0.12	0.12
FAR [-]	0.38	0.83
CSI [-]	0.11	0.08

Table 4: Statistical scores obtained from the comparison between H68 and radar acquisition, valid for 2 October 2019 at 04:30 UTC.

FINAL COMMENTS

In the present case of showers and thunderstorms during the night of 1 to 2 October, we obtain mixed results in the comparison between the radar and the product H68 data. As the results in Table 3 and Table 4 show, we have very similar statistical scores in both cases of 02:00 UTC and 04:30 UTC when all rain rates are taken into account (rr > 0.25 mm/h). However, the two cases differ substantially in spatial features as we see in Figure 3 and Figure 4. This is reflected in the very low POD values at 04:30 UTC.

3.4 Case study analysis in Slovakia (SHMI)

3.4.1 Case study: 2 September 2019 – 4 September 2019

PRODUCT NAME	H68
CASE STUDY PERIOD	2 Sep 2019 00 UTC – 4 Sep 2019 00 UTC
CASE STUDY AREA	Slovakia
METEOROLOGICAL EVENT	Intense waving cold front over Slovakia
VALIDATION INSTITUTE	Slovak Hydrometeorological Institute (SHMI)
PRODUCT DEVELOPER INSTITUTE	CNR-ISAC
OPERATIONAL CHAIN INSTITUTE	COMET

METEOROLOGICAL EVENT DESCRIPTION

On 1st of September 2019, a ridge of high pressure spread over the Carpathian region from the northeast and on its backside, very warm, originally tropical air from the south to the southeast flowed into our area. At the same time, a cold front, connected by a pressure low with a centre above the Norwegian Sea, advanced further east through Germany and the Alps. Behind this cold front a cold air mass began to penetrate over our territory on the next day. However, the weak airflow aloft in combination with the mountains slowed down the progress of the front in our area, and the front began to undulate, which contributed to large temperature differences within the territory as well as heavy rainfall in the following days.

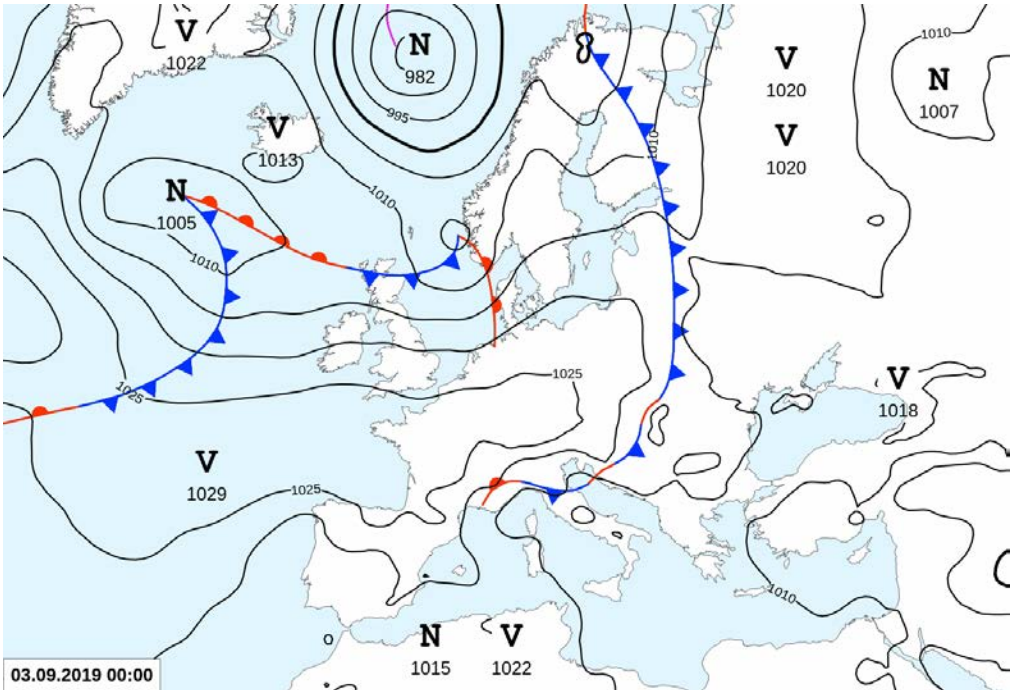

Figure 5: Synoptical analyses

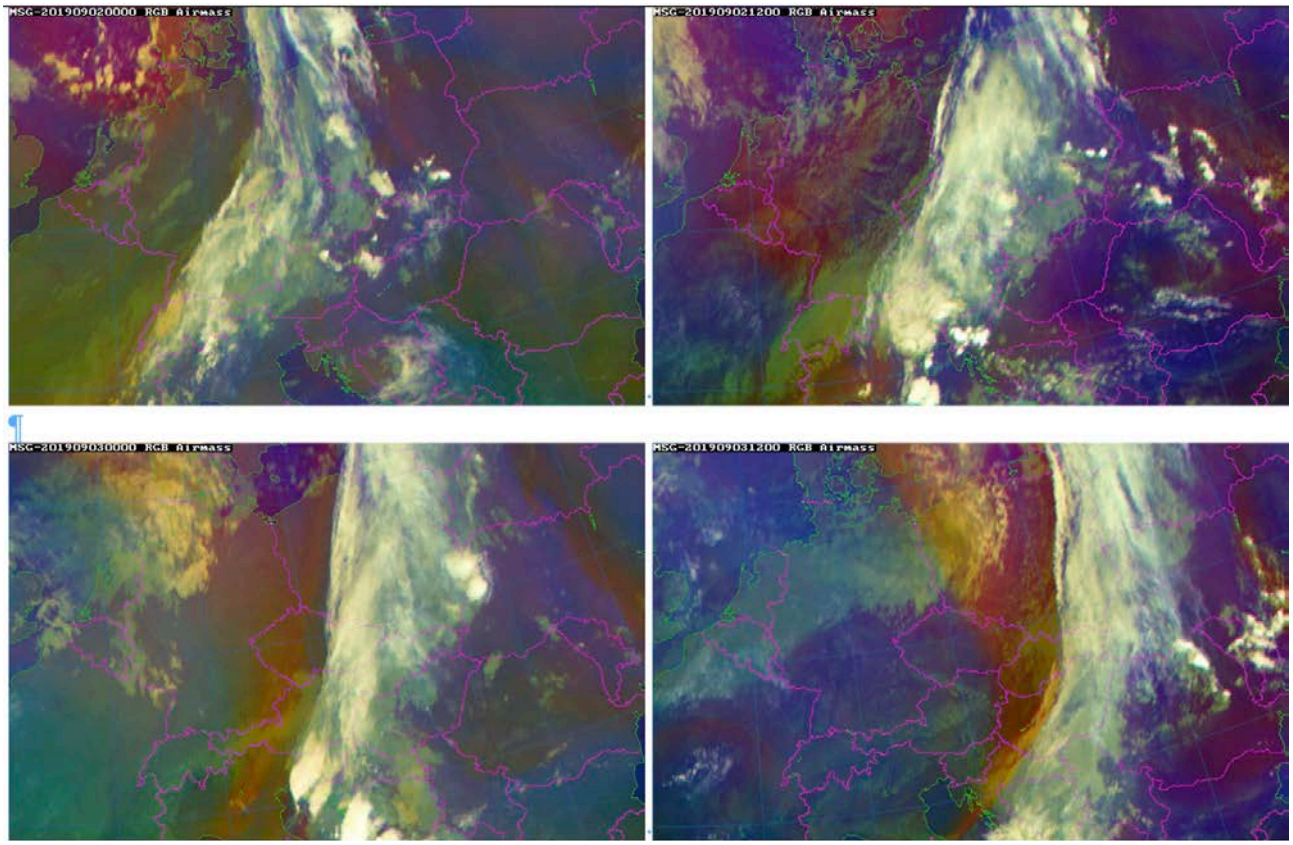

Figure 6: MSG Airmass RGB imagery documenting passage of waiving cold front over Slovakia during 2-3 Sep 2019

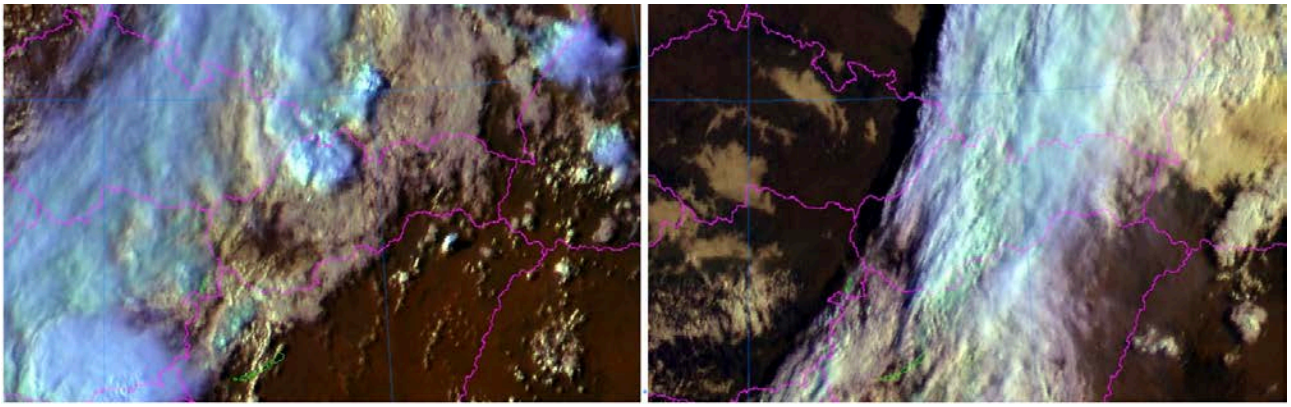

Figure 7: MSG HRV imagery showing formation of prefrontal thunderstorms over North Western Slovakia on 2 Sep 2019 15:00 UTC (left) and waving front cloudiness bringing stratiform precipitation over Slovakia on 3 Sep 2019 06:00 UTC (right)

DATA/PRODUCTS USED

P-IN-PMW precipitation intensities estimated over 30 minutes
Meteosat imagery to document synoptic situation
Precipitation intensities from SHMU radars over 24h derived from CAPPI 2km product using quality indices, thresholder to overall radar QI > 0.6
Precipitation intensity fields from SHMU radars (as above) upscaled into satellite projection

RESULTS OF COMPARISON

By visual comparison with radars, the H68 product detected successfully most of the precipitation (see examples in Figure 8). On the other hand, the satellite product in many cases overestimated the precipitation area (e.g. Figure 8 a), c) and d)).

The maximum intensities of convective precipitation that occurred on 2 Sep 2019 were mostly underestimated by the H68 product (Figure 8 a) and b)). In case of stratiform rain on the waving front on 3 Sep 2019, the precipitation intensities were comparable or slightly underestimated by the H68 as shown e.g. in Figure 8 d).

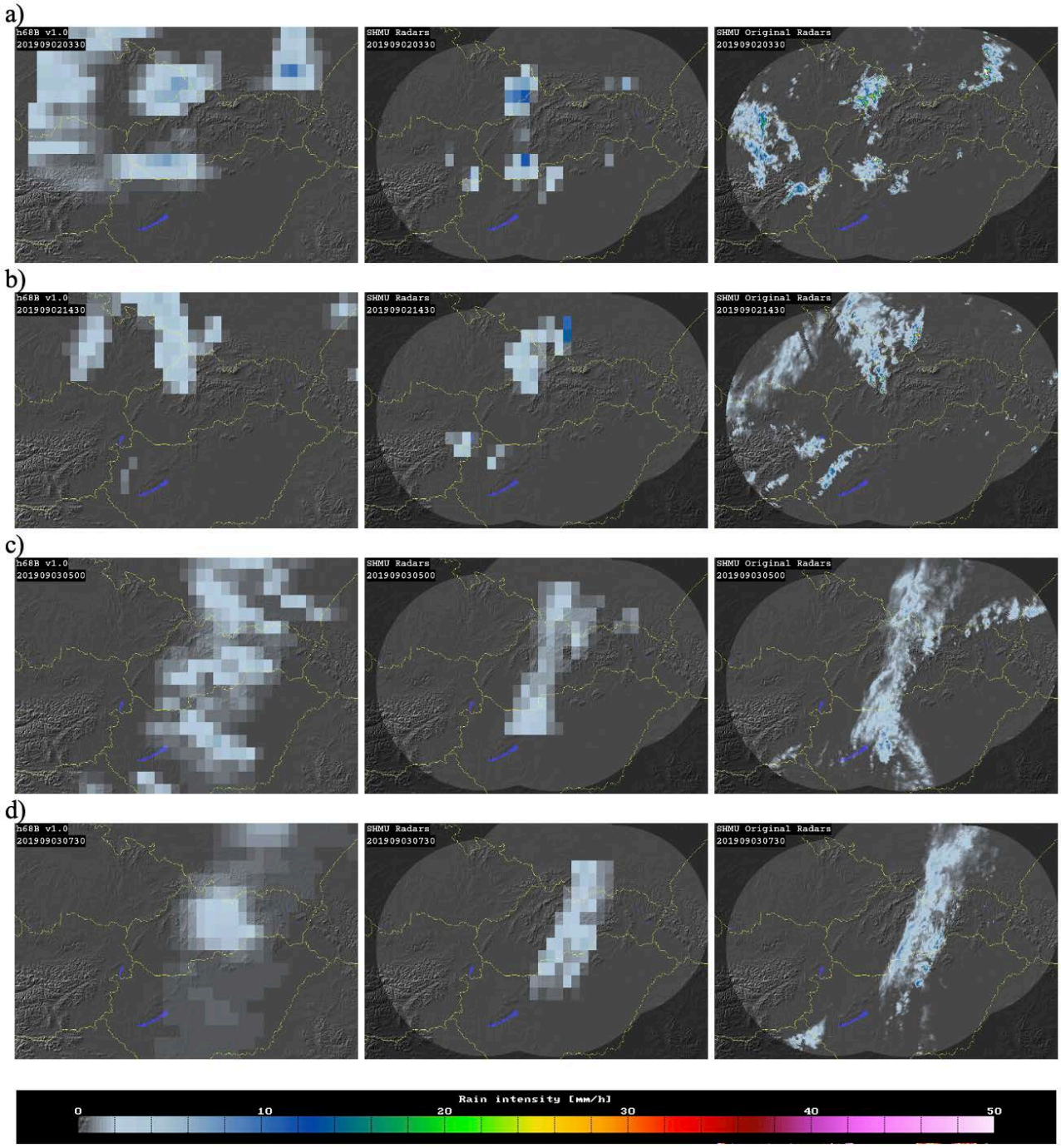

Figure 8: Precipitation intensity fields observed by H68 product (left column), SHMU radars upscaled to satellite grid (middle) and SHMU radars in original resolution (right column) on a) 2 Sep 2019 03:30 UTC and b) 14:30 UTC, c) 3 Sep 2019 05:00 UTC and 07:30 UTC.

Results of statistical comparison of the satellite product with radars are shown in the following tables.

Precipitation class (mm/h)	0.25 - 1	1 - 10	≥ 10	≥ 0.25
1 Number of satellite obs.	289	678	1	968
2 Number of radar obs.	269	378	12	659
3 Mean error (mm/h)	0.778	-0.325	-8.776	-0.029
6 Multiplicative bias	2.277	0.870	0.336	0.985
7 Correlation coefficient	0.125	0.401	-0.362	0.441
9 URD-RMSE (%)	258.7	71.1	69.7	174.1
10 Fractional Standard Error (%)	214.5	67.0	74.9	105.2
11 Nash-Sutcliffe Coefficient	-36.918	-0.072	-14.063	0.157

Table 5: Selected scores of continuous statistics

Precipitation threshold (mm/h	≥ 0.25	≥ 1
POD	0.939	0.849
FAR	0.361	0.513
CSI	0.614	0.449

Table 6: Selected scores of dichotomous statistics

Both Mean Error and Multiplicative Bias indicate slight overestimation of light precipitation (0.25-1 mm/h) by the H68 product (see Table 5). The same scores for the precipitation class 1-10 mm/h however show relatively good agreement of the satellite intensities with radars. The Mean Error and Multiplicative Bias for heavy precipitation (class ≥ 10 mm/h) show underestimation by the H68 which agrees with the visual comparison.
The POD reached high values confirming the observed good detection capability of the satellite product, especially for overall precipitation RR ≥ 0.25 mm/h with a value close to 1 (Table 6). The FAR reached a little bit less excellent results, especially for precipitation threshold of 8 mm. These results agree with the observed overestimation of the precipitation area. The CSI score reached relatively high value around 0.6 for the threshold 0.25 mm/h and 0.45 in case of the threshold 1 mm/h.

COMMENTS

The upscaled radar precipitation fields shown in this case study are limited to area with radar quality index higher than 0.6. Only the data lying inside this area are used for calculation of the statistical results.

During this event with passage of waving cold front, the H68 product showed excellent detection capabilities but, on the other side, often overestimated the precipitation area. The intensities of heavy precipitation were slightly overestimated by the H68. However, for medium precipitation (1-10 mm/h), the precipitation intensities were comparable with radars.

3.5 Case study analysis in Poland (IMWM-NRI)

3.5.1 Case study: 20 May 2019

PRODUCT NAME	H68
CASE STUDY PERIOD	20th May 2019
CASE STUDY AREA	Poland
METEOROLOGICAL EVENT	Severe precipitation events
VALIDATION INSTITUTE	IMWM-NRI
PRODUCT DEVELOPER INSTITUTE	CNR-ISAC
OPERATIONAL CHAIN INSTITUTE	COMET

METEOROLOGICAL EVENT DESCRIPTION

On the 20th of May 2019 one could observe the upper field slow transformation, a slow drift of the heat wedge of 500 hPa over the central and northwest part of European Russia and over the Baltic Sea and a large part of Scandinavia – this drift was not caused by any major pressure systems, but was due to the natural heating of the continent. In the middle of that week, the warmer air from the south with Arctic cold were clashing over northern Scandinavia and the White Sea, and the contrast on the front was strongly strengthened, which was being stationary for a few days extending from Labrador through the southern end of Greenland, Iceland, Tromso region, White Sea, Karelia and Northern Ural. In that time, a major part of Europe, including Poland, was in the area of relatively warm, humid air flowing from the eastern and south-eastern countries, it was quite natural to develop convection phenomena in those conditions. The warmer volumes of air and water vapor rised together in a convective thermal chimney reaching a condensation level usually located 800 to 1200 meters above the ground. Convection clouds were developing in the afternoon and evening on that day, being laid out in a clear line of rain squalls, starting from Roztocze region, on the line of Lublin and Siedlce, Ostrołęka, in the night reaching to Podlasie and Mazury regions. The storms appeared in Zamość at 1500, in Lublin at 1600, and in Siedlce at 1700 local time. The width of the zone of the most intense rainfall and storms was ~ 70 km, covering a large part of the Lublin and eastern Mazovia, then Podlasie and Mazury regions. In addition to the intense storms and simulatanous precipitation in those regions (12-16 mm per hour), a local convective precipitation exceeded 30 mm/h. There was also a rapid drop in temperature recorded (from 25 to 15 degrees C) and a lot of squall impacts occured (up to 25 m/s) or more depend on the development of individual Cumulonibus clouds *in situ*. Thus, the inhabitants of the eastern part of the country did not have a quiet evening and night, the roads were blocked by broken branches and tree trunks, power lines, roofs, advertising panels etc. Sudden and lasting several hours precipitation events resulted in numerous floodings of meadows and fields, especially in Roztocze region and Lubelszczyzna region. The lower Silesia region was covered by a continuous precipitation which moved slowly in the NW direction, during the day this rainfall zone turned over the Lubusz and Western Pomerania regions into a storm area with strong convection, but much weaker than in the east of the country.

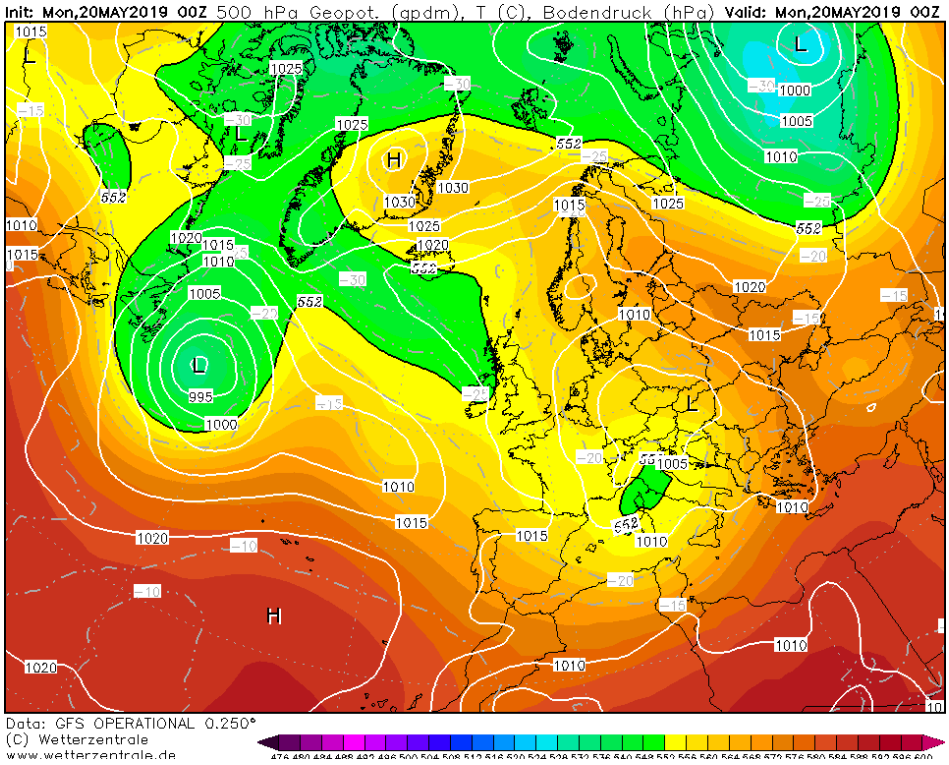

Figure 9: 500 hPa Geopotential chart valid for the 20th of May 2019 at 00 UTC.

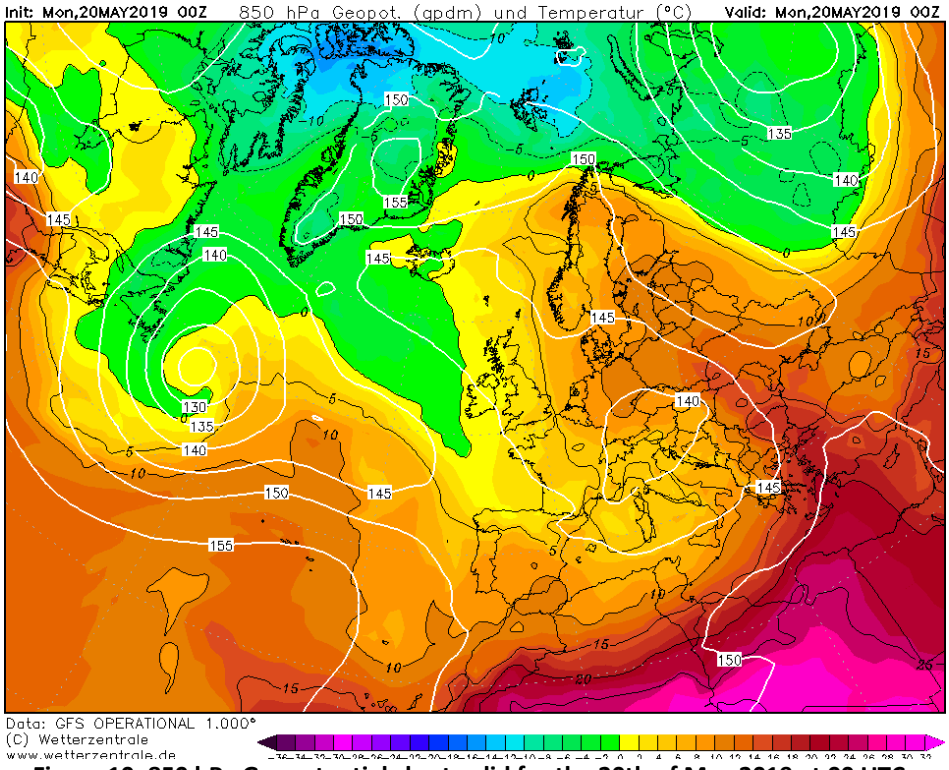

Figure 10: 850 hPa Geopotential chart valid for the 20th of May 2019 at 00 UTC.

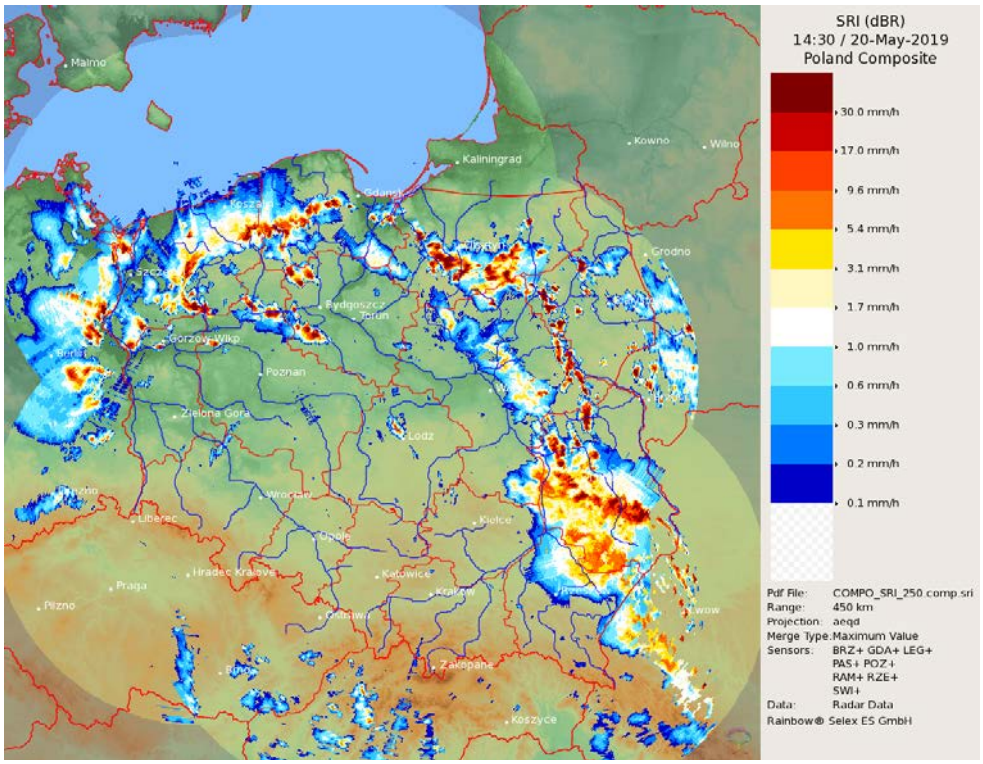

Figure 11: The radar composite map of Poland on the 20th of May 2019 at 1430 UTC.

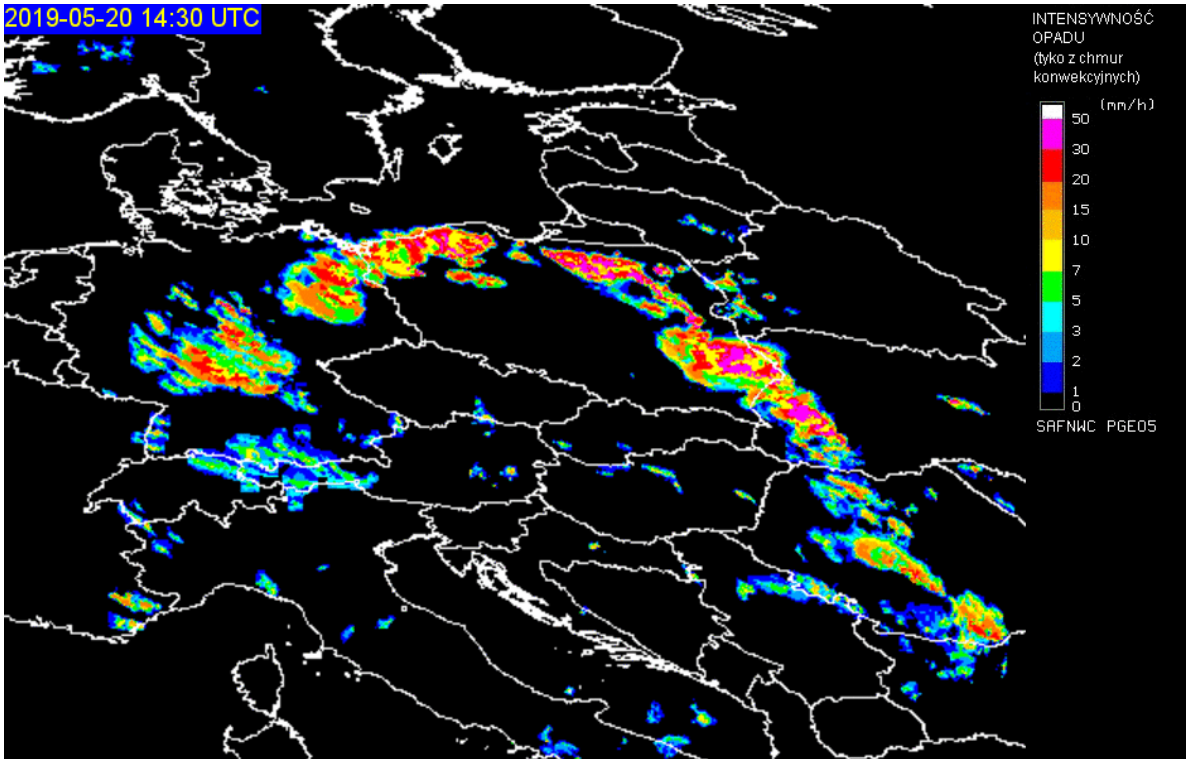

Figure 12: The SAF NWC product showing the convective rainfall rate at 1430 UTC, 20th of May 2019.

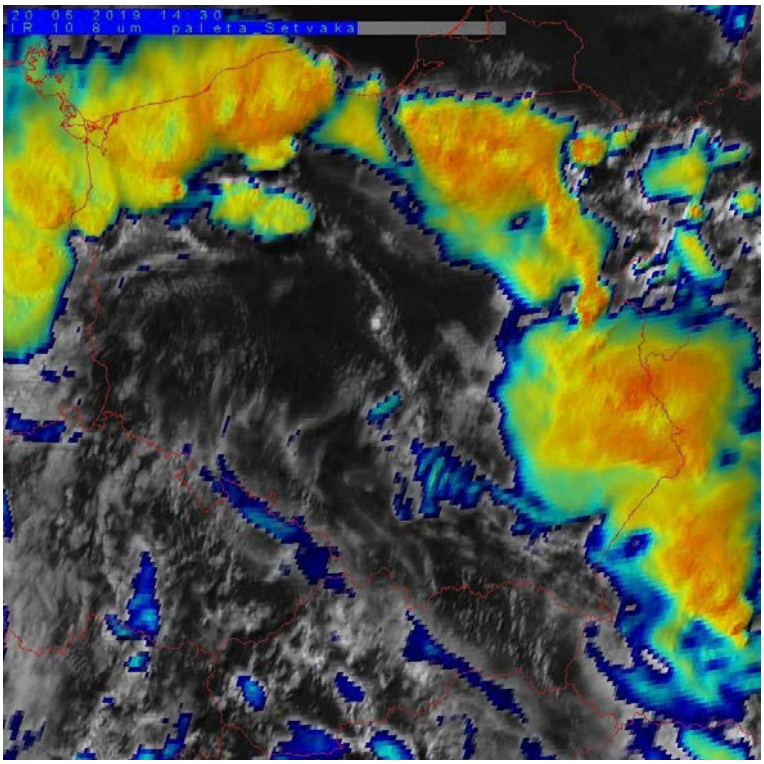

Figure 13: The 10,8 µm (Martin Setvak palette) product showing the convection over Poland at 1430 UTC, 20th of May 2019.

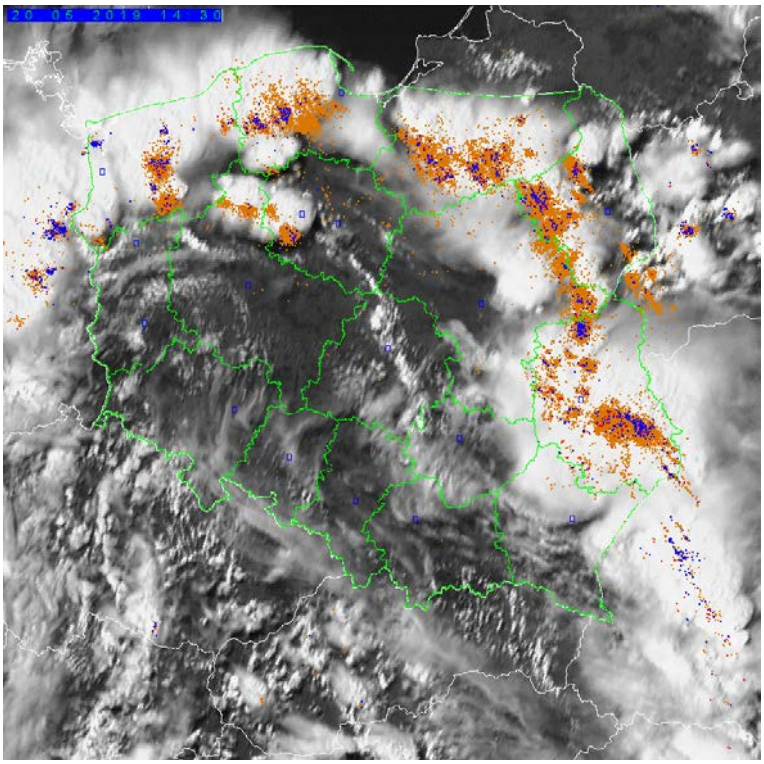

Figure 14: The image presents the lightning location proving the massive convective cores presence at 1430 UTC, 20th of May 2019. The lightning events are marked in colour: red – CG+, blue – CG-, orange – IC.

The composite radar map of Poland shows the horizontal extent of the precipitation on the 20th of May 2019 at 1430 UTC (Figure 11). Its spatial distribution is in very good agreement with the SAF NWC product showing the convective precipitation intensity at 14:30 UTC (Figure 12). It needs to

be emphasized that the SAF NWC product presents the precipitation from convective clouds only. The same convective phenomena are also visualized by the infra-red 10,8 µm product on Figure 13. The lightning recorded by the PERUN network in Poland (Figure 14 above) between at 1430 UTC on 20th of May 2019 shows a curved line of major and several smaller storm structures matching well both satellite and radar data fields, the storm centers seen on previous images are proven to be active due to the rapidly developing electrical activity within the storm cores.

DATA/PRODUCTS USED

Reference data:
Polish lightning detection and localization system PERUN
Polish meteorological radar composite map
Satellite images (EUMETSAT & IMWM-NRI)
Weather charts (www.wetterzentrale.de)

RESULTS OF COMPARISON

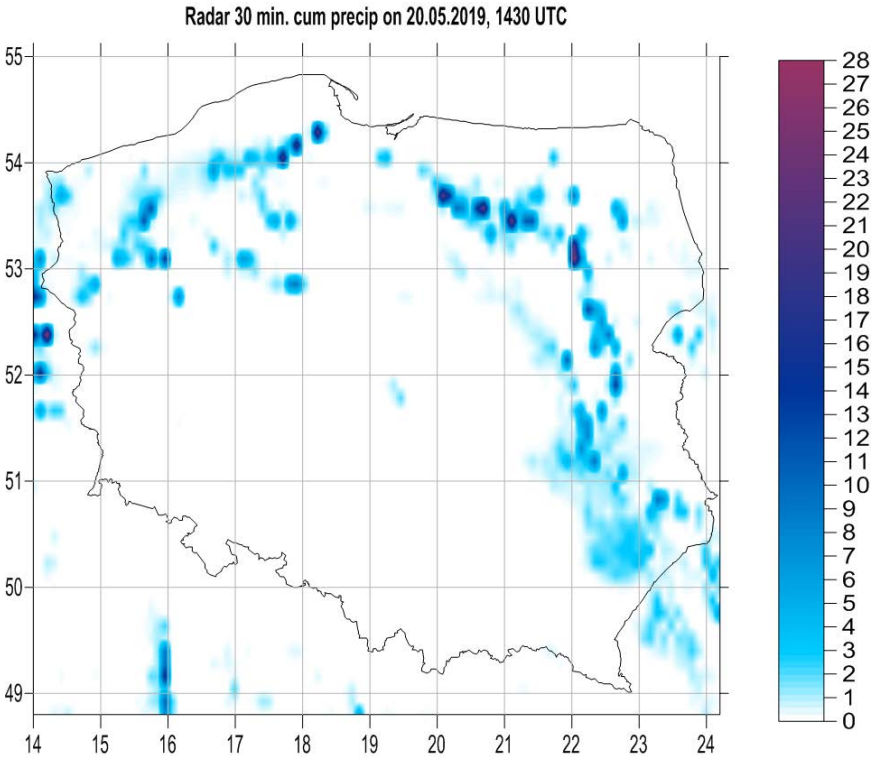

Figure 15: Radar 30 minutes cumulated precipitated on 20 May 2019 at 14:30 UTC

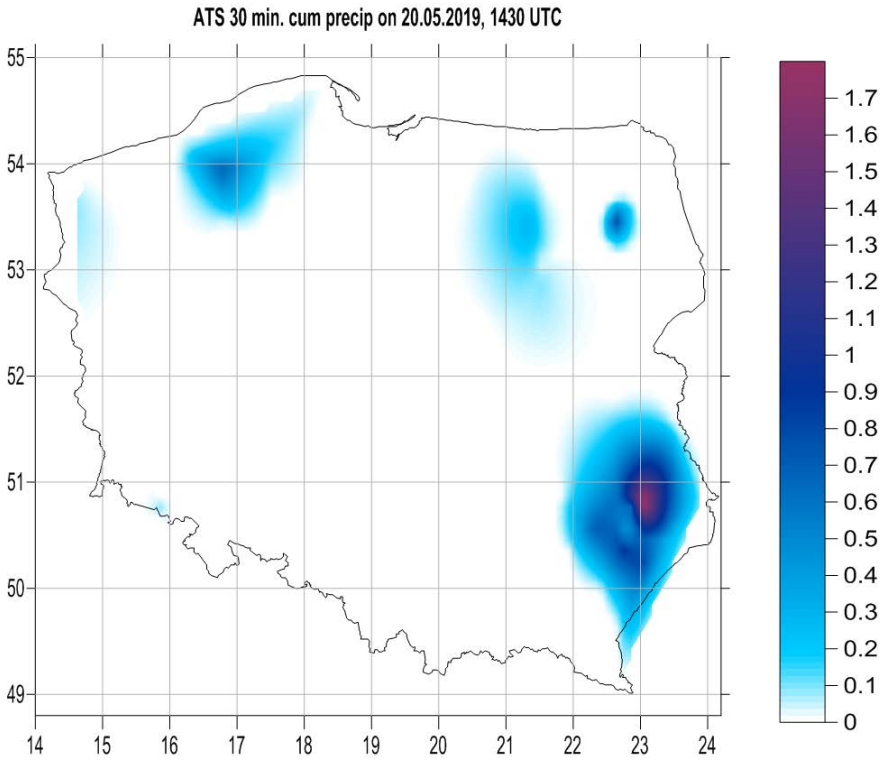

Figure 16: ATS 30 minutes cumulated precipitated on 20 May 2019 at 14:30 UTC

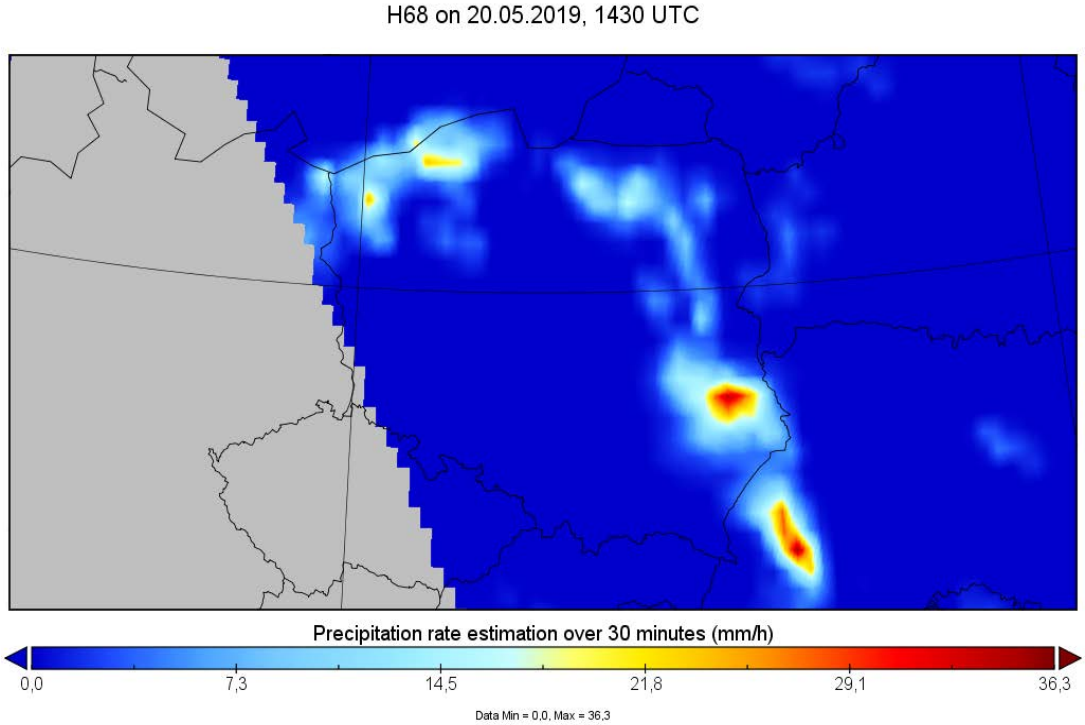

Figure 17: H68 on 20 May 2019 at 14.30 UTC

The visual comparison between the H68 product and the radar acquisition shows a good agreement between the areas with precipitation. However, the H68 product seems to be less accurate in terms of the precipitative area in comparison to the radar map (which is not a surprise). Also the top amounts of rainfall recorded by both of the sources are in good agreement.

The maximum intensity of precipitation observed by radar was 28 mm/h, at the same time rain gauge network maxed at 1.8 mm/h, while H68 recorded a maximum value of 36.3 mm/h.
Please note the scale differences between the data sources presented above.

FINAL COMMENTS

Overall, the H68 product has quite well observed the precipitation events in Poland on 20th of May 2019. However, it tends to overestimate the intensity of the point precipitation events and in the same time to underestimate the spatial extension of the precipitation areas (which is understandable in respect to its resolution). It needs to be mentioned that the Polish ATS network has failed to properly record both the special extent of the precipitable area and its max values. It seems that the most intense point precips visible on the radar image missed the networks rain gauges.

4 Validation results: long-term analysis

4.1 Overview

Product ID (Acronym)	H68 (P-IN-PMW)		
Product name	Gridded MW instantaneous precipitation rate based on intercalibrated PMW instantaneous precipitation rate estimates		
Algorithm version number	Latest version:		1.0
	Version considered for Q.A.:		1.0
Covered period	01/2019 – 12/2019		
Q.A. methods applied	Continuous statistics	ME, SD, MAE, MB, RMSE, FSE	
	Multi-categorical statistics	POD, FAR, CSI	
	Contributing countries	BE, BU, DE, HU, IT, PL, SK, TU	

The validation has been performed over the period between January and December 2019 by European countries belonging to PPVG and supervised by DPC. The product release currently in force at the time of writing has been evaluated. The results are showed both for European area in comparison with radar and rain gauge data (section 4.2), and over the H SAF extended area in comparison with DPR-NS product (section 4.3). The surface type classification is taken in account (land, sea and coast areas) as well as the three precipitation rate classes. The validation procedure evaluates precipitation of only liquid phase, excluding rain rate's retrievals with low quality ("poor quality"). Similarly, only high-quality precipitation has been considered as reference. Satellite Field Of Views not fully covered by reference data (or with percentage of coverage less than 50%) are discarded by the Q.A. procedure in order to increase the significance of the statistical sample.

4.2 Validation results over European area

Validation has been performed using rain gauge and radar data as reference in Belgium, Bulgaria, Germany, Italy, Hungary, Poland, Slovakia and Turkey, for the period as above descripted. Each institute has used the Unique Common Code (UCC Version 2.0) developed by PPVG to evaluate every H SAF precipitation product in terms of different statistical scores. More than 600 thousand of ground and satellite pairs of data were analyzed. For H68 product, the accuracy requirements depend by FSE score as indicated in Table 7.

Precipitation Rate	Threshold	Target	Optimal
≥ 1 mm/h	200	150	100

Table 7: Accuracy requirements for product P-IN-PMW in term of FSE(%).

The FSE score (mathematical formula shown in Table 18) defines the accuracy of the H SAF product under analysis.

4.2.1 Monthly accuracy

The monthly accuracy computed for H68 in comparison with radar, rain gauge and overall ground observations is shown in Figure 18 in panel a, b and c respectively. In each panel, the background color indicates the region inside each requirement accuracy threshold as defined in Table 7 and also used in Table 11. The black dotted line represents the mean FSE value over the whole period. Panel d shows the percentage contribution for different instruments and observation's surfaces respect to the full dataset.

The product has different trend and performances respect to radar and gauge. The overall accuracy is representative of all results computed: the mean value fully respects the target requirement. As for the gauge, the requirement score in four cases (March, April, May and July) is above the target (150%) globally the mean annual value equals 146%; whereas for the radar it is always below the target (<150%) with a mean annual value around 117%.

The percentage contribution highlights how radar over land (47%) and gauge (30%) represent most of the whole dataset. While coast and sea areas cover only 6% and 17%, respectively.

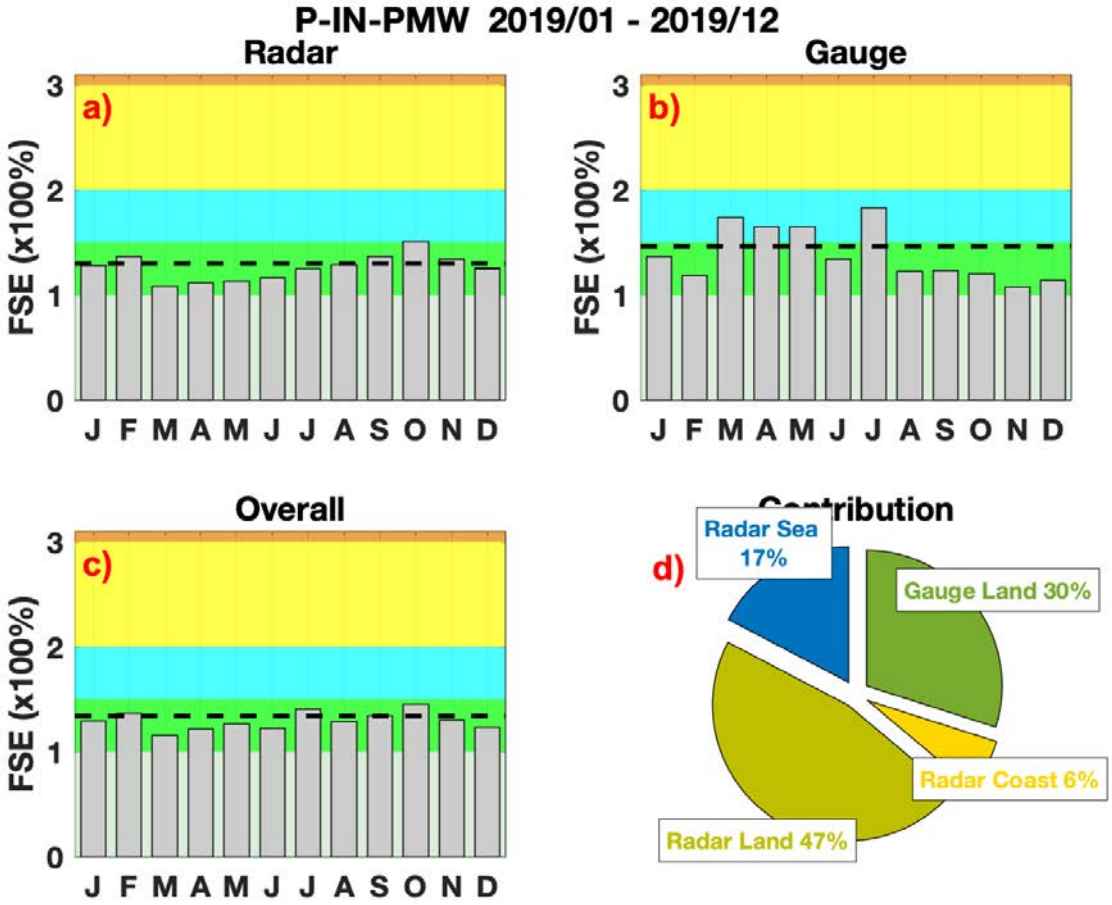

Figure 18: H68 monthly accuracy using Radar (a) and Gauge (b) as ground reference. The Overall Q.A. is shown in the panel c). Background colours highlight the requirement accuracy thresholds in terms of FSE as reported in Table 18 and Table 22. The horizontal black dotted line indicates the mean annual value. The single ground percentage contribution is shown in the panel d).

4.2.2 Monthly continuous statistical scores

In Figure 19 the H68 monthly trend respect to radar over land (green line), sea (blue line), coast (red line) and rain gauge (black dotted line) for all precipitation rates above 1 mm/h is shown for

continuous statistical scores (ME, SD, MAE, MB, RMSE and FSE). Results over land areas (mainly respect with radar measurements) are quite better in the various months than those over sea and coast.

The error coherence in time between radar and gauge is shown in trends of SD, MAE and RMSE score. ME and MB show a tendency to overestimate the precipitation intensity in the second half of the studied period. More continuous statistical scores are shown in Appendixes.

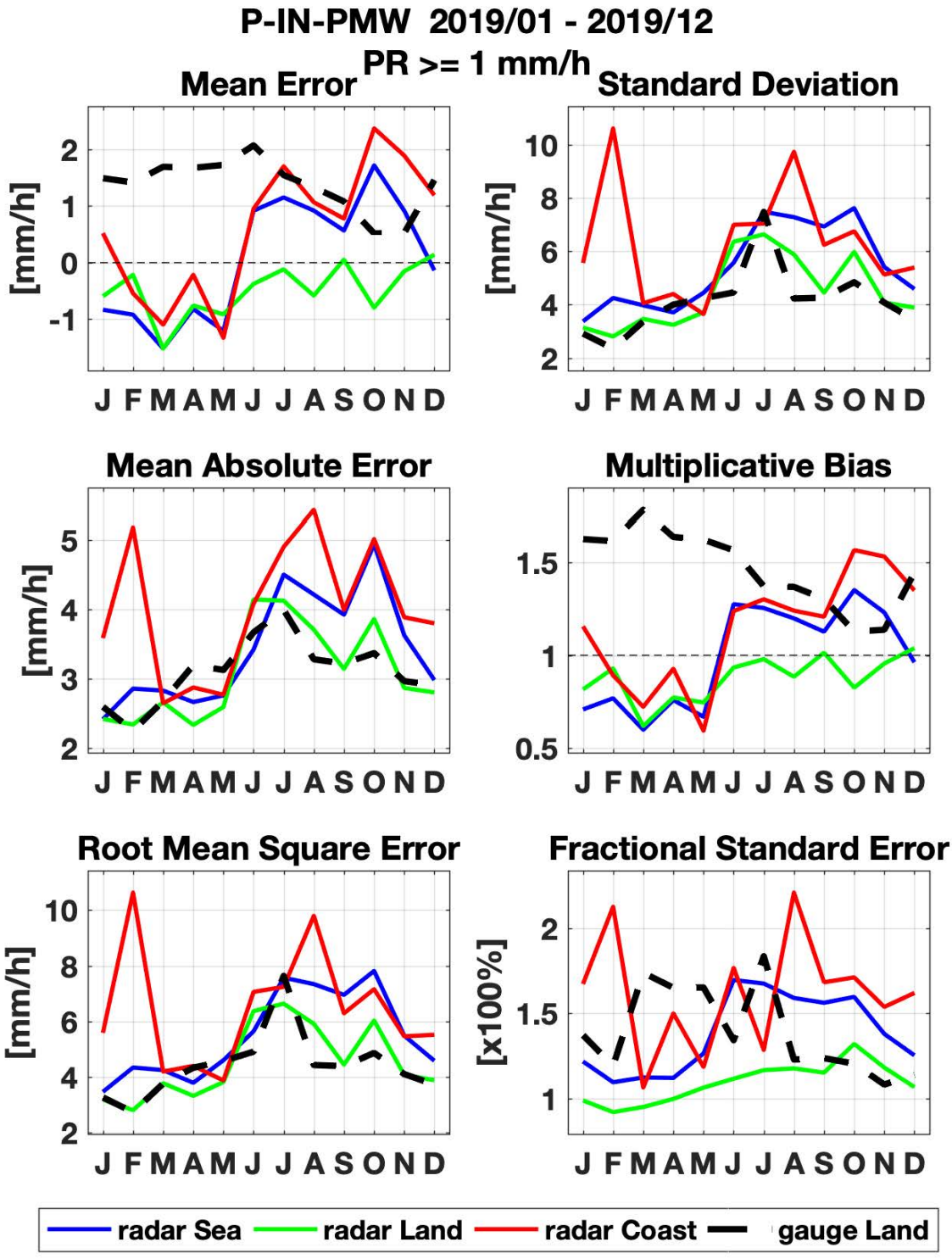

Figure 19: Monthly continuous statistical scores resulting for H68 relatively to the precipitation regime above 1 mm/h.

4.2.3 Multi-categorical statistics

The multi-categorical statistics are below shown. In each table, the first column indicates the precipitation classes of the satellite product, while along the columns are reported the ground precipitation classes. The first class detects the no-rain class (0≤PR<0.25 mm/h), the second class detects the light rain (0.25≤PR<1 mm/h), the third class identifies the stratiform rain rates (1≤PR<10 mm/h), while the last one classifies the convective rates (PR≥10 mm/h).
The H68 product well detects the no-rain area in 99% of cases. Light rain rates are not well detected at all (2%). An evident tendency to underestimate this intensity is observable (Land (78%), sea (82%) and coast (85%)). Stratiform rain rates are well detected in 60% of total cases, up to 73% in comparison with gauges. Finally, convective precipitation areas are correctly identified in only 29% of cases. More multi-categorical statistics are shown in Appendix.

Radar Land | Sea | Coast												
Multi-Categorical Statistics												
	[0 - 0.25[mm/h			[0.25 - 1[mm/h			[1 - 10[mm/h			≥10 mm/h		
[0 - 0.25[mm/h	99%	99%	100%	78%	82%	85%	31%	37%	45%	5%	7%	10%
[0.25 - 1[mm/h	0%	0%	0%	1%	4%	2%	1%	5%	3%	0%	1%	1%
[1 - 10[mm/h	1%	0%	0%	21%	12%	11%	63%	48%	38%	70%	57%	41%
≥10 mm/h	0%	0%	0%	1%	2%	2%	5%	9%	14%	25%	35%	49%

Table 8: Multi-categorical table for product H68 – radar validation over land, sea and coast areas. The precipitation classes along the columns (rows) are relative to ground (satellite) precipitation.

Gauge Land				
Multi-Categorical Statistics				
	[0 - 0.25[mm/h	[0.25 - 1[mm/h	[1 - 10[mm/h	≥10 mm/h
[0 - 0.25[mm/h	98%	57%	18%	4%
[0.25 - 1[mm/h	0%	1%	1%	0%
[1 - 10[mm/h	1%	40%	73%	68%
≥10 mm/h	0%	2%	8%	27%

Table 9: Multi-categorical table for product H68 – rain gauge validation over land. The precipitation classes along the columns (rows) are relative to ground (satellite) precipitation.

Overall				
Multi-Categorical Statistics				
	[0 - 0.25[mm/h	[0.25 - 1[mm/h	[1 - 10[mm/h	≥10 mm/h
[0 - 0.25[mm/h	99%	74%	30%	5%
[0.25 - 1[mm/h	0%	2%	2%	1%
[1 - 10[mm/h	1%	23%	60%	65%
≥10 mm/h	0%	1%	8%	29%

Table 10: Multi-categorical table for product H68 – Overall validation. The precipitation classes along the columns (rows) are relative to ground (satellite) precipitation.

4.2.4 Product requirement compliance

The resulting accuracy of H68 product for the validation period between January and December 2019 is reported in Table 11.
Generally, the accuracy is good, with FSE values below the target (150%). Only one, referred to the radar coast is between the threshold and the target requirement (162%). The overall accuracy for H68 product is equal to 134%.

Between target and optimal	Between threshold and target	Threshold exceeded by < 50 %	Threshold exceeded by ≥ 50 %

H68	Annual average of FSE (%)							
Precipitation Class	**Requirement (FSE %)**			**Radar (Land)**	**Radar (Sea)**	**Radar (Coast)**	**Gauge (Land)**	**OVERALL**
	thresh	**target**	**optimal**					
≥ 1 mm/h	200	150	100	117	145	162	146	**134**

Table 11: Product requirement and compliance analysis for product H68

4.3 Validation results over H SAF extended area

The validation procedure over the H SAF extended area has been developed by the PPVG and coordinated by DPC. DPR-NS product represents the reference for precipitation over the full area considered. As the validation on the European area, this one is performed over the same period and the FSE score defines the accuracy of H68 (as indicated in Table 7: Accuracy requirements for product P-IN-PMW in term of FSE(%)., mathematical formula shown in Table 18). More than 200,000 pairs of DPR and H68 gridded data over boxes of 0.5° x 0.5° are compared. Next sections deal about the statistical scores obtained between the two intersected products. In addition, a more detailed analysis for different geographical areas is reported in section 4.3.3. More maps over the FD area are shown in Appendix.

4.3.1 Monthly accuracy

The monthly accuracy computed for H68 in comparison with DPR-NS product is shown in Figure 20 over land, sea, and overall areas in panel a), b) and c) respectively. In every panel, the background color indicates the region inside each requirement accuracy threshold. The black dotted line represents the mean FSE value over the whole period (12 months). Panel d shows the percentage contribution for different areas respect to the full dataset. Sea areas represent the most part of dataset (73%) respect to land (25%) and coast areas (2%).
As for the land, for most months, the accuracy is close to the target value. The same happens for the sea. Overall results show a mean accuracy value quite close to the target (150%).

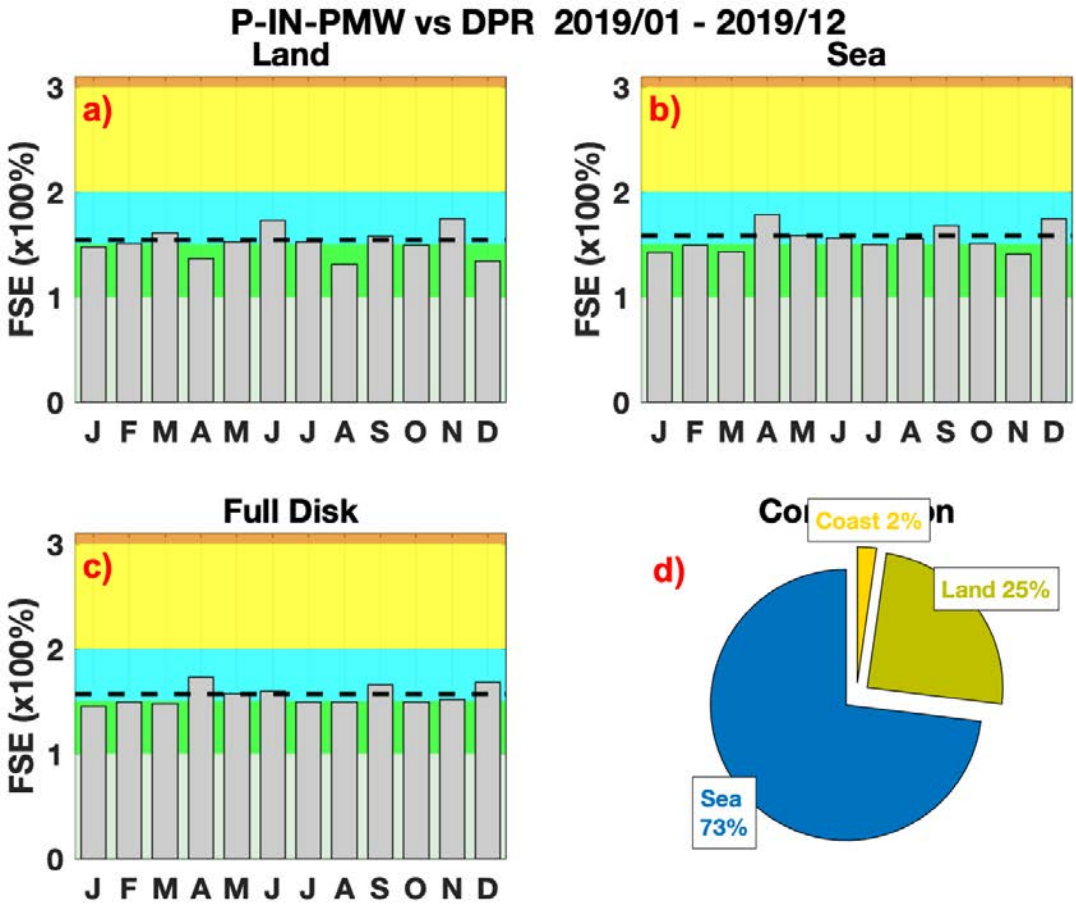

Figure 20: H68 monthly accuracy using DPR-NS as reference over Land (a) and Sea (b) H SAF extended areas. The Overall Q.A. is shown in the panel c). Background colours highlight the requirement accuracy thresholds in terms of FSE as reported in Table 7: Accuracy requirements for product P-IN-PMW in term of FSE(%). and Table 11. The horizontal black dotted line indicates the mean annual value. The single ground percentage contribution is shown in the panel d). Note: Coast is not shown.

4.3.2 Monthly continuous statistical scores

H68 monthly tendency over land (green line), coast (red line) and sea (blue line) areas for all rain rates above 1 mm/h is shown in Figure 21 for six continuous statistical scores (ME, SD, MAE, MB, RMSE and FSE). Results do not show a clear seasonal trend. Figures show as H68 tends to underestimate the precipitation in comparison with DPR: an average mean error close to -3 mm/h is evident for all surface types. More continuous statistical scores are shown in Appendix.

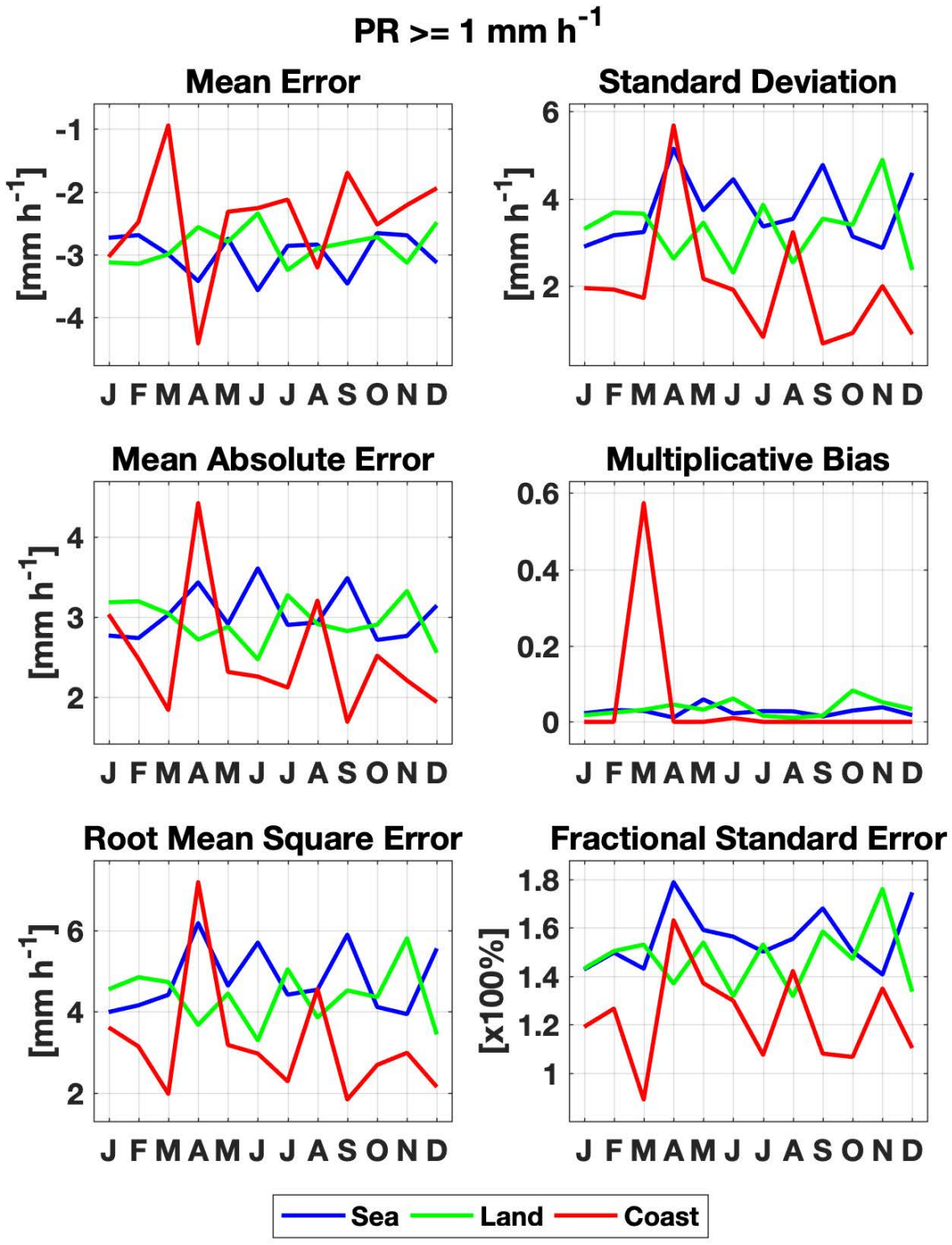

Figure 21: Monthly continuous statistical scores resulting for H68 vs DPR-NS over H SAF extended area relatively to the precipitation regime above 1 mm/h.

4.3.3 Analysis over different geographical areas

The analysis over different geographical areas is here shown. The full domain is divided over three regions: European area (36°N-66°N; 30°W-60°E), African area (36°S-36°N;30°W-60°E) and the rest part of the coverage namely "Ocean" (mainly oceans and Brazil). The spatial distribution of the 0.5°x0.5° DPR-H68 coincident grid boxes is shown in Figure 22.

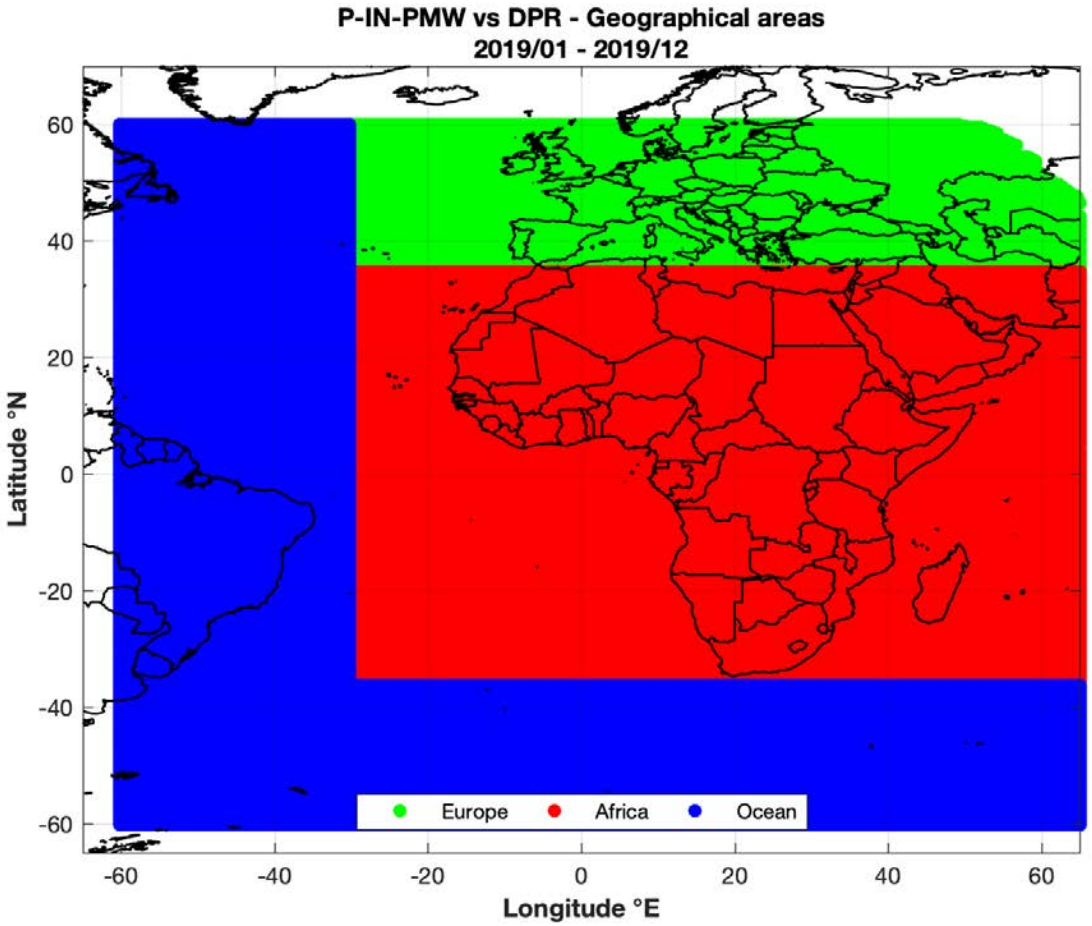

Figure 22: Spatial distribution of 0.5°x0.5° DPR-H68 intersection grid box over three geographical areas.

The tendency of the statistical scores calculated for different areas with respect to the DPR rain rates ranging between 0 and 5 mm/h are shown in Figure 23. In the panel on the left the numerosity of 0.5° x 0.5° grid boxes is displayed: the full dataset contains over $2x10^6$ data (for all DPR rainfall rates) and the number of intersections decreases up to $5x10^3$ grid boxes for rain rates above 5 mm/h. The FSE shown in the panel on the right highlights as over European area the result is better respect to all other regions. More detailed maps on the FSE distribution over FD area and over European and African areas are shown in Figure 24 and Figure 25.

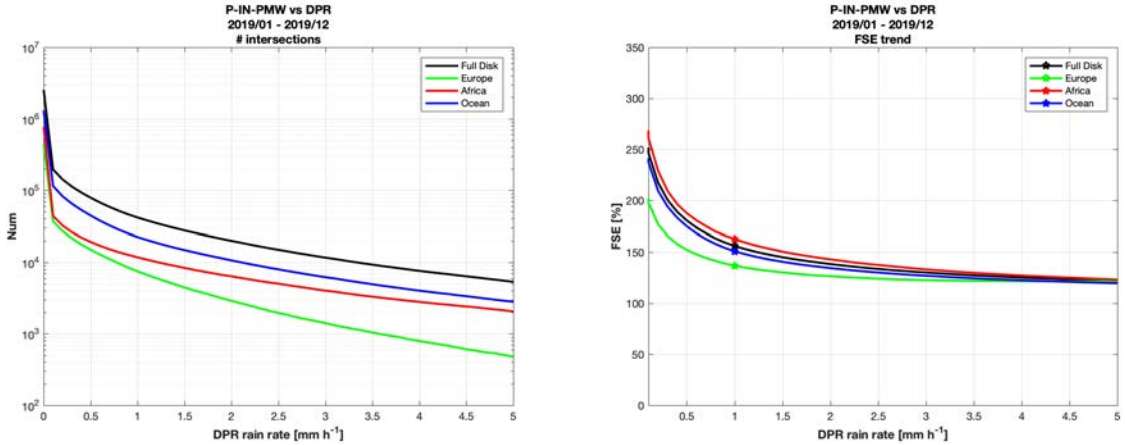

Figure 23: For different geographical areas: (on the left) number of intersection grid points between H68 and DPR as function of DPR rain rates; (on the right) the FSE score trend for various DPR rain rates.

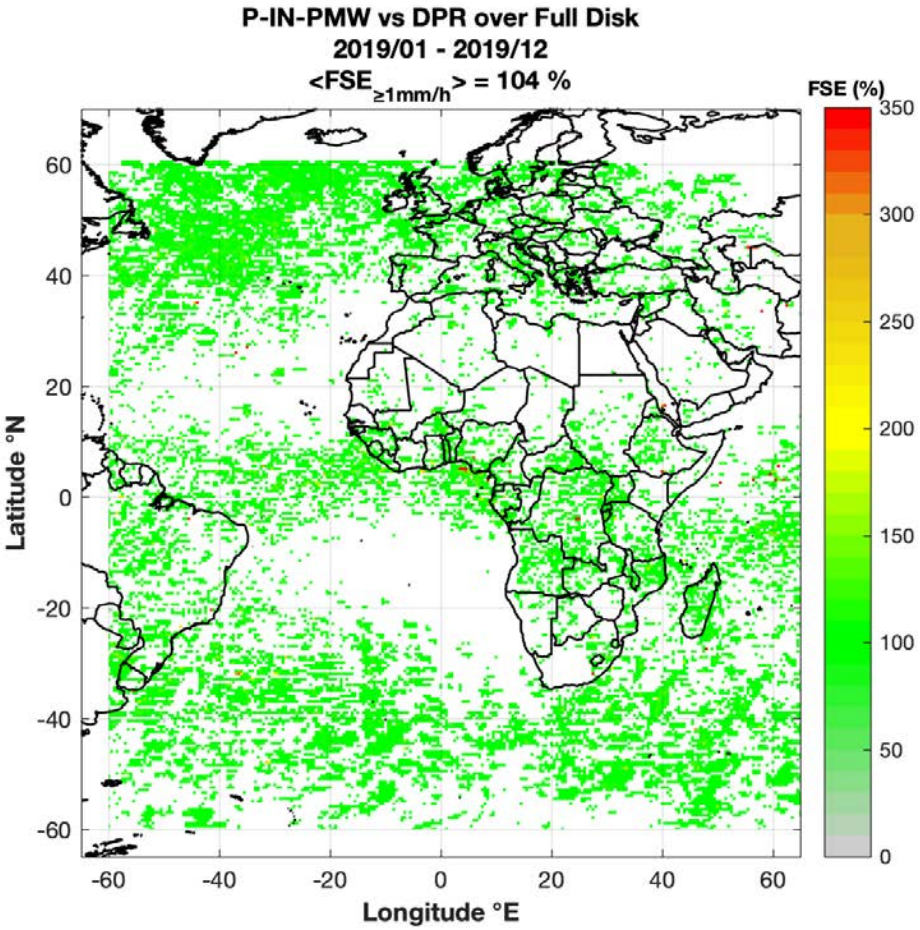

Figure 24: FSE map over FD area computed by comparison between H68 and DPR estimates over 1 year dataset. Note: FSE mean value indicated (104%) is computed as mean value of all grid points (and not as mean value of all data).

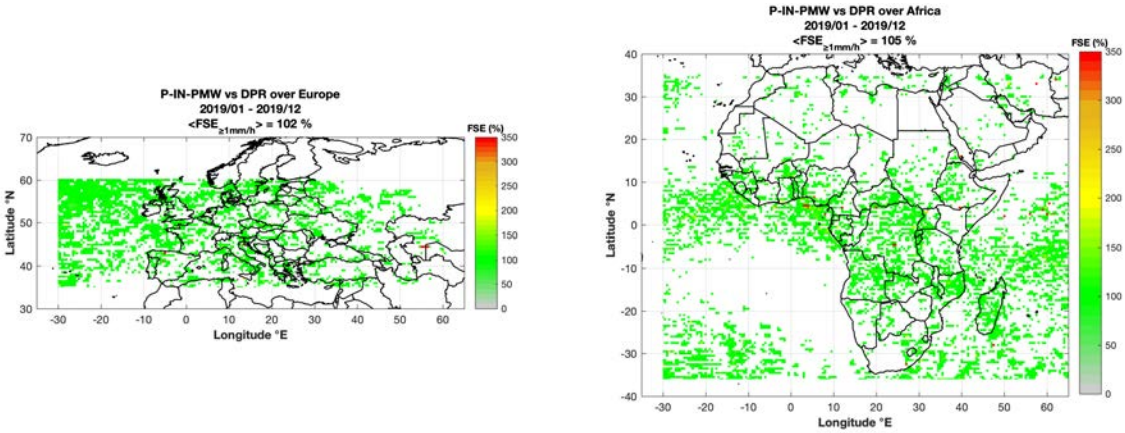

Figure 25: FSE map over EU area (on the left) and over African area (on the right) computed by comparison between H68 and DPR estimates over 1 year dataset. Note: FSE mean value indicated (102% and 105%) are computed as mean value of all grid points (and not as mean value of all data).

4.3.4 Product requirement compliance

The accuracy of H68 over FD area for the period between January and December 2019 is reported in Table 12. FSE score values for land and sea are between threshold and target and quite close to the target requirement (150%). Result over coast are even below the target. The resulting mean annual overall accuracy for H68 product over the MSG FD area reaches the value of 157%.

Between target and optimal	Between threshold and target	Threshold exceeded by < 50 %	Threshold exceeded by ≥ 50 %

H68 vs DPR	Annual average of FSE (%)						
Precipitation Class	**Requirement (FSE %)**			**Land**	**Sea**	**Coast**	**OVERALL**
	thresh	**target**	**optimal**				
≥ 1 mm/h	200	150	100	154	158	148	157

Table 12: Product requirement and compliance analysis for H68 in comparison with DPR-NS product.

5 Conclusions

The H68 (P-IN-PMW) product has been validated by the PPVG on the period of data January 2019-December 2019. Each Country/Team has provided long statistics analysis and case studies using ground data (radar and rain gauge) as reference following the common validation methodology reported in Appendix 1. A huge effort has been made in the development of the Unique Common Code (UCC) used by all members of the validation cluster to improve it. The use of a UCC guarantees that the results obtained by every partner are obtained in the same way.

A validation outside the European area was also performed. The Quality Assessment of H68 product was evaluated over the H SAF extended area in comparison with the DPR Normal Scan precipitation product estimated by DPR instrument onboard of GPM Core Observatory satellite. As for the UCC, the development of the validation procedure over full domain has involved the entire Validation Cluster. Results of comparison with DPR-NS product was obtained by Italian DPC and reported in this document.

It is well known that radar and rain gauge rainfall estimation is influenced by several error sources that should be carefully handled and characterized before using these data as reference for ground validation of any satellite-based precipitation products. Each Country/Team has independently evaluated the quality of its radar data to optimize the satellite data validation.

Much effort has been made to define a standard radar quality data. Rain gauge quality data has been standardized to all members by use of the same interpolation method (GRISO).

Different case study analysis of H68 have been here reported in section 3. Case studies, analysed in different geographical regions, highlight the behavior to slightly overestimate precipitation intensity and low success ratio to detect precipitation patterns.

In section 4 the validation results of the H68 long statistics analysis obtained for the entire period have been presented. To assess the degree of compliance of the product with product requirements, each Country/Team has provided the monthly statistical scores. The results have been showed using both European ground (radar and rain gauge) data and DPR-NS estimates as benchmark over land, sea and coast areas.

The results of the Precipitation Validation Programme are reported in this Product Validation Report (PVR). H68 reaches the target accuracy requirement in both validation procedures. Better performances are observed in comparison with ground measurements respect to the DPR estimates. The analysis for different geographical areas highlights as better performance is reached over European region. Contingency tables show as the no-rain is well estimated, while the light intensities are often underestimated. Finally, intermediate and heavy rainfall estimates are not always accurate.

END MAIN DOCUMENT

Appendix 1 Validation strategy, methods and tools

The quality assessment procedure, methodologies and instruments used to assess the performances of precipitation products are described in this chapter.

A1.1 Validation team and work plan

To evaluate the satellite precipitation product accuracy, a Validation Group has been established by the beginning of the Validation Phase in the H SAF project. The Precipitation Product Validation team is composed of experts from the National Meteorological and Hydrological Institutes of Belgium, Bulgaria, Germany, Hungary, Italy, Poland, Slovakia, and Turkey (Table 13). Hydrologists, meteorologists, and precipitation ground data experts, coming from these countries are involved in the product validation activities (Table 14).

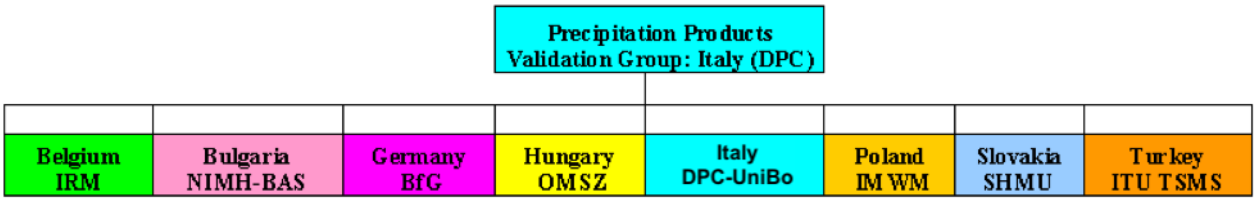

Table 13: Structure of the Precipitation products validation team.

Validation team for precipitation products			
Name	**Institute**	**Country**	**e-mail**
Silvia Puca (Leader)	Civil Protection Department (DPC)	Italy	silvia.puca@protezionecivile.it
Marco Petracca	Civil Protection Department (DPC) National Research Council (CNR - ISAC)	Italy	M.Petracca@isac.cnr.it
Alexander Toniazzo	Civil Protection Department (DPC)	Italy	alexander.toniazzo@protezionecivile.it
Alessandra Mascitelli	Civil Protection Department (DPC)	Italy	alessandra.mascitelli@protezionecivile.it
Gianfranco Vulpiani	Civil Protection Department (DPC)	Italy	gianfranco.vulpiani@protezionecivile.it
Emanuela Campione	Civil Protection Department (DPC)	Italy	emanuela.campione@protezionecivile.it
Pierre Baguis	Royal Meteorological Institute of Belgium (RMI)	Belgium	Pierre.Baguis@meteo.be
Emmanuel Roulin	Royal Meteorological Institute of Belgium (RMI)	Belgium	Emmanuel.Roulin@meteo.be
Eram Artinyan	National Institute of Meteorology and Hydrology (NIMH)	Bulgaria	eram.artinian@meteo.bg
Petko Tsarev	National Institute of Meteorology and Hydrology (NIMH)	Bulgaria	petko.tsarev@meteo.bg
Georgy Koshinchanov	National Institute of Meteorology and Hydrology (NIMH)	Bulgaria	georgy.koshinchanov@meteo.bg
Claudia Rachimow	Bundesanstalt für Gewässerkunde (BfG)	Germany	rachimow@bafg.de
Peter Krahe	Bundesanstalt für Gewässerkunde (BfG)	Germany	krahe@bafg.de
Márta Diószeghy	Hungarian Meteorological Service (OMSZ)	Hungary	dioszeghy.m@met.hu
Ildikó Szenyán	Hungarian Meteorological Service (OMSZ)	Hungary	szenyan.i@met.hu
Dóra Cséke	Hungarian Meteorological Service	Hungary	cseke.d@met.hu

	(OMSZ)		
Federico Porcu'	Department of Physics and Astronomy, University of Bologna (UniBo)	Italy	federico.porcu@unibo.it
Bozena Lapeta	Institute of Meteorology and Water Management (IMWM)	Poland	Bozena.Lapeta@imgw.pl
Rafal Iwanski	Institute of Meteorology and Water Management (IMWM)	Poland	Rafal.Iwanski@imgw.pl
Ján Kaňák	Slovenský Hydrometeorologický Ústav (SHMÚ)	Slovakia	jan.kanak@shmu.sk
Ľuboslav Okon	Slovenský Hydrometeorologický Ústav (SHMÚ)	Slovakia	luboslav.okon@shmu.sk
Mariàn Jurasek	Slovenský Hydrometeorologický Ústav (SHMÚ)	Slovakia	marian.jurasek@shmu.sk
Ladislav Méri	Slovenský Hydrometeorologický Ústav (SHMÚ)	Slovakia	ladislav.meri@shmu.sk
Ahmet Öztopal	Istanbul Technical University (ITU)	Turkey	oztopal@itu.edu.tr

Table 14: List of the people involved in the validation of H SAF precipitation products (PPVG)

The Precipitation products validation programme started with a first workshop in Rome, 20-21 June 2006, soon after the H SAF Requirements Review (26-27 April 2006). The first activity was to lay down the Validation plan, that was finalised as first draft early as 30 September 2006. After the first Workshop, other ones followed, at least one per year to exchange experiences, problem solutions and to discuss possible improvement of the validation methodologies. Often the Precipitation Product Validation workshop are joined with the Hydrological validation group.

The results of the Product Validation Programme are reported in this Product Validation Report (PVR) and are published in the validation section of the H SAF web page. A new structure and visualization of the validation section of H SAF web page is in progress to consider the user needs. This validation web section is continuously updated with the last validation results and studies coming from the Precipitation Product Validation Group (PPVG).

A1.2 Validation objects and issues

The products validation activity has to serve multiple purposes:

- to provide input to the product developers for improving calibration for better quality of baseline products, and for guidance in the development of more advanced products;
- to characterise the product error structure in order to enable the Hydrological validation programme to appropriately use the data;
- to provide information on product error to accompany the product distribution in an open environment, after the initial phase of distribution limited to the so-called “beta users”.

Validation is a challenging task in the case of precipitation, both because the sensing principle from space is very much indirect, and because of the natural space-time variability of the precipitation field (sharing certain aspects with fractal fields), that poses severe sampling problems.

It is known that an absolute ‘ground reference’ does not exist. In the H SAF project the validation is based on comparisons of satellite products with **European ground data**: radar, rain gauge and radar integrated with rain gauge. During the Development phase some main problems have been pointed out. First of all, the importance to characterize the error associated to the ground data used by PPVG. Secondly to develop software for all steps of the Validation Procedure, a software

available to all the members of the PPVG. The radar and rain gauge Working Group (WG) have been composed to solve these problems.

In CDOP-3, with the release of more than 30 products **over the MSG full disk area,** the Validation Cluster had to develop new methodologies to compare precipitation estimates on almost global area coverage. The Associated Scientist analysis (H_AS16_03 DPC/CNR-ISAC 2016) has been identified the DPR (Dual-frequency Precipitation Radar) onboard of GPM-CO (Global Precipitation Measurement – Core Observatory) satellite as worthy instrument reference for the estimation of instantaneous precipitation on a global scale. In particular, the 2A-DPR NS V05 (**DPR**) was considered as most suitable product for potential use within the H SAF Precipitation Product Validation activity **for instantaneous precipitation estimates.** For more details, refer to Sebastianelli, 2017.

For accumulated precipitation products, instead, the Triple Collocation (**TC)** methodology (Brocca et al., 2014) was used to perform the validation activity. TC requires the simultaneous availability of three products with mutually uncorrelated errors with similar spatial coverage, resolution and accumulation time.

In the following three sections, the validation methodologies and data used as reference to perform the comparisons are described.

A1.3 Validation methodology respect to GROUND reference data

From the beginning of the project it was clear the importance to define a common validation procedure in order to make the results obtained by several institutes comparable and to better understand their meanings. The main steps of this methodology have been identified during the development phase inside the validation group, in collaboration with the product developers, and with the support of ground data experts. This common procedure has given rise to a single common code for all members of the PPVG, named Unique Common Code (UCC). This common validation methodology is based on ground data (radar and rain gauge) comparisons to produce **large statistic** (multi-categorical and continuous), and **case study analysis.** Both components (large statistic and case study analysis) are considered complementary in assessing the accuracy of the implemented algorithms. Large statistics helps in identifying existence of pathological behaviour, selected case studies are useful in identifying the roots of such behaviour, when present.
The main steps of the validation procedure are:

- ground data error analysis: radar and rain gauge;
- point measurements (rain gauge) spatial interpolation;
- up-scaling of radar data versus satellite grid (radar data gridded on satellite grid);
- temporal comparison of precipitation products (satellite and ground);
- statistical scores (continuous and multi-categorical) evaluation;
- case study analysis.

Ground data and tools used for validation

Both rain gauge and radar data have been used for H SAF product validation. Working groups have been set up to solve specific items in the validation procedure and to develop a common software. A complete knowledge of the ground-based data characteristics, used within the PPVG, was the first

step necessary to define the procedure to select the most reliable data (ground reference) and to understand the validation results.

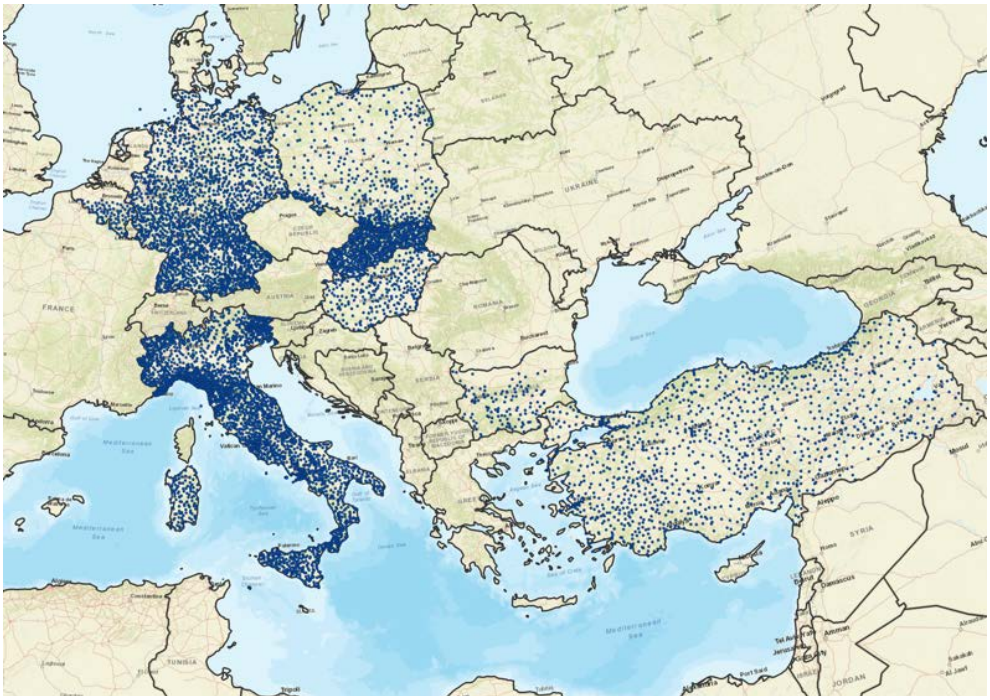

Figure 26: The network of 8,404 rain gauges used for H SAF precipitation products validation

The rain gauge networks of PPVG is composed of approximately 8400 stations across 8 Countries (Figure 26). A key characteristic of such networks is the distance between each raingauge and the closest one, averaged over all the instruments considered in the network and it is a measure of the raingauge density. Instruments number and density are summarized in the following Table 3.

Country	Total number of gauges *	Average minimum distance (km)
Belgium	92	15.2
Bulgaria	123	25.2
Germany	2,299	12.9
Hungary	270	17.0
Italy	2,934	11.3
Poland	540	24.0
Slovakia	911	13.6
Turkey	1,235	26.5

*** the number of raingauges could vary from day to day due to operational efficiency within a maximum range of 10-15%.**

Table 15: Number and density of raingauges within H SAF validation Group

Most of the gauges used in the National networks by the PPVG Partners are of the tipping bucket type, and hourly cumulated.

74 C-band radars (Figure 27**)** are used by the H SAF PPVG for assessing the satellite product accuracy. An inventory on radar data networks and products used in PPVG has pointed out that all the institutes involved in the PPVG declared the system are kept in a relatively good status and all

of them apply some correction factors in their processing chain of radar data. Only the radar data, which passes the quality control of the owner Institute, are used by the PPVG for validation activities. Please note that the Validation procedure is the same for all countries of PPVG.

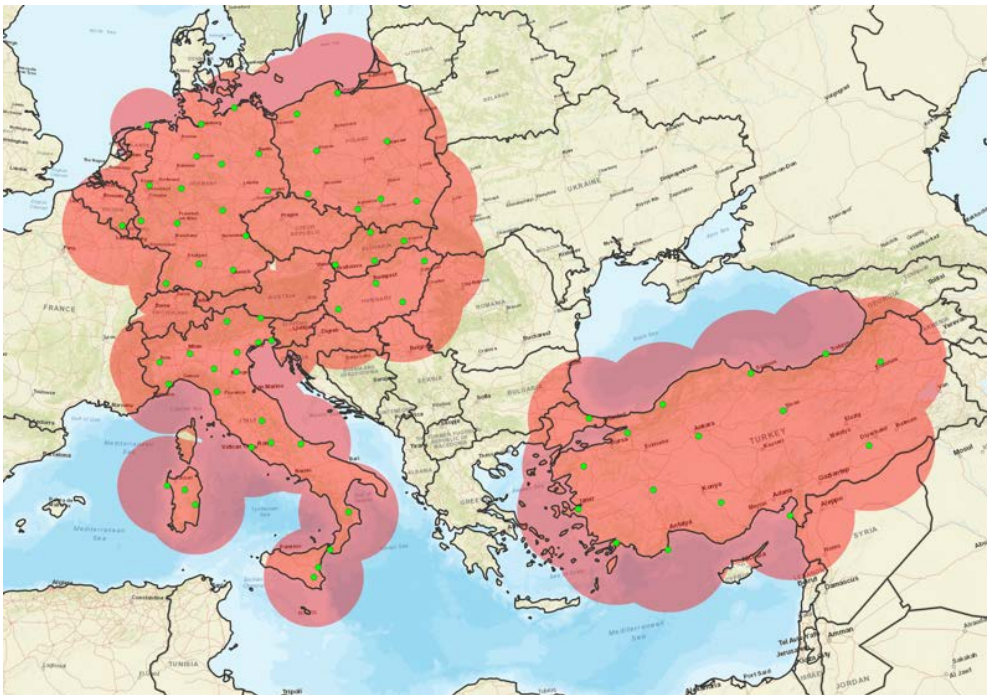

Figure 27: The networks of 74 C-band radars used by the H SAF PPVG.
Note1: Turkish radars are not used in validation activities. Note2: Only one out of four belgian radars is shown.

Instruments number and average minimum distance in each country are summarized in Table 16.

Country	Total number of radar	Average minimum distance (km)
Belgium	4	120
Bulgaria	-	-
Germany	16	163
Hungary	4	190
Italy	22	141
Poland	8	186
Slovakia	4	137
Turkey	16*	253

Table 16: Number and density of radars used by the H SAF PPVG.
*** Not used in validation activities.**

Common procedure for the validation

The UCC developed by PPVG during CDOP-2 and improved in CDOP-3 has been used to validate satellite data respect to radar and rain gauge data considered as ground reference.

Common procedure for the validation with RADAR data

Selection of satellite pixels falling into the region of interest

In order to avoid time-consuming useless calculation, every country restricts the validation to a specific Area of Interest (normally the area covered by the RADAR data of the country), which is detected implicitly by the common validation algorithm.

Taking into account quality index information
The UCC considers the quality index for each radar pixel. It depends mainly by distance from radar site and by interferences or beam-blocking. Each country independently calculates the quality of its data. This quality information is used for validation purposes since CDOP2.

Selection of the RADAR data time-synchronous with the satellite ones
The RADAR data whose temporal characteristics are congruent with the data of the satellite product to be compared (instantaneous or mean value or daily cumulated) are selected. For instantaneous acquisitions, the maximum time difference allowed for satellite comparison is 10 minutes.

Up-scaling of RADAR data at the product satellite resolution
Radar data, whose spatial resolution (0.25 ÷ 1 km) is typically greater than satellite products (5 ÷ 25 km), is rescaled to the satellite product grid (we refer it as "radar upscaled"). The information on the radar data density for each grid point is kept in order to eliminate those grid points that are not representative of the radar data (whose spatial coverage is limited or less than 50%).

Calculation of corresponding satellite and RADAR rainfall values
For each single satellite file, a separate up-scaling procedure reads the look up table and assigns to each satellite pixel the RADAR rainfall average calculated from the values of the radar pixels belonging to the satellite pixel in the look-up table.
Averaging is simply arithmetical as investigations so far have shown that the averaging method does not have an impact on the statistical scores.
The flag indicating if the satellite pixel is coast, land or sea is matched to each satellite-radar data pair calculated in this step.

Common procedure for the validation with RAIN GAUGE data

Selection of satellite pixels falling into the region of interest:
In order to avoid time-consuming useless calculation, every country restricts the validation to a specific Area of Interest (normally the area covered by the rain gauge data of the country), which is detected implicitly by the common validation algorithm.

Selection of rain gauge data synchronous with the satellite ones
Gauges with different cumulation intervals are considered, and if the interval is longer than the time resolution of the product (15 or 30 minutes), more satellite images are averaged. For H68 product two consecutive images (2 x 30' every image) are summed for comparing with one-hourly accumulated gauges.

Interpolation of the rain gauge data:
All partners of the Validation Group have been used the same interpolation technique, named GRISO (a like-Kriging interpolation technique for rain gauge data, Pignone et al. 2010; Feidas et al. 2018), to get spatially continuous rainfall maps (over 5x5 km grid) from individual gauge measurements.

The GRISO technique is the interpolation method chosen for the common validation.

Taking into account quality index information
GRISO technique produces a quality index map for each instantaneous acquisition as function of distance from each rain gauge station. This quality information was used for validation purposes in CDOP2.

Matching between satellite and rain gauge data:
The satellite data is matched with the rain gauge interpolated grid using the nearest-neighbor method.

A1.4 Validation methodology of INstantaneous precipitation products over Full Disk coverage

As the validation with respect to ground data, even this methodology was developed in communion with European experts belonging to the VC. But, differently from the first one, this is not performed by all countries but only by Italian DPC because all DPR products over global area are freely available from GPM website. All instantaneous satellite precipitation products, with extension area over FD area, are evaluated following these main steps:

- regridding of DPR and H SAF data versus a regular 0.5° equi-distance grid;
- temporal and spatial matching between precipitation products;
- statistical scores (continuous and multi-categorical) evaluation;

The methodology, as the previous one, produces **large statistic** (multi-categorical and continuous) scores.

DPR products used for validation
The spatial coverage of both rain gauge and ground radar networks is not suitable to detect precipitation on a global scale. At the contrary, satellite observations provide estimates on a synoptic scale, although there are some issues related to their accuracy. It was discussed in the Visiting Associated analysis in comparison with ground radar network (Sebastianelli, 2017). The DPR is a Dual frequency Precipitation Radar located on board of the GPM Core Observatory (Figure 28). It uses the Ka (~35 GHz) and Ku bands (~13 GHz) to construct three-dimensional precipitation and drop size distribution maps. The GPM Core Observatory (Figure 28) flies in a non-sun-synchronous orbit at 65° inclination to cover a larger latitudinal extension with respect to the TRMM orbit, which extended from 35°S to 35°N. Both Ku- and Ka-band radars perform cross-track type scans (perpendicular to the direction of the satellite motion) estimating the precipitation during the day and the night over land and ocean. The Ku-band radar performs a normal scan (NS) acquisition mode that is composed by 49 footprints (IFOV) of 5 km in diameter. In fact, away from the scanning center, footprints tend to widen and overlap (edge effects) because of a geometric distortion. The term swath indicates the width of each scan of 245 km. The range resolution is 250 m. The Ka-band radar can perform a matched scan (MS) or a high sensitivity scan (HS) acquisition mode. The MS footprints match the central 25 footprints of the Ku-band and the range resolution is 250 m. Therefore, MS scan is composed of 25 footprints of 5 km in diameter and the swath is 125 km. When Ka-band radar operates in HS mode footprints are interlaced with the matched beams, the range resolution is 500 m and there are 24 footprints along a swath. Figure shows the different DPR scanning modes with respect the flight direction.

It must to be noted that the range resolution is different from the spatial resolution. In fact, the sampling is carried out for 19 km above the sea level and then along the vertical there are many footprints of 250 m height (range resolution). In addition, footprint size decreases as the sampling height increases due to the antenna aperture. The sampling distance between the centers of two adjacent footprints is 5.2 km, and it is constant throughout the scan to the edges. Apart the other problems which affects the DPR estimates, the main issues deal with the attenuation and the ground clutter. The K-band radar estimates are affected by attenuation when they sample through very intense precipitations (convective cells). Ground clutter is a non-meteorological echo which causes an overestimate of precipitations.

DPR products (level 2A) referred to single frequency radar are 2A-Ku, 2A-Ka-MS and 2A-Ka-HS, as showed in Figure 29. Three different DPR products combining Ka and Ku bands precipitation rate estimates (prEs) also exist depending on the IFOV to which data are referred. The IFOV can be related to the NS Ku-band, or to the MS or HS Ka-band, and the corresponding DPR products for prEs are 2A-DPR-NS, 2A-DPR-MS and 2A-DPR-HS, respectively. Results of Visiting Associated activity (Sebastianelli, 2017) highlight as 2A-DPR-NS product performs better with respect to ground-based radar estimates. For this reason, the prEs by 2A-DPR-NS product (hereafter also referred as DPR-NS) was used as precipitation reference to validate the H SAF satellite precipitation products.

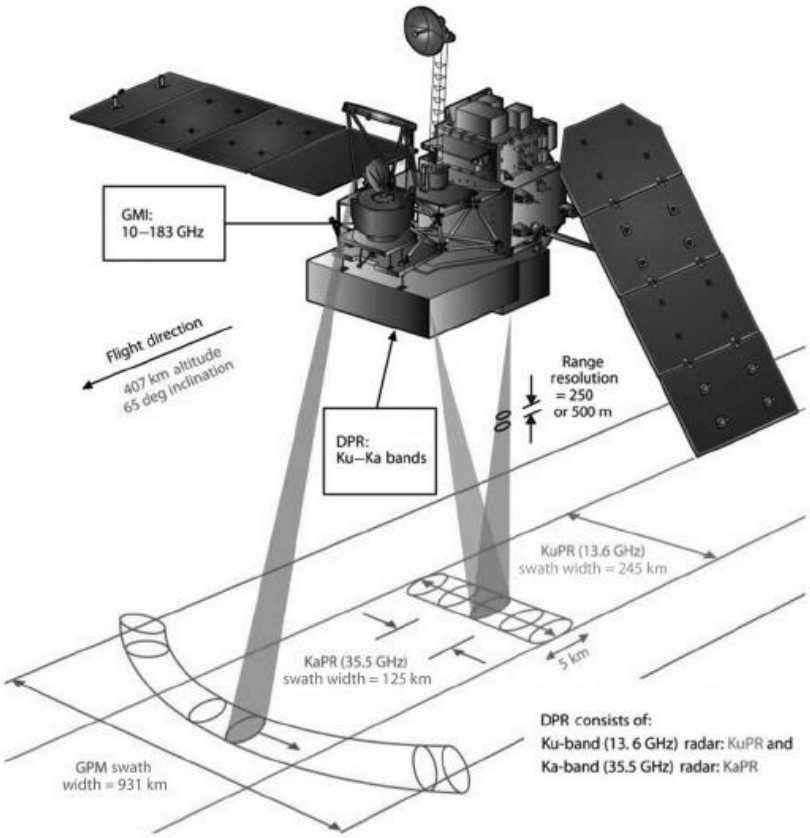

Figure 28: The GPM Core Observatory and the GMI and DPR ground tracks.

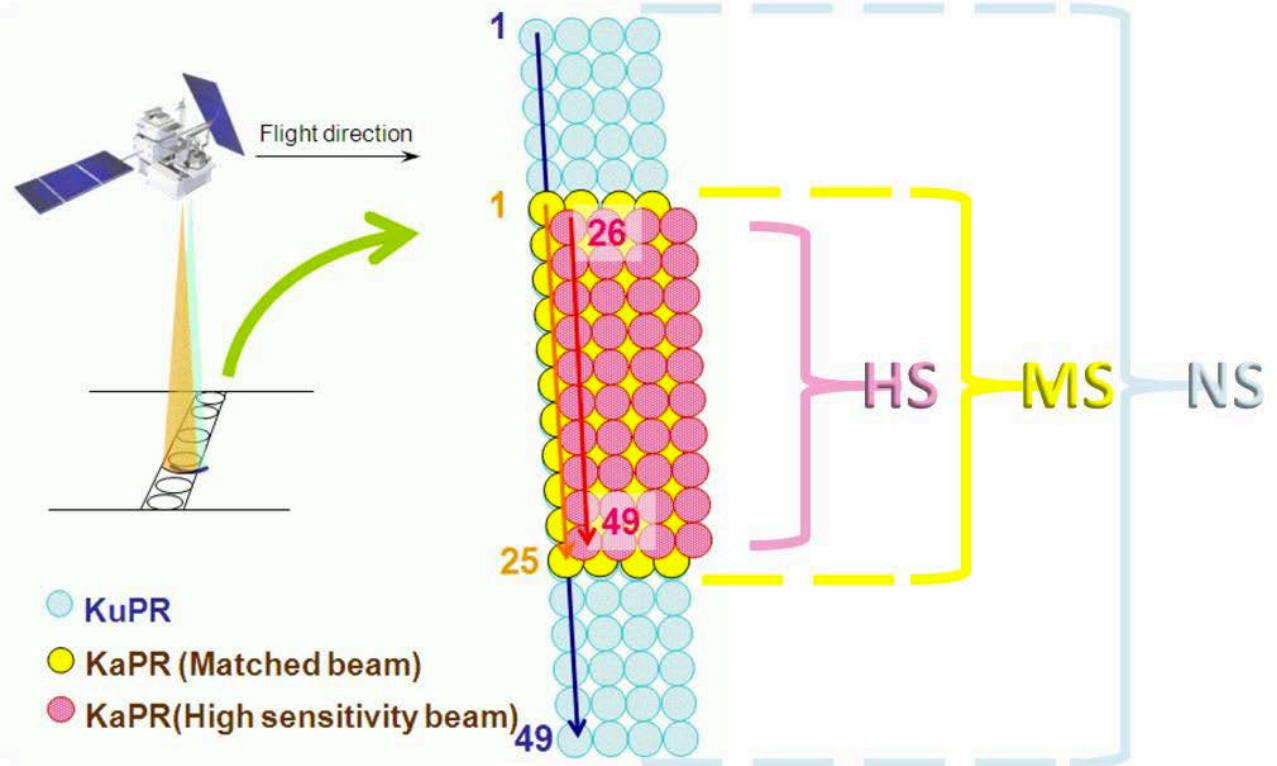

Figure 29: Different DPR scanning modes with respect to the flight direction. The Normal Scan corresponds to Ka-band radar, whereas matched and high sensitivity scans are performed by Ka-band radar.

Common procedure for the validation with DPR-NS

The comparison between DPR-NS and H SAF precipitation products is performed following the procedure below described.

Selection of synchronous data (first check)

Both DPR and H SAF filenames contain the start and finish time. Only files with consistent time intervals are considered and evaluated to avoid time-consuming useless computation.

Data re-gridding over regular grid

Both, DPR and H SAF data are re-gridded over the same equi-distance 0.5° grid. All satellite parameter (continuous) values are averaged over the new grid cell. For discrete parameters (such as sea/coast/land flag or precipitation phase flag) the most frequent value is considered.

Temporal and spatial matching between the two regridded data

DPR and H SAF gridded data are temporal- and spatial- matched. Only overlapping grid cells with maximum time difference within ±15 minutes (from the average time of validity of the H SAF product) are stored and evaluated for statistical score analysis.

A1.5 Validation methodology of ACcumulated precipitation products over Full Disk coverage

In order to assess the quality of accumulated precipitation products over FD area the new TC methodology analysis was successfully tested by Brocca et al. (2014). This technique requires three wholly independent rainfall datasets on global scale without the availability of ground-based rainfall accumulation data.

Given three estimates of the same variable, the main assumptions of the TC method are the (i) stationarity of the statistics, (ii) linearity between the three estimates (vs. the same target) across all timescales and (iii) existence of uncorrelated error between the three estimates.
TC provides error and correlations of three products if each of the ones is afflicted by mutually independent errors.

The main steps of the TC validation procedure are:

- temporal (daily) and spatial (0.5° x 0.5° grid) matching between three precipitation datasets;
- TC main procedure;
- statistical scores (continuous and multi-categorical) evaluation;

The methodology, as the previous one, produces **large statistic** (multi-categorical and continuous) scores.

For more details on the TC main procedure, see the H SAF Visiting Scientist Final Report titled "Leveraging coincident soil moisture and precipitation products for improved global validation of satellite-based rainfall products" by Chen F. and Crow W. T. : https://hsaf.meteoam.it/VisitingScientist/GetDocument?fileName=Final_Report_H_AS18_04.pdf

Data and products used

In this analysis, TC is applied to the rainfall accumulation estimates derived from H SAF satellite product and by GPCC (Global Precipitation Climatology Centre, https://climatedataguide.ucar.edu/climate-data/gpcc-global-precipitation-climatology-centre) and GLDAS (Global Land Data Assimilation System, https://ldas.gsfc.nasa.gov/gldas) projects.

GPCC

The GPCC provides gridded gauge-analysis products derived from quality-controlled station data. In this analysis is used the GPCC First Guess Daily Product (hereafter named as GPCC): daily global land-surface precipitation based on the station database (SYNOP) available via the Global Telecommunication System (GTS) of the World Meteorological Organization (WMO) at the time of analysis (3 - 5 days after end of the analysis month). This product contains the daily totals for a month on a regular latitude/longitude grid with a spatial resolution of 1.0° x 1.0° latitude by longitude. Interpolation is made for the daily relative quota of the monthly total, i.e., the daily total divided by the monthly total, the latter has the DOI:**10.5676/DWD_GPCC/FG_M_100**. The temporal coverage of the dataset ranges from January 2009 to the most recent month for which GTS based SYNOP data is available, i.e. the previous month, 3-5 days after its completion. In Figure 30 is shown an example of spatial extension and resolution of the GPCC product.

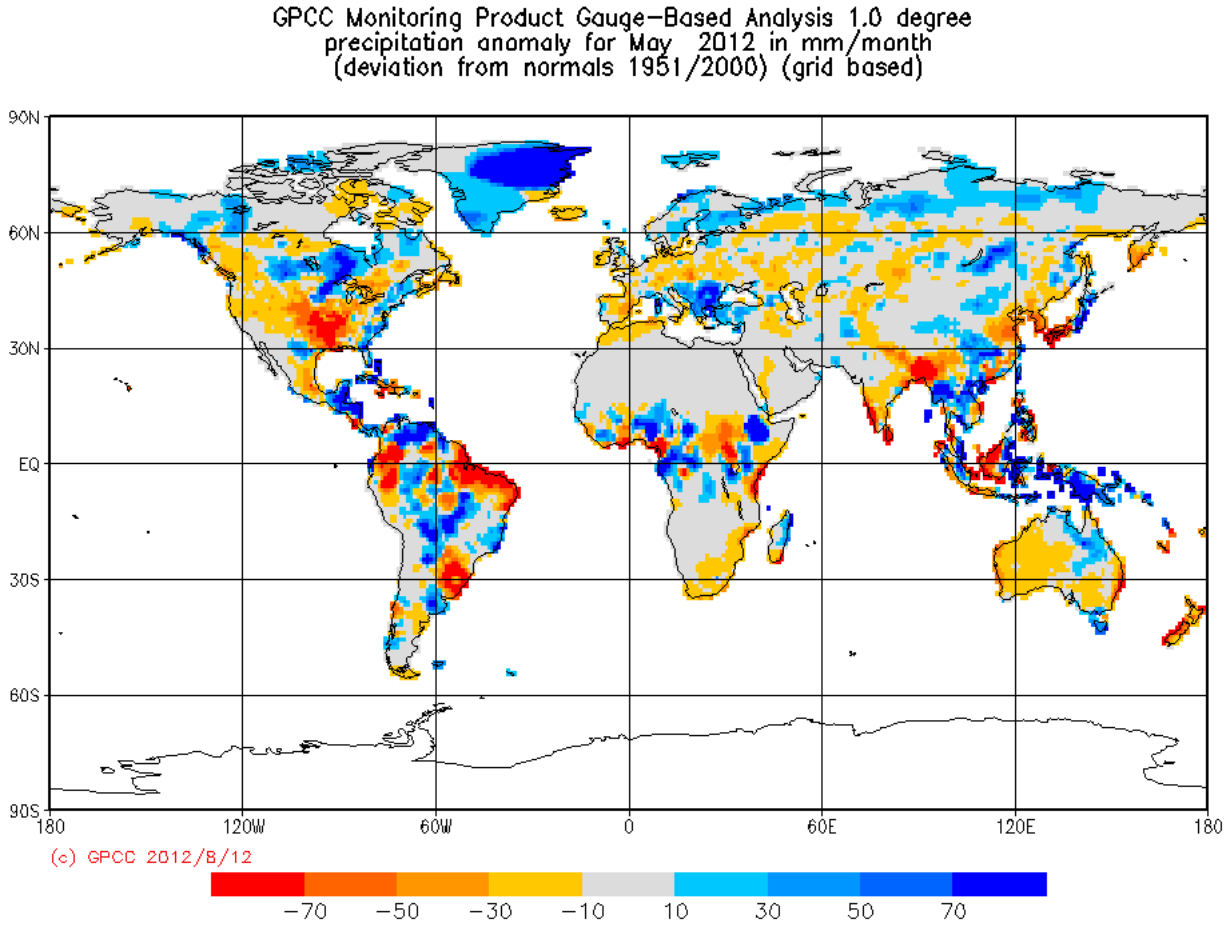

Figure 30: Example of data available in GPCC. The daily precipitation data used in TC methodology have the spatial extent as shown in the figure and the spatial resolution of 1.0 degree

GLDAS

NASA Global Land Data Assimilation System Version 2 (GLDAS-2) has three components: GLDAS-2.0, GLDAS-2.1, and GLDAS-2.2. GLDAS-2.0 is forced entirely with the Princeton meteorological forcing input data and provides a temporally consistent series from 1948 through 2014. GLDAS-2.1 is forced with a combination of model and observation data from 2000 to present. GLDAS-2.2 product suites use data assimilation (DA), whereas the GLDAS-2.0 and GLDAS-2.1 products are "open-loop" (i.e., no data assimilation). The choice of forcing data, as well as DA observation source, variable, and scheme, vary for different GLDAS-2.2 products.

The 3-hourly data product was simulated with the Noah Model 3.6 in Land Information System (LIS) Version 7 (https://lis.gsfc.nasa.gov/sites/default/files/LIS/public_7_3_releases/LIS_usersguide.06-dec-2021.pdf). The data product contains 36 land surface fields from January 2000 to present. In this analysis GLDAS-2.1 data are used. These data are archived and distributed in NetCDF format (DOI:10.5067/E7TYRXPJKWOQ). In Figure 31 is shown an example of spatial extension and resolution of the GLDAS product used.

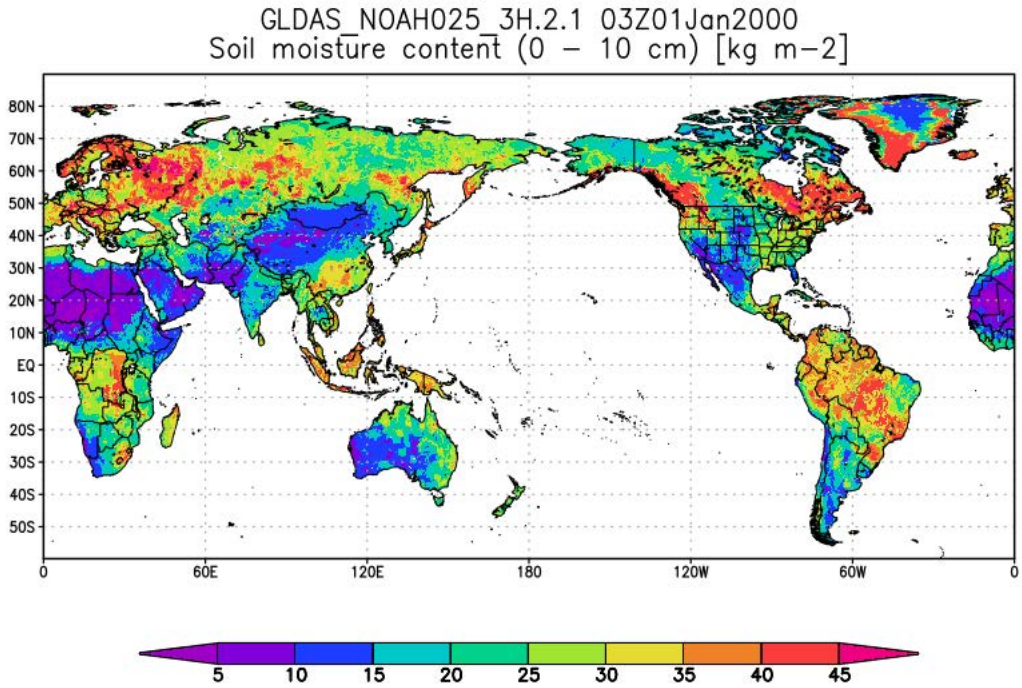

Figure 31: Example of data available in GLDAS. The 3-hourly precipitation data used in TC methodology have the spatial extent as shown in the figure and the spatial resolution of 0.25 degree

GLDAS 2.1 uses GPCC observations via the ingestion of the disaggregated Global Precipitation Climatology Project (GPCP) V1.3 Daily Analysis precipitation fields. In order to assess whether this has an impact on the TC analysis, pixel-based cross-correlated errors between GPCC and GLDAS by quadruple collocation (QC) analysis have been calculated (Perdicca et al., 2015, Gruber et al., 2016) using GPCC first guess data, GLDAS 2.1, ERA5 and SM2RAIN-ASCAT derived daily rainfall at the global scale. QC is a viable way to estimate the cross-correlated errors between two of the datasets included in the quadruplet (see Chen et al. 2020).

The analysis has been carried out at 0.25° of spatial resolution for the year 2017. Despite the use of a single year, the analysis shows that cross correlated errors between GPCC and GLDAS are very low (R=0.05 in median). If we zoom over the H SAF Extended Area (HEA) the median value decreases to 0.044 (see Figure 32 and Figure 33). In the inset it is reported the histogram of the R-values, showing how most of the pixels provided very low values of error correlation. This point should assure the independence of the datasets used for performing the analysis and thus, should allow to use TC analysis for validating H SAF products not only over the HEA, but also at the global scale.

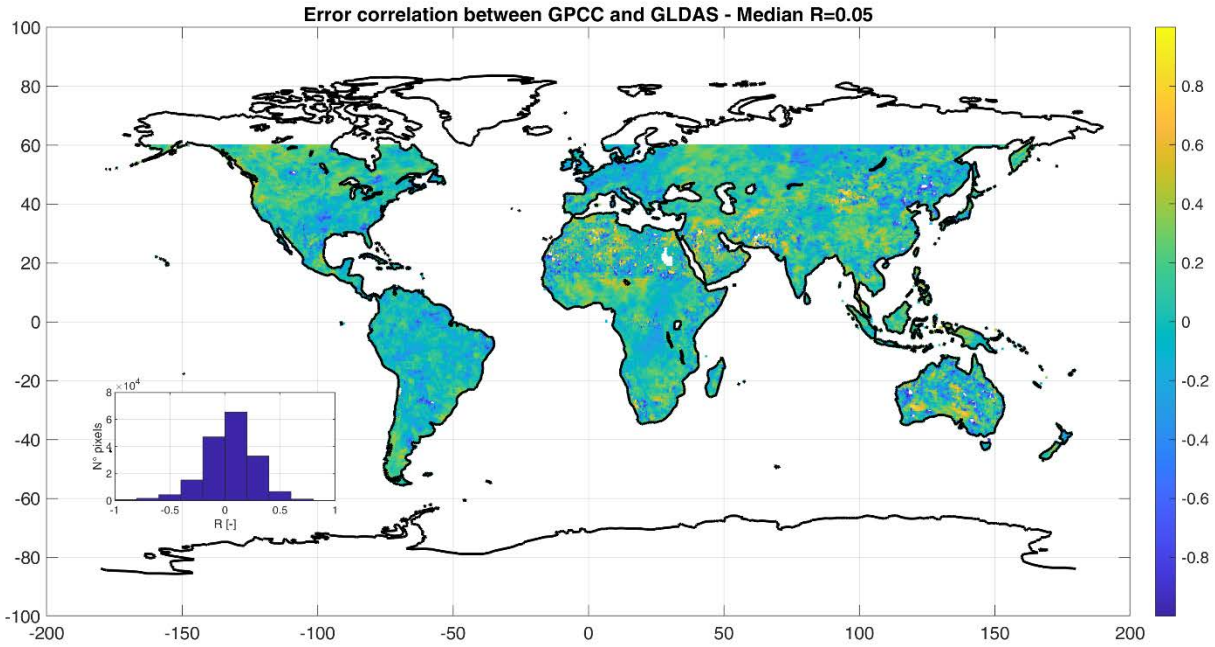

Figure 32: Cross correlated errors between GPCC and GLDAS over global scale for the year 2017.

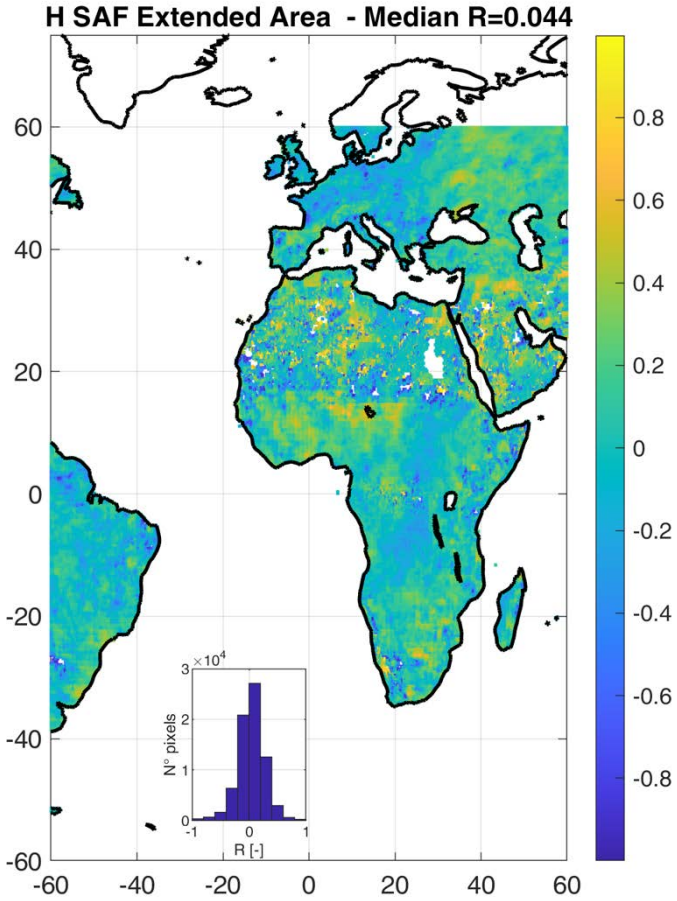

Figure 33: Cross correlated errors between GPCC and GLDAS over H SAF extened area for the year 2017.

A1.6 Large statistic

The large statistical analysis allows to point out the existence of pathological behavior in the satellite product performance. The application of the same validation technique step by step is guaranteed in all institutes take part of the PPVG and in both validation methodologies above described.

The large statistical analysis in PPVG is based on the evaluation of monthly and seasonal ***Continuous verification*** and ***Multi-Categorical*** statistical scores on one full year of data. It was decided to evaluate both continuous and multi-categorical statistics to give a complete view of the error structure associated to the H SAF product. Since the accuracy of precipitation measurements depends on the type of precipitation or, to simplify matters, on the intensity or accumulated precipitation, the verification is carried out on three precipitation classes (for accumulated precipitation products) as descripted in Table 17: Classes for evaluating cumulated precipitation products.

Accumulated Precipitation Classes (CR)	1	2	3
	≥ 1 mm/daily	≥5 mm/ daily	≥ 10 mm/ daily

Table 17: Classes for evaluating cumulated precipitation products

The impact of different background is also considered in the product performances. Statistical scores are separately computed for land, sea and coast areas. The Precipitation Product Validation Leader collects all validation results as computed by European institutes, verifies the consistency of these results and evaluates the monthly and seasonal common statistical results as reported in Chapter 4.

Continuous statistics

Continuous statistics are provided for each month and season of assessment. The main statistical scores are here listed:

Score	*Acronym*	*Range*	*Perfect score*	*Calculation*
Number of Satellite samples	NS	N.A.	N.A.	N.A.
Number of Reference (radar/rain gauge) samples	N	N.A.	N.A.	N.A.
Mean Error or Bias	ME	- ∞ to ∞	0	$ME = \frac{1}{N}\sum_{k=1}^{N}(sat_k - obs_k)$
Mean Absolute Error	MAE	0 to ∞	0	$MAE = \frac{1}{N}\sum_{k=1}^{N}\lvert sat_k - obs_k \rvert$
Standard Deviation	SD	0 to ∞	0	$SD = \sqrt{\frac{1}{N}\sum_{k=1}^{N}(sat_k - obs_k - ME)^2}$
Multiplicative Bias	MB	- ∞ to ∞	1	$MB = \frac{\frac{1}{N}\sum_{1}^{N} sat_K}{\frac{1}{N}\sum_{1}^{N} obs_K}$

Score	*Acronym*	*Range*	*Perfect score*	*Calculation*
Correlation Coefficient	CC	- 1 to 1	1	$CC = \frac{\sum_{k=1}^{N}(sat_k - \overline{sat})(obs_k - \overline{obs})}{\sqrt{\sum_{k=1}^{N}(sat_k - \overline{sat})^2 \sum_{k=1}^{N}(obs_k - \overline{obs})^2}}$
Root Mean Square Error (or Root Mean Square Difference)	RMSE	0 to ∞	0	$RMSE = \sqrt{\frac{1}{N}\sum_{k=1}^{N}(sat_k - obs_k)^2}$
Fractional Standard Error (%)	FSE	0 to ∞	0	$FSE = [RMSE / \overline{obs}] *100\%$

Table 18: Continuous statistical scores

In the Table 18:
- N represents the total number of observation samples and equivales to all satellite/observation pairs for computing all the statistical scores;
- NS indicates the number of product satellite estimates with given characteristics (e.g.; with estimated rain rate > 1 mm/h);
- the index "k" represents the spatial and temporal grid point at the scale of the common reference grid;
- *obs* and *sat* stand for rainfall value acquired by reference observations and satellite estimations, respectively.

The FSE score represents the accuracy for H SAF satellite precipitation products. The User requirements thresholds are below indicated:

Accuracy for CR ≥ 1 mm/daily		
Threshold	Target	Optimal
FSE% = 200%	FSE% = 150%	FSE% = 100%

Table 19: Precipitation products user requirements (UR)

The FSE score is not appropriate to define the accuracy in the TC methodology. In this case the Correlation Coefficient (CC) is used to define the product accuracy with thresholds as below indicated:

Accuracy for all precipitation rates (CR ≥ 0 mm/daily)		
Threshold	Target	Optimal
CC = 0.50	CC = 0.65	CC = 0.80

Table 20: UR for accumulated precipitation products using TC methodology

Multi Categorical statistics

Multi categorical statistics are derived by the following contingency table:

		Observation		
		yes	**no**	**total**
	yes	hits	false alarms	forecast yes

Satellite	no	misses	correct negatives	forecast no
	total	observed yes	observed no	total

Table 21: Multi-categorical statistics contingency table

where:
hit: $Sat_k \geq R_{th}$ and $Obs_k \geq R_{th}$
miss: $Sat_k < R_{th}$ and $Obs_k \geq R_{th}$
false alarm: $Sat_k \geq R_{th}$ and $Obs_k < R_{th}$
correct negative: $Sat_k < R_{th}$ and $Obs_k < R_{th}$
$\mathbf{R_{th}}$ is the threshold between the "rain" and "no rain" conditions. The scores evaluated from the contingency table are:

Score	Acronym	Range	Perfect score	Calculation
Probability Of Detection	POD	0 to 1	1	$POD = \frac{hits}{hits + misses} = \frac{hits}{observed\ yes}$
False Alarm Rate	FAR	0 to 1	0	$FAR = \frac{false\ alarms}{hits + false\ alarms} = \frac{false\ alarms}{forecast\ yes}$
Critical Success Index	CSI	0 to 1	1	$CSI = \frac{hits}{hits + misses + false\ alarm}$

Table 22: Multi-categorical statistics scores

A1.7 Case study analysis

Each institute, in addition to the large statistics verification, produces a case study analysis based on ***the knowledge and experience of the institute itself***, following a standard format as below reported. The institute decides whether to use ancillary data such as lightning data, SEVIRI images, the output of numerical weather prediction and nowcasting products.

The main sections of the standard format are:

- description of the meteorological event;
- comparison of ground data and satellite products;
- visualization of ancillary data;
- discussion of the satellite product performances;
- indication on the ground data (if requested) availability into the H SAF project.

Case study analysis are reported in Chapter 3.

References

Chen, F., Crow, W.T., Ciabatta, L., Filippucci, P., Panegrossi, G., Marra, A.C., Puca, S., Massari, C., 2020. Enhanced large-scale validation of satellite-based land rainfall products. Journal of Hydrometeorology 1. https://doi.org/10.1175/JHM-D-20-0056.1

Feidas, H., F. Porcù, S. Puca, A. Rinollo, C. Lagouvardos, and V. Kotroni, 2018: Validation of the H SAF precipitation prod- uct H03 over Greece using rain gauge data. Theor. Appl. Cli- matol., 131, 377–398, https://doi.org/10.1007/s00704-016-1981-9.

Gruber, A., C.-H. Su, W. T. Crow, S. Zwieback, W. A. Dorigo, and W. Wagner, 2016a: Estimating error cross-correlation in soil moisture data sets using extended collocation analysis. J. Geophys. Res. Atmos., 121, 1208–1219.

Pierdicca, N., F. Fascetti, L. Pulvirenti, R. Crapolicchio, and J. Muñoz-Sabater, 2015: Quadruple collocation analysis for soil moisture product assessment. IEEE Geosci. Remote Sens. Lett., 12, 1595–1599.

Pignone, F., N. Rebora, F. Silvestro, and F. Castelli, 2010: GRISO (Generatore Random di Interpolazioni Spaziali da Osservazioni incerte) - Piogge. Rep. 272/2010, 353 pp.

Sebastianelli, 2017: Potentials and limitations of the use of GPM-DPR for validation of H SAF precipitation products: study over the Italian territory, Associated Visiting Scientist H SAF, Final Report,116 pp. https://hsaf.meteoam.it/VisitingScientist/GetDocument?fileName=Final_Report_Stefano_Sebastianelli.pdf

Appendix 2 Ground data used for validation activities

In the following sections the precipitation ground data networks used in the PPVG are described: radar and rain gauge data the following countries: Belgium, Bulgaria, Germany, Hungary, Italy, Poland, Slovakia, and Turkey. It is well known that radar and rain gauge rainfall estimation is influenced by several error sources that should be carefully handled and characterized before using these data as reference for ground validation of any satellite-based precipitation products.

The rain gauge in PPVG is composed by more than 8000 instruments across the partner Countries. These data are, as usual, irregularly distributed over ground and are generally deduced by tipping bucket type instruments. Moreover, most of the measurements are hourly cumulated. So probably the raingauge networks used in this validation activities are surely appropriated for the validation of cumulated products (1 hour and higher), while for the validation of instantaneous estimates the use of hourly cumulated ground measurements could introduce a large error. Moreover, the revisiting time (3,4 hours) of the product makes impossible or not reasonable to validate the product for 1-24 hours cumulated interval. The first object of PPVG *(Rain Gauge- WG)* was to quantitatively estimate the errors introduced in the validation procedure comparing the instantaneous satellite precipitation estimation with the rain gauge precipitation cumulated on different intervals.

The radar data in the PPVG is composed by 74 C-band radars across the 7 countries: Belgium, Germany, Hungary, Italy, Slovakia, Poland, Turkey. The rain gauge network responsible declared that the systems are kept in a relatively good status. The rain gauge inventory pointed out that different correction factors are applied. This means that the corresponding rainfall estimates are diverse, and the estimation of their errors cannot be homogenized. The first step in PPVG *(Radar – WG)* was to define a quality index on the base of the study performed by the Slovakian team and the scheme published by J. Szturc et all. 2008. The evaluation of this quality index has allow to increase the confidence of radar estimates with the selection of more reliable radar data in the PPVG.

In this chapter a description of the ground data available in the PPVG is reported country by country. chapter has the object to provide ground data information and to highlight their error sources.

A1.1 Ground data in Belgium (IRM)

Radar Data

The network

There are four radars in Belgium (Figure 34 and Table 23): two operated by the RMI (in Wideumont - Ardennes range - and Jabbeke - near the coast), one by Belgocontrol (Zaventem airport near Brussels) and the radar coverage is also provided by a fourth radar in France, operated by Meteo France. Of particular interest is the Wideumont radar, located in one of the highest locations of the country with clear horizon in every direction. This is very important in order to have the best possible precipitation picture in this hilly area giving rise to many tributaries of the Meuse river.

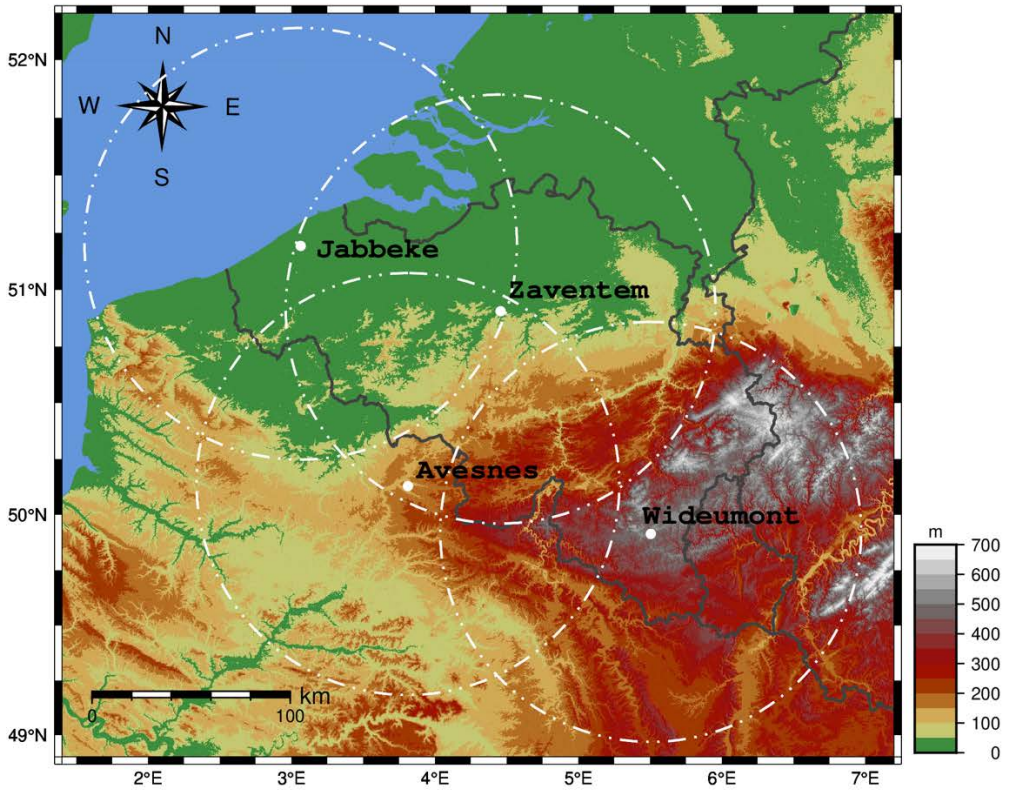

Figure 34: Meteorological radars in Belgium (elevation data from Danielson, J.J., and Gesch, D.B., 2011, Global multi-resolution terrain elevation data 2010 (GMTED2010): U.S. Geological Survey Open-File Report 2011–1073, 26 p.)

Radar location	Frequency Band	Polarization	Reflectivity Z = aR^b
Wideumont	C	Single	a = 200, b = 1.6
Jabbeke	C	Dual	a = 200, b = 1.6
Zaventem	C	Single	a = 200, b = 1.6
Avesnes	C	Dual	a = 200, b = 1.6

Table 23: Meteorological radars in Belgium, main features

Data processing

Raw reflectivity data are contaminated by off-shore wind farms and marine traffic clutter over the North Sea. The sea clutter is detected and removed using the module available in Selex Rainbow 5

software for this purpose. Rainfall rate estimation is based on a PCAPPI at a given height (depending on the radar) combined with the Marshall-Palmer relationship between reflectivity and rainrate. For grid points where several estimates are available from different radars, the maximum value is taken.
A 5-min accumulation is generated based on the rainrates at t and t-5. If the rainrate at t-5 is missing, the rainrate at t-10 is used to generate the 5-min accumulations at both t and t-5. This means than 1 missing file is tolerated. Accumulations of higher durations are made by summing accumulations of lower duration.

Acknowledgement (elevation data for the radar map)
Danielson, J.J., and Gesch, D.B., 2011, Global multi-resolution terrain elevation data 2010 (GMTED2010): U.S. Geological Survey Open-File Report 2011–1073, 26 p.

A1.2 Ground data in Bulgaria (NIMH)

Rain gauge

The network

The maximum number of available manually measured daily accumulated rain gauges is up-to 300, irregularly distributed over the country. These stations are measured every day at 6:30 UTC by emptying the collected in the past 24hours rain.
The hourly measuring automatic rain gauges are varying on daily basis and range from 70 units to 130 units. Number of stations is varying mainly because in winter months not heating gauges data is discarded from the operational database when air temperature drops below 0° C. Other specific measurement errors that are detected by the operators as funnel clogging, sensor failure etc.

The average minimum distance between closest stations is about 20 km. Most dense network of automatic gauges is built in South-Central Bulgaria where a number of European funded projects permitted to purchase and install more than 50 telemetric gauges. Spatial distribution of automatic gauges is described in (Naldzhiyan et al., 2017)[1]. One of main objectives was to consider mountain structures because of the need to measure snowfall accumulation in winter months.
This points out that the distribution of gauges could be able to describe the spatial structures of precipitation fields in case of wintertime rainfall. This objective is reached in central and South Bulgaria but much less in Western and Eastern parts of the country.

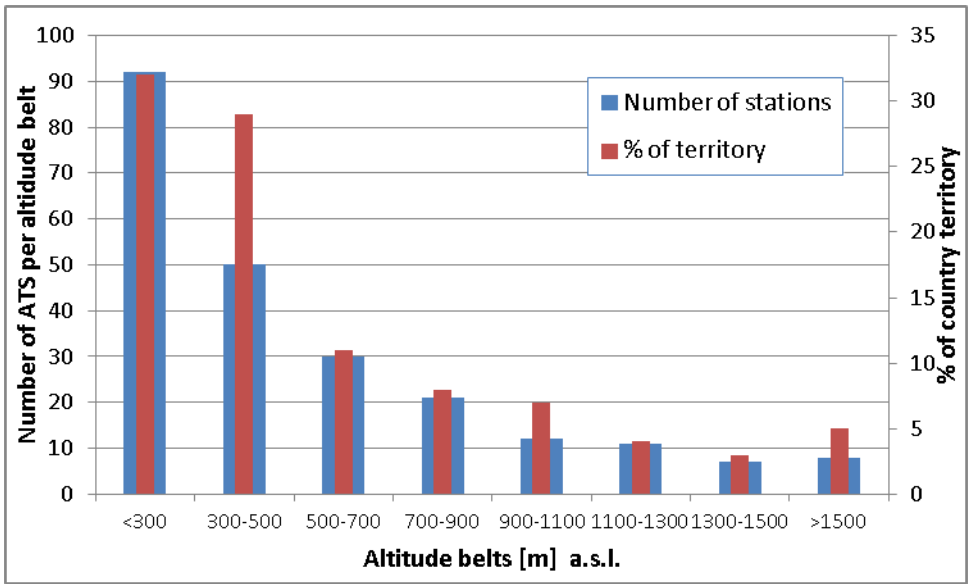

Figure 35: Spatial distribution of automatic telemetric gauges in Bulgaria (NIMH)

In following figure the distribution of working stations over Bulgaria is shown.

[1] Naldzhyian A, Georguiev O., Artinyan E., 2017: "From the sensors to the models, integrated hydro-meteorological systems in NIMH – BAS, Bulgaria". International Conference on Automatic weather stations ICAWS-2017.

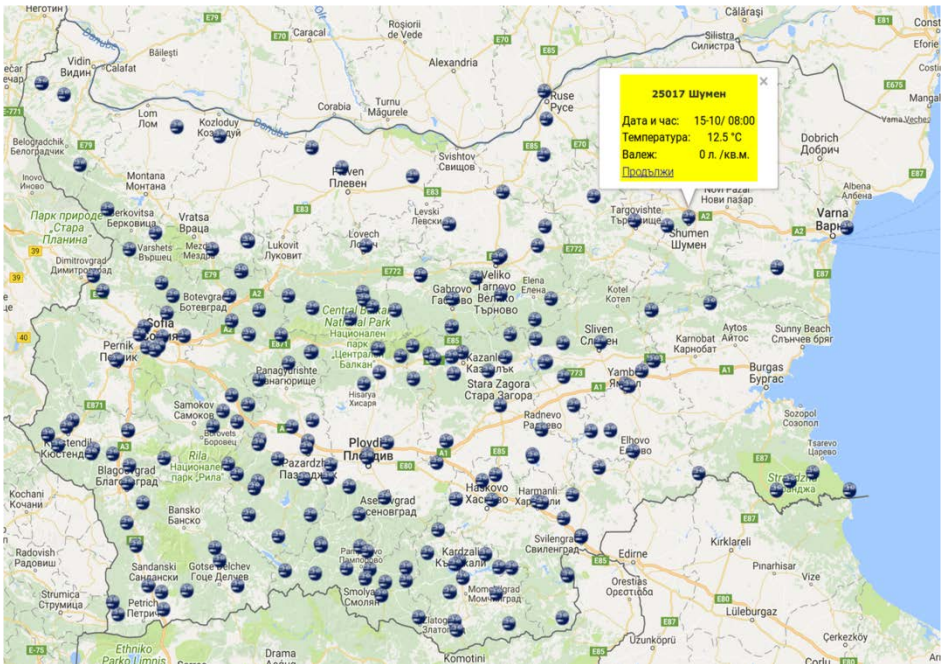

Figure 36: Distribution of the automatic stations of the Bulgaria network collected by NIMH.

The instruments – hourly measuring rain gauges:

- About 50 raingauges are of weighing type so they can measure snowfall without heating; however some of them have orifice heating (where 220V supply is available). Examples of such sensors are Vaisala VRG101, SEBA TRW 200cm^2 and SUTRON TPG
- About 80 raingauges are of tipping bucket type so they need 220 V supply to switch on the heater in winter conditions, however half of them are installed beside rivers so 220V supply is not available; The sensors types are mostly SEBA RG50, DELTA-OHM 400cm^2 and MTX 400 cm^2
- Most of the raingauges have a minimum detected quantity of 0.1 mm, others have 0.2 mm.
- The maximum rain rate (with acceptable quality) that can be measured by the gauges ranges between 33 and 120 mm^{-1} over one minute, depending on the manufacturer.

The rainrate is measured over 1 minute and 1-hour accumulation intervals depending on the hardware specifications.

At the moment, the NIMH officially provides only daily data from manually measured rain gauges. Shorter accumulation times could be available for scientific studies but not publicly distributed.

The data processing

Quality control is performed on the data, after daily visual comparison check, but only on YES/NO basis. When rain sensor fails it may be seen in few days or not be seen by the operators specially when it doesn't rain.

For NIMH internal usage hourly accumulated rain data is converted into 3 h sums and then interpolated using a kriging technique to 8 km regular grid. The method also incorporates the 24h

accumulated data from manually measured tin cans, thus enhancing the spatial and vertical quality of the field (Artinian et al., 2007)[2]

For H SAF validations a subset of country's automatic gauges is used (between 70 and 90) because of the much denser network in South-Central Bulgaria – an area of about 34000 km^2. Other parts of the country have much sparse gauge networks, data from which is not suitable to be interpolated using the GRISO technique.

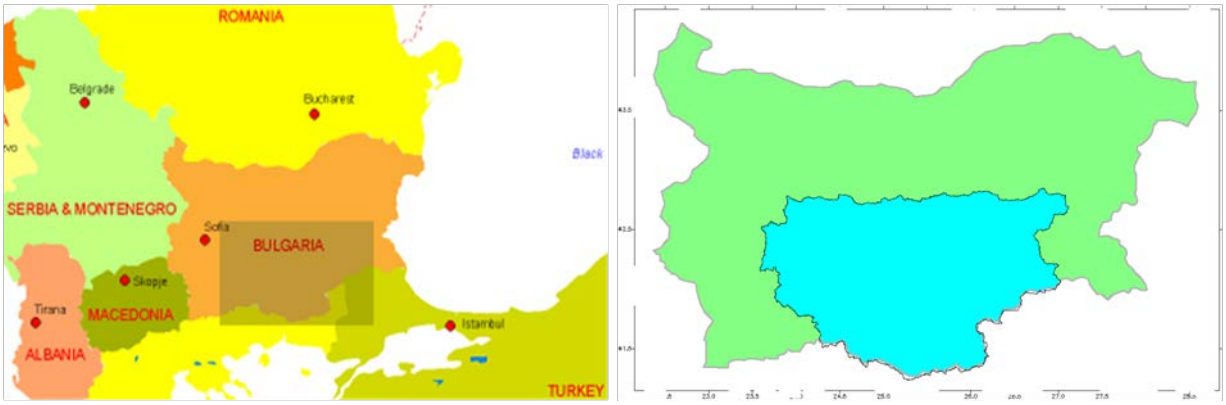

Figure 37: The area in Bulgaria used for H SAF validation with hourly accumulated rain data

[2] Artinyan, E. et al, 2007: "Modelling the water budget and the riverflows of the Maritsa basin in Bulgaria", Modelling the water budget and the riverflows of the Maritsa basin in Bulgaria. Hydrology and Earth System Sciences. 12. 10.5194/hessd-4-475-2007.

A1.3 Ground data in Germany (BfG)

The H SAF products are validated for the territory of Germany by use of two observational ground data sets: SYNOP - precipitation data based on the network of synoptical stations, provided by the German Weather Service (DWD) and RADOLAN-RW - calibrated precipitation data based on the radar network of DWD and calibrated by DWD by use of measurements at precipitation stations.

Data	Number/Resolution	Time interval	Delay	Annotation
Synoptical stations	~ 200	6h / 12h	Near-real-time	
Precipitation stations	~ 1100	hourly	Near-real-time	Automatic precipitation stations
RADOLAN RW	16 German radar sites, ~1 km x ~1 km	1 hour,	Near-real-time	Quantitative radar composite product RADOLAN RW (Radar data after adjustment with the weighted mean of two standard procedures)

Table 24: Precipitation data used at BfG for validation of H SAF products

Rain gauge

The network

The data used are compiled from ~1300 rain gauges. About 1000 are operated by DWD while about 300 are operated by other German authorities. The average minimum distance between stations is 17 km.

The instruments

The measurement instruments are precipitation sensors OTT PLUVIO of Company Ott[3] [4]. They continually and precisely measure quantity and intensity of precipitation in any weather, based on balance principle with temperature compensation (heated funnel) and by an electronic weighing cell. The absolute measuring error is less than 0.04 mm for a 10 mm precipitation amount and the long-term (12months) stability is better than 0.06 mm. The operating temperature ranges from –30°C to +45°C. The minimum detected quantity (sensitivity) is 0,05 mmh^{-1}. The maximum possible measured rain rate is 3000 mmh^{-1}. The operational accumulation interval theoretically is one minute.

The data processing

Continuous, automatic measurement of liquid and solid precipitation data are collected, accumulated (intervals: from 1hour until 1day) and provided as SYNOP tables by DWD. These data are error corrected and quality controlled in four steps with checks of completeness, climatologic temporal/spatial consistency and marginal checks.

[3] http://www.ott.com/web/ott_de.nsf/id/pa_ottpluvio2_vorteile.html?OpenDocument&Click=

[4] **Precipitation amount and intensity measurements with the Ott Pluvio, Wiel Wauben, Instrumental Department, INSA-IO, KNMI, August 26, 2004**

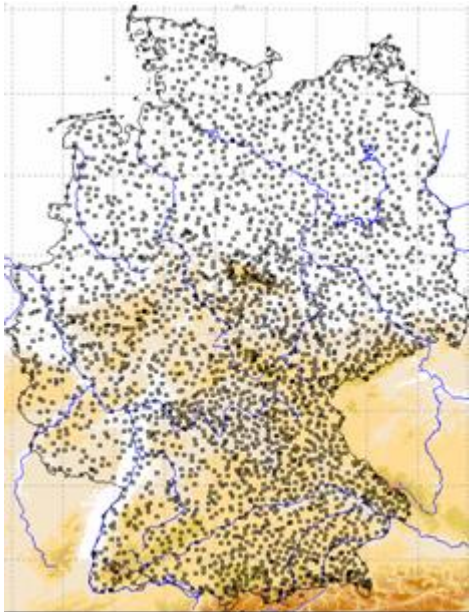

Figure 38: (left): Network of rain gauges in Germany - Figure 39: (right): Pluvio with Remote Monitoring Module

Radar data

Radar-based real-time analyses of hourly precipitation amounts for Germany (RADOLAN) is a quantitative radar composite product provided in near-real time by DWD. Spatial and temporal high-resolution, quantitative precipitation data are derived from online adjusted radar measurements in real-time production for Germany. Radar data are calibrated with hourly precipitation data from automatic surface precipitation stations. [5]

The combination of hourly point measurements at the precipitation stations with the five-minute-interval radar signals of the 16 weather radars (C-Band Doppler) provides gauge-adjusted hourly precipitation sums for a ~1km x ~1km raster for Germany in a polar stereographic projection.

Radar site	Latitude (N)	Longitude (E)	WMO No.	Radar site	Latitude (N)	Longitude (E)	WMO No.
München	48° 20’ 14’’	11° 36’ 46’’	10871	Rostock	54° 10’ 35’’	12° 03’ 33’’	10169
Frankfurt	50° 01’ 25’’	08° 33’ 34’’	10630	Ummendorf	52° 09’ 39’’	11° 10’ 38’’	10356
Hamburg	53° 37’ 19’’	09° 59’ 52’’	10147	Feldberg	47° 52’ 28’’	08° 00’ 18’’	10908
Berlin-Tempelhof	52° 28’ 43’’	13° 23 17’’	10384	Eisberg	49° 32’ 29’’	12° 24’ 15’’	10780
Essen	51° 24’ 22’’	06° 58’ 05’’	10410	Flechtdorf	51° 18’ 43’’	08° 48’ 12’’	10440
Hannover	52° 27’ 47’’	09° 41’ 54’’	10338	Neuheilenbach	50° 06’ 38’’	06° 32’ 59’’	10605
Emden	53° 20’ 22’’	07° 01’ 30’’	10204	Türkheim	48° 35’ 10’’	09° 47’ 02’’	10832

5 http://www.dwd.de/bvbw/appmanager/bvbw/dwdwwwDesktop?_nfpb=true&_windowLabel=dwdwww_main_book&T14609949251144921180881gsbDocumentPath=Navigation%2FWasserwirtschaft%2FUnsere__Leistungen%2FRadarniederschlagsprodukte%2FRADOLAN%2Fradolan__node.html%3F__nnn%3Dtrue&switchLang=en&_pageLabel=_dwdwww_spezielle_nutzer_forschung_fkradar

Neuhaus	50° 30’ 03’’	11° 08’ 10’’	10557	Dresden	51° 07’ 31’’	13° 46’ 11’’	10488

Table 25: Location of the 16 meteorological radar sites of the DWD

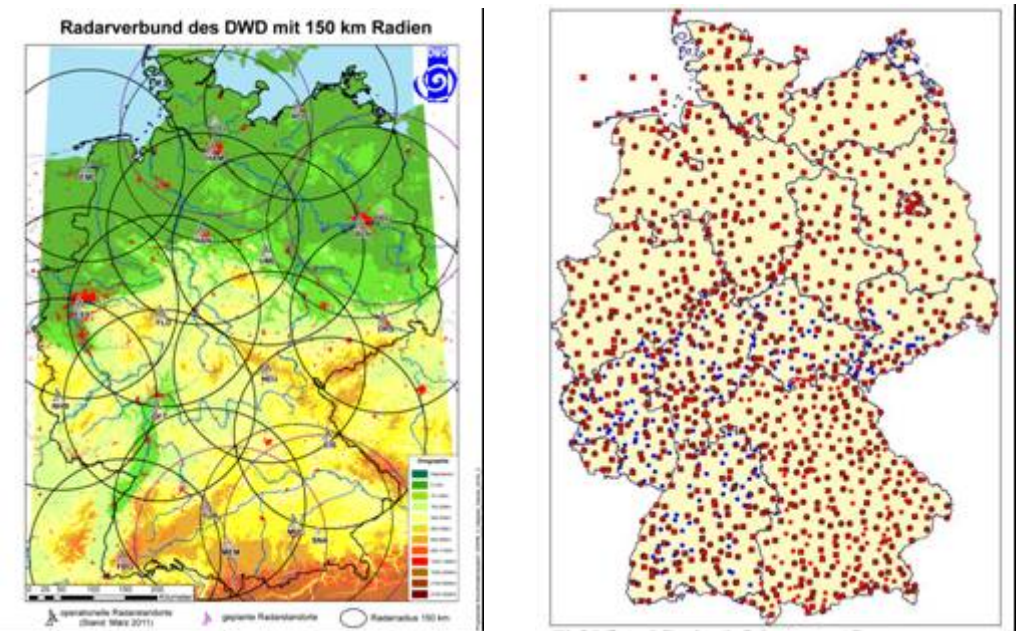

Figure 40: (left) radar compound in Germany (March 2011) ; Figure 41: (right) location of ombrometers for online calibration in RADOLAN; squares: hourly data provision (about 500), circles: event-based hourly data provision (about 800 stations)6.

The flowchart of online calibration method applied in RADOLAN is depicted in Figure 42.

[6] Bartels, H.: Projekt RADOLAN. Routineverfahren zur Online-Aneichung der Radarniederschlagsdaten mit Hilfe von automatischen Bodenniederschlagsstationen (Ombrometer), Abschlussbericht 2004

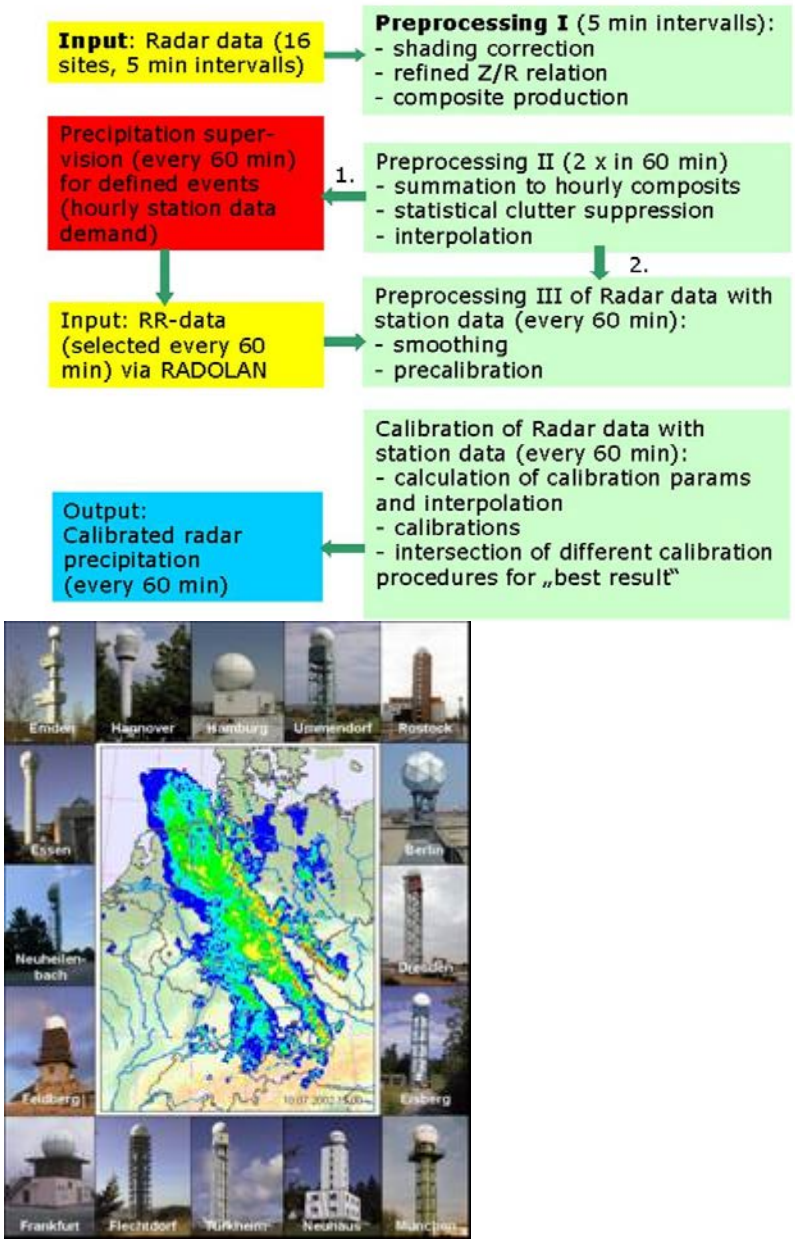

Figure 42: Flowchart of online calibration RADOLAN (DWD, 2004)

A1.4 Ground data in Hungary (OMSZ)

The radar network

The main data used for validation in Hungary would be the data of meteorological radars. There are four C-band dual polarized Doppler weather radars operated routinely by the OMSZ-Hungarian Meteorological Service. The location of the four Hungarian radars and the measurement characteristics are listed in Table 26. All four radars are calibrated periodically, with an external (calibrated) TSG, the periodicity is kept every 1 year.

Year of installation	***Location***	***Radar type***	***Parameters measured***
1999	*Budapest*	*Dual-polarimetric Doppler radar*	Z,Z_{DR},K_{DP},Φ_{DP}
2003	*Napkor*	*Dual-polarimetric Doppler radar*	Z,Z_{DR},K_{DP},Φ_{DP}
2004	*Poganyvar*	*Dual-polarimetric Doppler radar*	Z,Z_{DR},K_{DP},Φ_{DP}
2014	Szentes	*Dual-polarimetric Doppler radar*	Z,Z_{DR},K_{DP},Φ_{DP}

Table 26: Main characteristics of the Hungarian radar network

Instrument characteristics

The Hungarian radar network is composed by four Doppler radars, which are measuring in the C-band, mainly at same frequencies. The scan strategy is the same for all the radars. The parameters of the instruments and the measurement campaigns are listed in Table 27.

	Budapest	***Napkor***	***Poganyvar***	***Szentes***
Frequency band	C-Band, 5625MHz	C-Band, 5610MHz	C-Band, 5610MHz	C-Band, 5640MHz
Polarization (Single/Double)	double	double	double	double
Doppler capability (Yes/No)	Yes	Yes	Yes	Yes
Scan strategy: elevations, maximum nominal range distance, range resolution	*scan freq: 5 min* *Elevaions(deg):* *0 0.5 1.1 1.9 3.0 4.7 7.0 10.0 14.2* *Range 240 Km*	*scan freq: 5 min* *Elevaions(deg):* *0 0.5 1.1 1.9 3.0 4.7 7.0 10.0 14.2* *Range 240 Km*	scan freq: 5 min Elevaions(deg): *0 0.5 1.1 1.9 3.0 4.7 7.0 10.0 14.2* Range 240 Km	scan freq: 5 min Elevaions(deg): *0 0.5 1.1 1.9 3.0 4.7 7.0 10.0 14.2* Range 240 Km

	Resolution:125 m	*Resolution:125 m*	Resolution:125 m	Resolution:125 m

Table 27: Characteristics of the four radar instruments in Hungary

Data processing and radar products

Radar field corrections

Radar measurements are influenced by many error sources that should be minimized as much as possible. As such, in case of the Hungarian radar data many correction methods are applied to filter out false radar reflectivity measurements. Clutter removal, WLAN filter and clear-air echo filter is implemented in the processing chain of all four-radar data. The beam blockage correction is also implemented in the processing chain in order to correct serious underestimation of precipitation amounts behind mountains. Attenuation correction (the attenuation of electromagnetic waves in water environment, water drops) was implemented in 2019. Hungary does not apply VPR (Vertical Profile Reflectivity) correction.

Precipitation intensity is derived from radar reflectivity with the help of an empirical formula, the Marshall-Palmer equation (R=a*Z^b, where a=200, b=1.6). From the four radar images a composite image over the territory of Hungary is derived every 5 minutes applying the maximum reflectivity in one column method, in order to make adjustments in overlapping regions.

Rain gauge correction of the radar precipitation fields

The non-corrected precipitation field can be corrected by rain gauge measurements. In Hungary, we do not make corrections to instantaneous 5 minutes radar data. In our institute, we only use a correction for the total precipitation for 1, 3-, 6-, 12- and 24-hour periods.

For the accumulated products, we use a special method to accumulate rainfalls: we interpolate the 5-minutes measurements for 1-minute grid by the help of displacement vectors also measured by the radar, and then sum up the images which we got after the interpolation. It is more precise especially when we have storm cells on the radar picture, because a storm cell moves for 5 minutes and thus we do not get continuous precipitation fields when we sum up only with 5 minute periods. This provides satisfying results. However, there is still a need for rain-gauge adjustment because there are obviously places (behind mountains) that the radar does not see.

The radars are corrected with rain gauge data every hour. The correction method using rain gauge data for 1-hour total precipitation consists of two kinds of corrections: the spatial correction which becomes dominant in the case of precipitation extended over a large area, whereas the other factor, the distance correction factor prevails in the case of sparse precipitation. These two factors are weighted according to the actual situation. The weighting factor depends on the actual effective local station density, and also on the variance of the differences of the bias between radar and rain gauge measurements. On the whole, we can say that our correction method is efficient within a radius of 100 km from the radar. In this region, it gives a final underestimation of about 10%, while at bigger distance; the underestimation of precipitation fields slightly increases.

Resolution, projection, threshold of detection

The resolution of the radar data used for validation is 1km by 1km. This is true for the accumulated and the instantaneous products as well. Hungarian radar data is available operationally in stereographic (S60) projection.

References

Péter Németh: Complex method for quantitative precipitation estimation using polarimetric relationships for C-band radars. Proceed. of 5th European Radar Conference (ERAD), Helsinki (Finland) (http://erad2008.fmi.fi/proceedings/extended/erad2008-0270-extended.pdf)

Raingauge network

Distribution of the raingauge stations in Hungary

The automated precipitation measurement network of OMSZ Hungarian Meteorological Service (OMSZ) consist of the following types of instruments:

96 instruments are tipping bucket type (34 Lambrecht Lambrecht 15183H, 62 Lambrecht 15180H), and 37 instruments are weighing type (4 Lambrecht 15184H, 23 OTT Pluvio2, 8 Geonica Datarain4000, 2 EWS HWI).

In addition, 142 weighing type instruments (OTT Pluvio2) belonging to the General Directorate of Water Management of Hungary (OVF) are also maintained by OMSZ and integrated into its network.

Altogether more than 270 automated raingauges are available, but the number is constantly increasing with new installations.

All data of the precipitation network are collected in every 10 minutes and they undergo on a quality check procedure.

Traditional precipitation measurements by human observers (either spacialists or amateurs) are not used for HSAF validation work in Hungary.

The map below shows the Hungarian automated precipitation measurement network, the stations of OMSZ are red and the stations of OVF are green.

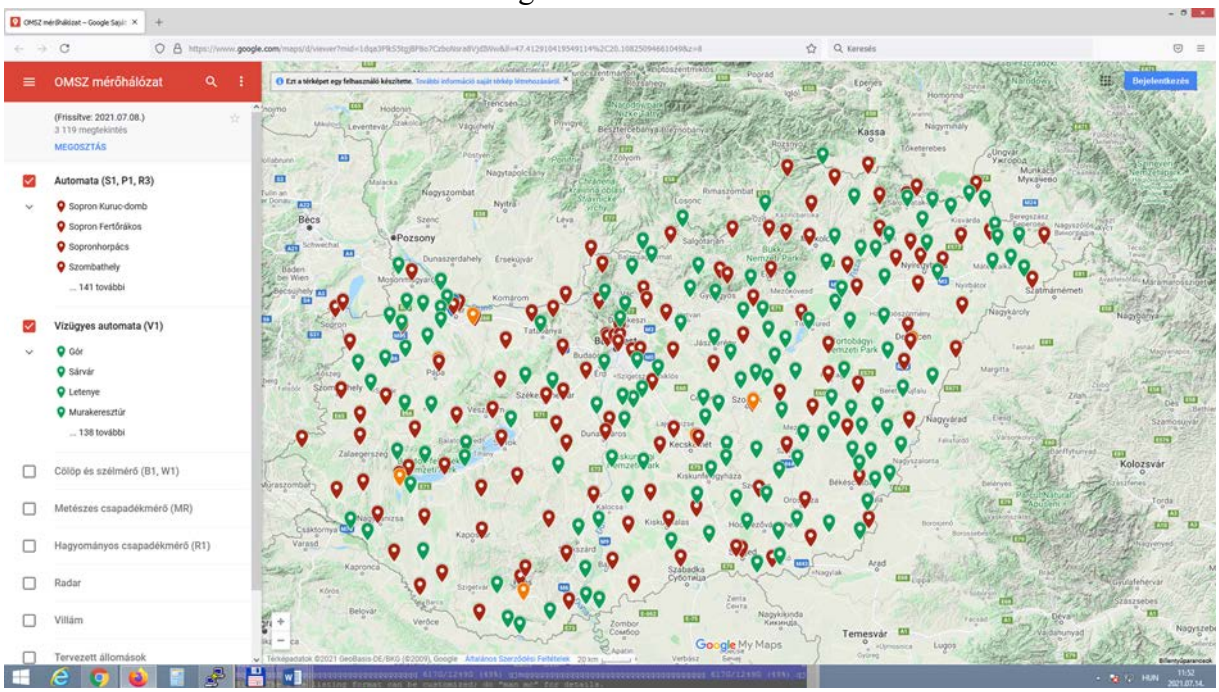

Figure 43: Hungarian automated precipitation measurement network.

A1.5 Ground data in Italy (DPC, UniBo)

Rain gauge

The network

The maximum number of available raingauges is about 3000, irregularly distributed over the surface. On the average, however, a number of stations have low quality data, failure or data transmission problems and their data are missing (-9999 recorded). This number of no data stations is highly varying on hourly/daily basis and ranges from few units to a hundred. In case of data acquired but not transmitted/recorded, the first transmitted measure is the cumulated value over the time when the data were not transmitted.

The average minimum distance between closest stations is about 11 km, with a very high variance: in some regions (such as Tuscany in central Italy) it is below 5 km, while in Emilia Romagna (Po Valley) it is more than 20 km. A study of the decorrelation distance between stations as function of the mutual distance has been carried out for the 2009 dataset. The decorrelation distance is defined as the minimum distance between two observations that makes the Pearson correlation coefficient between the two measures decrease below e^{-1}. Results are shown in Figure 44, where the decorrelation distance is plotted as function of the distance between stations. It appears that there is a large variability of this parameter from higher values (around 60 km for cold months when large precipitating systems dominate and reduces to roughly 10 km when small scale convection is more likely to occur (warm months).
This points out that the distribution of gauges could be able to describe the spatial structures of precipitation fields in case of wintertime rainfall, while may be inadequate for spring/summer convective events.

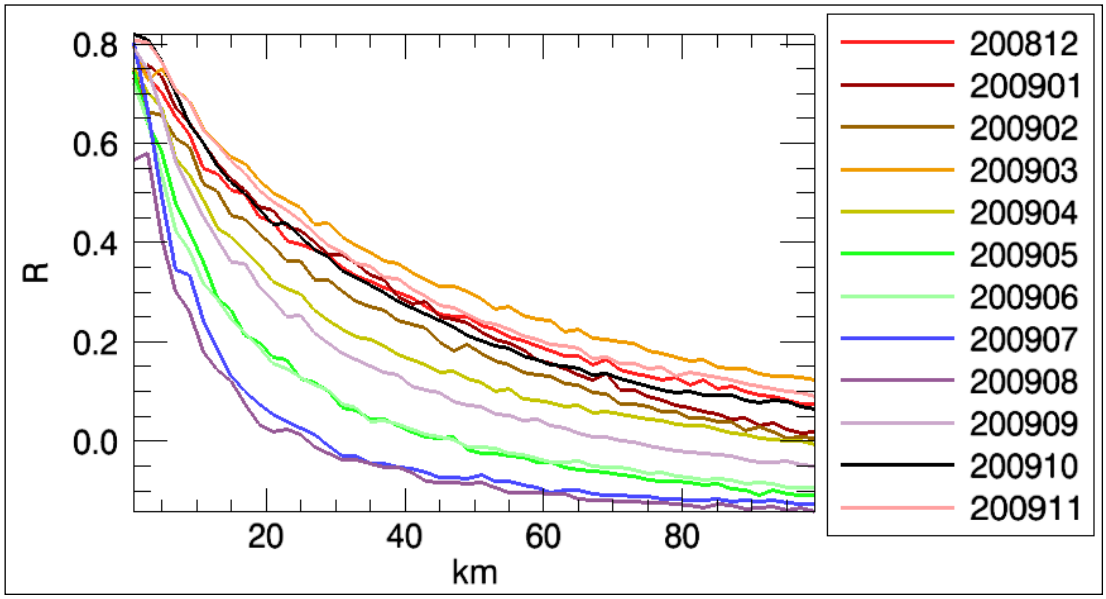

Figure 44: Correlation between rainrates detected by two close stations as function of the distance between the two stations. Colors refer to the month along 2009

In Figure 45 the distribution of working stations over Italy is shown.

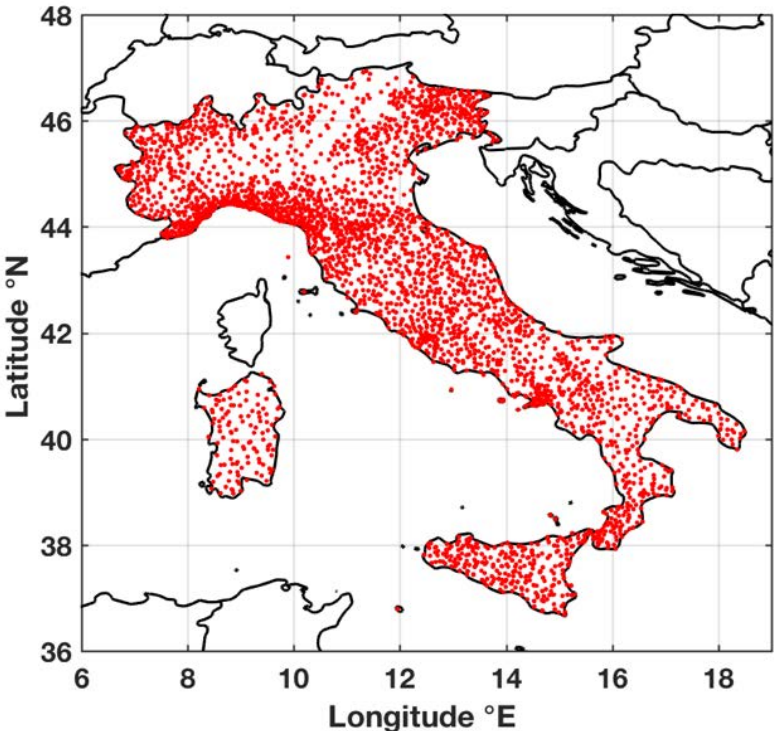

Figure 45: Distribution of the raingauge stations of the Italian network collected by DPC.

The instruments

This section provides the following information:

- All the available raingauge are of tipping bucket type;
- Most of the raingauge have a minimum detected quantity of 0.2 mm, others have 0.1 mm.
- The maximum rainrate that can be measured by the gauges ranges between 300 and 500 mm^{-1} over one minute, depending on the manufacturer.

The rainrate is measured over different cumulation intervals by the different local administrations managing the network, but the data disseminated are all integrated over 60 minutes.

At the moment, the National network made available by DPC provides only hourly data, shorter cumulation times could be available for case studies after specific agreements with local management authorities.

Only a small subset (about 300 stations) of gauges have heated funnel, especially in alpine regions (such as Valle d'Aosta and Piedmont), and this is a clear source of errors in both summer (due to hailfall) and in autumn/winter (due to snowfall).

The data processing

To homogenize the two ground datasets, rain gauge data, preprocessed according to range, persistence, step, and spatial consistency (Shafer et al. 2000) to screen out suspect values, have been interpolated over a regular grid (5 km x 5 km) through the Random Generator of Spatial Interpolation from uncertain Observations (GRISO). The GRISO (Pignone et al. 2010; Feidas et al. 2018) is an improved kriging-based technique implemented by the International Centre on Environmental Monitoring (CIMA Research Foundation). This technique preserves the values observed at the rain gauge location, allowing for a dynamical definition of the covariance structure associated

with each rain gauge by the interpolation procedure. Each correlation structure depends both on the rain gauge location and on the accumulation time considered. GRISO is adopted by all European participating countries in the H SAF validation procedure (Puca et al. 2014). The resulting grid is a 5x5 km regular grid with 240 columns and 288 lines. Moreover, a Digital elevation model is used to provide a mask of Italy in order to: 1) screen out sea-pixels too far from the coastlines and 2) process the pixels with the elevation above sea level.

Radar data

The network

The Italian Department of Civil Protection (DPC) is the authority leading the national radar coverage project in order to integrate the pre-existent regional systems. Currently, the radar network is composed by 22 systems (20 C-band and 2 X-band systems), most of them with dual-polarization. The network is composed by 8 C-band fixed regional installations (five of them are polarimetric), five systems owned by the Italian company for air navigation services (ENAV), 9 dual-polarization systems managed by DPC (7 using C-band and 2 X-band).
The Figure 46 shows the spatial radar coverage of the Italian territory.

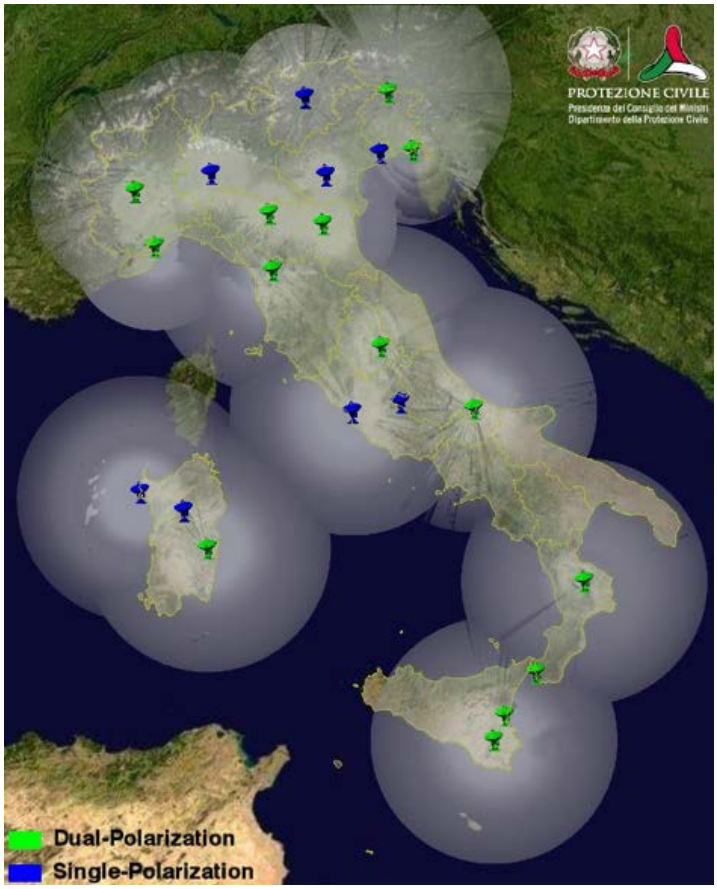

Figure 46: Italian radar network coverage. The green and blue radar symbol stands for dual- and single-polarization system, respectively.

Radar Data processing

The operational radar processing chain is briefly described in this section.

It aims at compensating or at least identifying most of the uncertainty sources conditioning the radar rainfall estimation process (Friedrich et al., 2006). Among them, the following error sources are primarily considered: contamination by non-weather returns (clutter), Partial Beam Blocking (PBB), beam broadening at increasing distances, vertical variability of precipitation (Germann and Joss, 2002; Joss and Lee, 1995; Marzano et al., 2004) and rain path attenuation (Bringi and Chandrasekar, 2001; Carey et al., 2000; Testud et al., 2000; Vulpiani et al., 2008). Every error source is quantified through specific tests ending with the estimation of specific (partial) quality matrices and, when possibile, is compensated for. The overall data quality (Q) is then obtained as a combination of the partial quality matrices. The quality model described in Rinollo et al. (2013) is embedded within the overall processing chain schematically depicted in Figure 24.
In this schematic representation, the sequential flow among consecutive computational steps is specified by black arrows, while the blue ones identify the data input (or output) to (or from) a specific processing module.
The processing chain can be summarized through the following few steps as follows:

i. As typical, the raw volumetric data must be first filtered from non-weather returns. This step is here achieved using the fuzzy-logic approach proposed in Vulpiani et al. (2012) for polarimetric radar systems.
ii. The next step is the correction for Partial Beam Blocking (PBB) based on the retrieved 3-D occlusion map (Bech et al., 2003) that, assuming the e.m. waves propagate in a standard atmosphere, is evaluated only once for a given radar scanning strategy.
iii. The rain path attenuation is just qualitatively evaluated in case the considered radar system has single-polarization capability (Rinollo et al., 2013), otherwise it is compensated for by means of the differential phase shift that needs to be preliminarly processed. In this framework, the iterative moving-window range derivative approach proposed in Vulpiani et al. (2012) is applied here.
iv. The range-related deterioration of radar data quality is modeled through a non-linear function as in Rinollo et al. (2013).
v. Once the attenuation is evaluated and, eventually, compensated for through the so-called ZPHI method (Testud et al., 2000), the overall data quality is computed as geometric mean of the partial quality matrices.

$$Q = q_{clutter} \cdot q_{vertical} \cdot q_{PBB} \cdot q_{distance} \cdot q_{attenuation}$$

vi. The retrieved mean Vertical Profile of Reflectivity (VPR) is applied to the entire volumetric scan with the aim to use all the observations along the vertical to retrieve the surface rainfall rate. All the clutter-filtered and attenuation-corrected (if applicable) PPIs are projected at ground by means of the average Vertical Profile of Reflectivity (VPR).
vii. The Surface Rainfall Intensity (SRI) map is computed as a quality-weighted average of each rain rate map, obtained by each ground-projected reflectivity sweep (Vulpiani et al., 2014).
viii. The SRI composite is built by combining the single-radar rainfall maps through a squared-quality-weighted approach. In case of dual-polarization systems, the composite rainfall retrieval algorithm proposed in Vulpiani and Baldini (2013).

As descripted in Petracca et al. (2018), only radar data with Q values greater than 0.60 are used for comparison with satellite data.

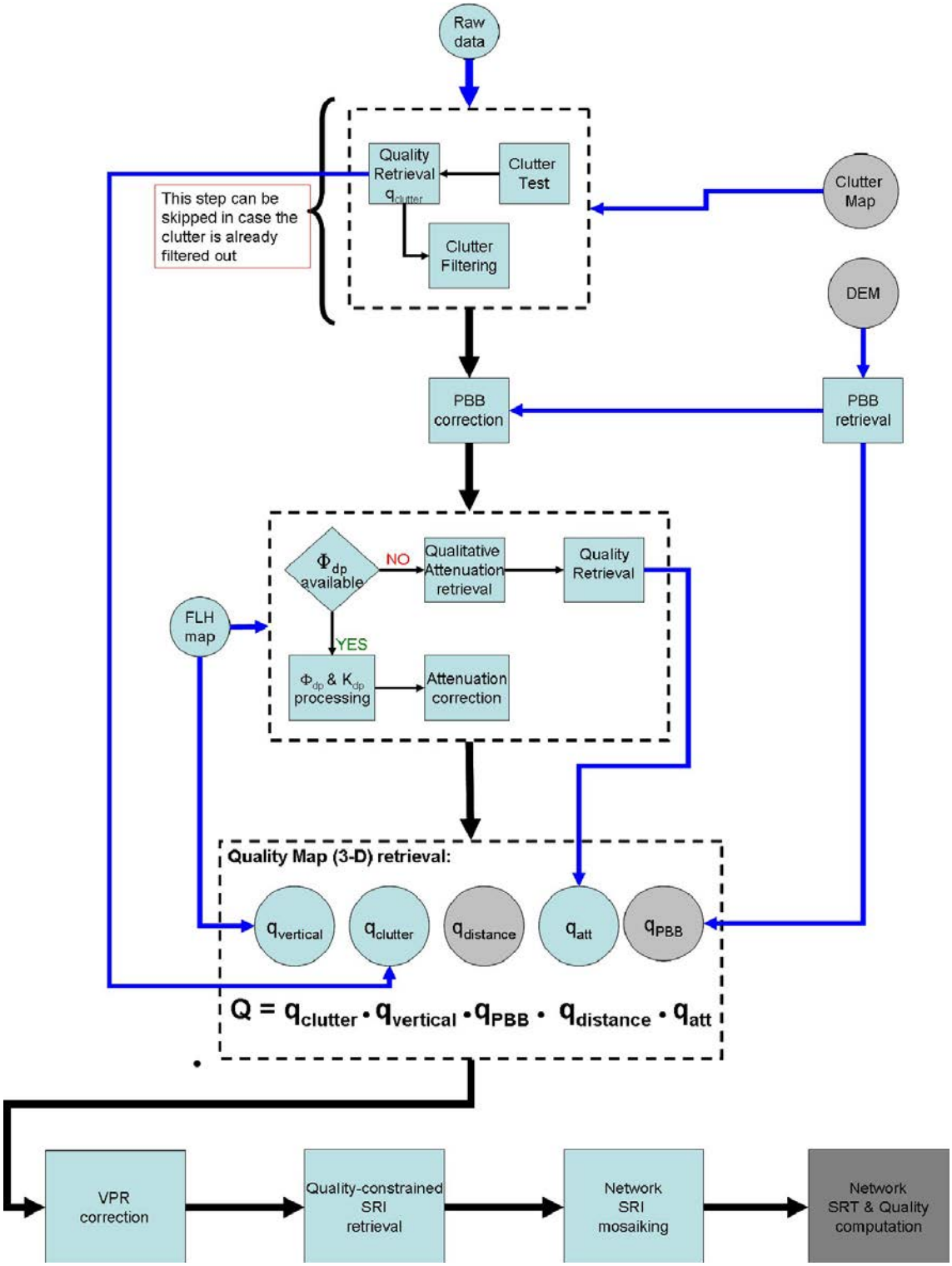

Figure 47: Schematic representation of the Italian radar data processing chain.

References

Bech, J., B. Codina, J. Lorente, and D. Bebbington, 2003: The sensitivity of single polarization weather radar beam blockage correction to variability in the vertical refractivity gradient. J. Atmos. Oceanic Technol., 20, 845–855.

Bringi, V. N. and V. Chandrasekar, 2001: Polarimetric doppler weather radar. Cambridge University Press, 636 pp.

Carey, L. D., S. A. Rutledge, and D. A. Ahijevych, 2000: Correcting propagation effects in c-band polarimetric radar observations of tropical convection using differential propagation phase. J. Appl. Meteor., 39, 1405–1433.

Feidas, H., F. Porcù, S. Puca, A. Rinollo, C. Lagouvardos, and V. Kotroni, 2018: Validation of the H SAF precipitation prod- uct H03 over Greece using rain gauge data. Theor. Appl. Cli- matol., 131, 377–398, https://doi.org/10.1007/s00704-016-1981-9.

Friedrich, K., M. Hagen, and T. Einfalt, 2006: A quality control concept for radar reflectivity, polarimetric parameters, and doppler velocity. J. Atmos. Ocean. Tech., 23, 865–887.

Germann, U. and J. Joss, 2002: Mesobeta profiles to extrapolate radar precipitation measurements above the alps to the ground level. J. Appl. Meteorol., 41, 542–557.

Joss, J. and R. Lee, 1995: The application of radar-gauge comparisons to operational precipitation profile corrections. J. Appl. Meteorol., 34, 2612–2630.

Petracca, M., D'Adderio, L.P., Porcù, F., Vulpiani, G., Sebastianelli, S., Puca, S., Validation of GPM Dual-frequency Precipitation Radar (DPR) rainfall products over Italy, Journal of Hydrometeorology, 19, 907-925, 2018, doi: 10.1175/JHM-D-17-0144.1

Pignone, F., N. Rebora, F. Silvestro, and F. Castelli, 2010: GRISO (Generatore Random di Interpolazioni Spaziali da Osservazioni incerte)-Piogge. Rep. 272/2010, 353 pp.

Puca, S., Baguis, P., Campione, E., Ertürk, A., Gabellani, S., Iwański, R., Jurašek, M., Kaňák, J., Kerényi, J., Koshinchanov, G., Kozinarova, G., Krahe, P., Łapeta, B., Lábó, E., Milani, L., Okon, L., Öztopal, A., Pagliara, P., Pignone, F., Porcù, F., Rachimow, C., Rebora, N., Rinollo, A., Roulin, E., Sönmez, İ., Toniazzo, A., Vulpiani, G., Biron, D., Casella, D., Cattani, E., Dietrich, S., Laviola, S., Levizzani, V., Melfi, D., Mugnai, A., Panegrossi, G., Petracca, M., Sanò, P., Zauli, F., Rosci, P., De Leonibus, L. "The validation service of the hydrological SAF geostationary and polar satellite precipitation products", Nat. Hazards Earth Syst. Sci., 14, 871–889, 2014 www.nat-hazards-earth-systsci.net/14/871/2014/ doi:10.5194/nhess-14-871-2014

Rinollo, A., Vulpiani, G., Puca, S., Pagliara, P., Kanák, J., Lábó, E., Okon, L'., Roulin, E., Baguis, P., Cattani, E., Laviola, S., and Levizzani, V.: Definition and impact of a quality index for radar-based reference measurements in the H SAF precipitation product validation, Nat. Hazards Earth Syst. Sci., 13, 2695–2705, doi:10.5194/nhess-13-2695-2013, 2013.

Shafer, M. A.,C.A. Fiebrich, D. S. Arndt, S. E. Fredrickson, andT.W. Hughes, 2000: Quality assurance procedures in the Oklahoma Mesonetwork. J. Atmos. Oceanic Technol., 17, 474–494, https:// doi.org/10.1175/1520-0426(2000)017,0474:QAPITO.2.0.CO;2.

Testud, J., E. L. Bouar, E. Obligis, and M. Ali-Mehenni, 2000: The rain profiling algorithm applied to polarimetric weather radar. J. Atmos. Oceanic Technol., 17, 332–356.

Vulpiani, G. and L. Baldini, 2013: Observations of a severe hail-bearing storm by an operational X-band polarimetric radar in the mediterranean area. Proceed. of the 36th AMS Conference on Radar Meteorology, Breckenridge, CO, USA.

Vulpiani, G., M. Montopoli, L. D. Passeri, A. Gioia, P. Giordano, and F. S. Marzano, 2012: On the use of dual-polarized C-band radar for operational rainfall retrieval in mountainous areas. J. Appl. Meteor and Clim., 51, 405–425.

Vulpiani, G., P. Tabary, J. P. D. Chatelet, and F. S. Marzano, 2008: Comparison of advanced radar polarimetric techniques for operational attenuation correction at c band. J. Atmos. Oceanic Technol., 25, 1118–1135.

Vulpiani, G., A. Rinollo, S. Puca, m. Montopoli, 2014: A quality-based approach for radar rain field reconstruction and the H SAF precipitation products validation. The eighth European Radar conference on radar in meteorology and hydrology. Garmish-Partenkirken (Germany) 1-5 Sept., 2014.

A1.6 Ground data in Poland (IMWM)

Rain gauge

The network

The maximum number of rain gauges in the Polish ATS (Automatic Telemetric Station) national network is 950. Each ATS post is equipped with two independent rain gauges of the same sort. One of them is heated during the winter period and the other one is not. Therefore precipitation information is derived from 475 points at the time. Fact that rainfall is measured by two equally sensitive instruments two meters away from each other at the same post, enables to apply simple in situ data quality control during summertime. During winter non-heated rain gauge is covered with a cup to prevent it from being clogged by the ice and damaged. Because of that the precipitation information derived from ATS network in winter cannot be verified using this method. It can be stated that during the wintertime precipitation information might be a slightly bigger measuring error.

The number of rain gauges available for H SAF validation activities varies from day to day due to operational efficiency of ATS network in Poland and depends on large number of independent factors. It can be stated that the number varies between 330 and 475 rain gauges for each day of operational work.

Mean minimum distance between precipitation measuring ATS posts (between each pair of rain gauges) in Polish national network is 13,3 km.

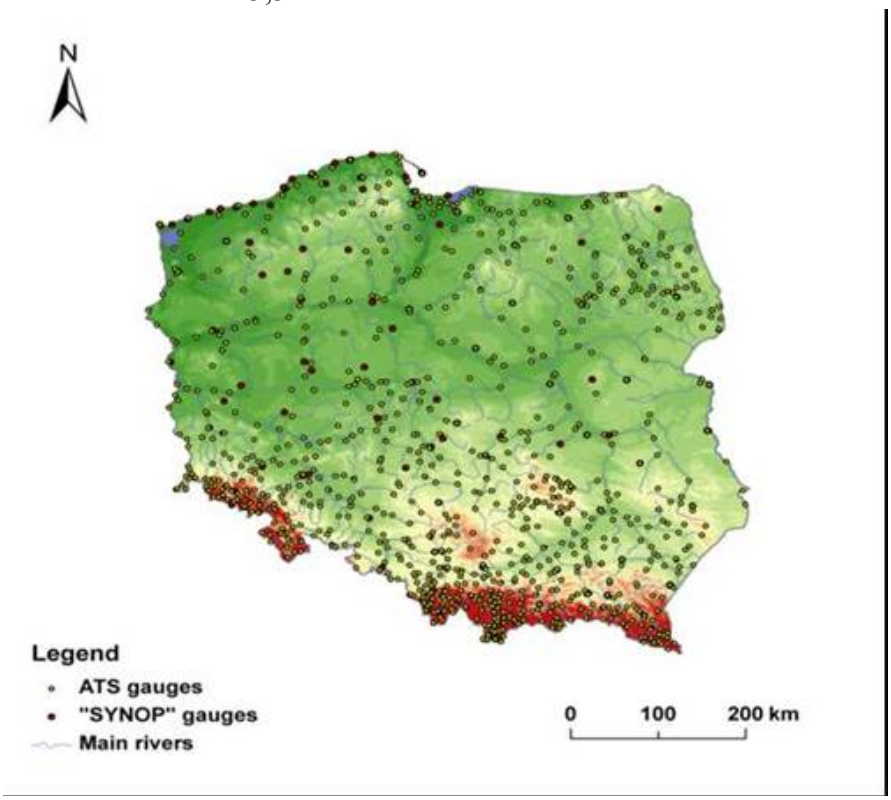

Figure 48: ATS national network in Poland

The instruments

All rain gauges working within Polish ATS national network are MetOne tipping bucket type instruments. Minimum detected quantity that can be measured by those rain gauges is 0,1 mm/h which means that each tilt of rain gauge bucket adds 0,1mm to the total sum of the measured precipitation. During very heavy precipitation events MetOne rain gauges tend to underestimate real precipitation by factor of 10%. Maximum measured rainrate *(mmh^{-1})* by MetOne instruments in

Poland was recorded in 5.06.2007 at ATSO Koscielisko Kiry at the foot of Tatra Mountains. The recorded values reached 65 mm/h. Operational cumulation interval *(min)* of ATS network rain gauges is set for 10 minutes and can be adjusted according to given needs. There is possibility to have very short cumulation intervals for case studies - theoretically 1 minute - but not on every given precipitation post. It depends on local DCS settings.

The data processing

As stated above the data quality control can be achieved by comparison on two rainfall datasets collected by two independent rain gauges at the same ATS post. It is done operationally during summertime. There is no such possibility during the winter because of lack of non-heated rain gauge dataset. In case that one pair of rain gauges at the same ATS post provide two different rainfall readings the higher one is taken into account.

No specialization technique is used for standard validation process. However, for some case studies, the Natural Neighbor technique is applied for satellite and ground precipitation data. To match the precipitation information with satellite data spatial and temporal matching are applied.

- Spatial matching: for each given satellite pixel, the posts situated within that pixel were found. The pixel size was taken into account, however, its shape was assumed to be rectangular. If more than one rain gauge were found within one satellite pixel, the ground rain rate value was calculated as a mean of all rain gauges measurements recorded within that pixel;
- Temporal matching: satellite derived product is combined with the next corresponding ground measurement. As the ground measurements are made with 10 minute time resolution, the maximum interval between satellite and ground precipitation is 5 minutes.

Radar data

The Polish meteorological radar network called POLRAD (initially Doppler Radar System METEOR) consists of eight devices and was produced by Gematronic Weather Radar Systems GmbH SELEX Sistemi Integrati GmbH. The system had been installed in Poland starting from year 2001 and has its 20th anniversary this year. The software running within this system is Rainbow 5 (and it's later updates). The radars are using band C (frequency 5,6 GHz and subsequently 5,4 cm wavelength). All of the radars are Doppler instruments operationally run in 10 min. scan frequency and two of them (Ramża and Pastewnik) in dual polarisation mode.

Eight basic radars working within the POLRAD network.

Station location	Latitude	Longitude	Elevation a.m.s.l.	Antenna height a.t.l.	Radar type
Legionowo	52°24'18,79''	20°57'39,28''	89,0 m	29,0 m	Doppler radar METEOR 1500 C
Rzeszów	50°06'49,79''	22°02'12,09''	206,5 m	30,0 m	Doppler radar METEOR 1500 C
Brzuchania	50°23'39,13''	20°05'00,35''	388,5 m	35,0 m	Doppler radar METEOR 500 C
Ramża	50°09'04,59''	18°43'29,86''	320,7 m	36,0 m	Dual polarisation Doppler radar METEOR 1600C
Pastewnik	50°53'32,81''	16°02'22,17''	666,5 m	23,5 m	Dual polarisation Doppler radar

					METEOR 1600C
Poznań	52°24’47,73’’	16°47’49,40’’	95,1 m	35,0 m	Doppler radar METEOR 500 C
Świdwin	53°47'40,25"	15°50'16,97"	121,1 m	30,0 m	Doppler radar METEOR 500 C
Gdańsk	54°23’03,17’’	18°27’23,00’’	135,2 m	20,0 m	Doppler radar METEOR 1500 C

Table 28: Radars in Poland

The original radar arrangement in Poland (when installed).

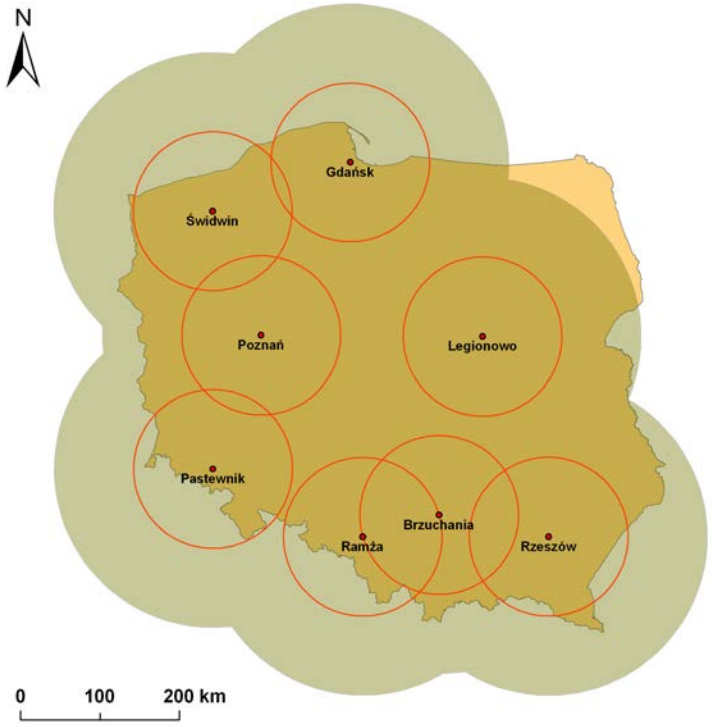

Figure 49: Radar dislocation in Poland

The radar ranges drawn above represent both 125 km and 250 km ranges respectively.

The spatial resolution of the radar scan is 1 km, the data resolution in azimuth is 1° on average, hence within a circumference of a given radius 200 km one elevation angle returns 72 000 virtual measurement points. The basic max reflectance radar information is gathered from 10 elevation angles so one measurement cycle (max reflectance only, no Doppler wind information received) returns 720 000 points. To make this information valid, one point requires 256 levels – 8 bits of information. Concluding, one reflectance only measurement cycle requires 720 kB.

Since the beginning of the millennium Poland has operational meteorological radar data exchange with neighbouring countries. The current composite radar map of Poland looks as follows (incorporating radar data received on the basis of transnational radar data exchange).

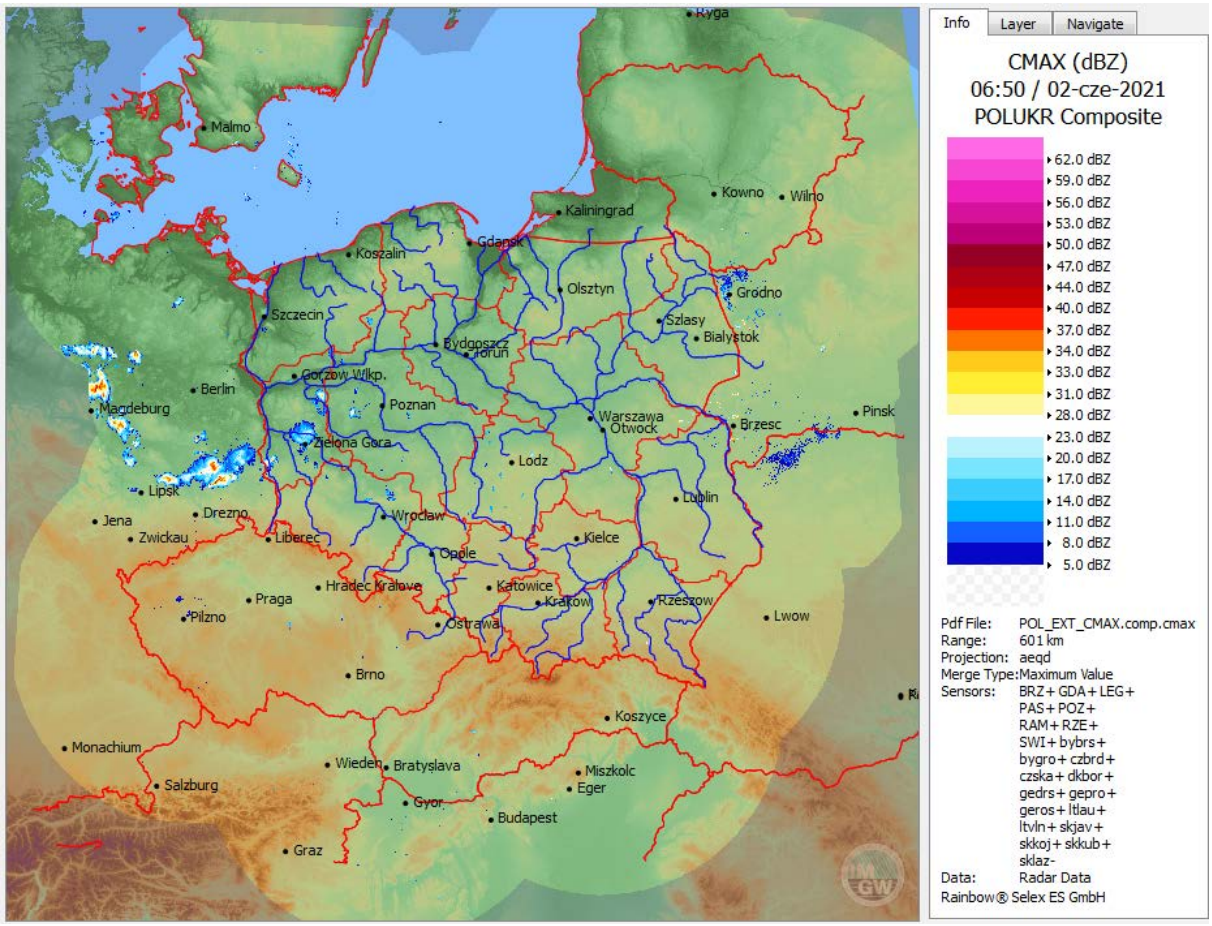

Figure 50: Radar composite map in Poland

The operational radar data exchange is maintained with Germany, Czechia, Denmark and Slovak Republic. The cooperation was initiated in 1998 within Baltrad and Opera projects and is still kept valid.

Foreign radars that provide data on operational basis.

Station location	Longitude	Latitude
Brdy-Praha	13.817800	49.658300
Skalky	16.788500	49.501100
Kojsovska	20.987277	48.782895
Maly Javornik	17.153100	48.256100
Kubinska Hola	19.249350	49.271670
Spani Laz	19.257430	48.240430
Protzel	13.858210	52.648660
Rostock	12.058070	54.175660
Dresden	13.768630	51.124630
Bornholm	14.887517	55.112750

Table 29: Operational foreign radars.

The non-operational radar data exchange is carried out with Belarus, Ukraine and Latvia. The data aren't operationally provided and sometimes are very burdened with artificial errors, hence they are not included in the operational composite radar map of Poland.

Foreign radars that provide test or non-operational data.

Station location	Longitude	Latitude
Laukuva	22.239500	55.609040
Traky	25.106780	54.626220
Grodno	24.048889	53.651943
Minsk	28.040277	53.865833
Brzesc	23.898611	52.115276
Lviv	23.900514	49.848378

Table 30: Non-operational foreign radars.

It is worth mentioning that in the current year 2022 the POLRAD system is being upgraded to new instruments and software. The work will continue in the next year (2023). All new radars will be Doppler class magnetron instruments with dual polarisation. In addition, there will be two completely new radars located in Użranki and Góra Św. Anny.

The new radars that will be installed in 2023.

Station location	Longitude	Latitude
Użranki	21,4121	53,8557
Góra Św. Anny	18,1530	50,4640

Table 31: New radars with forthcoming installation

A1.7 Ground data in Slovakia (SHMÚ)

Rain gauge

The network

In Slovakia there are overall 98 automatic rain gauge stations potentially available for the H SAF project. The real number of usable gauges varies with time because on average about 20 of them are out of operation.

Mean minimum distance between rain-gauges in the complete network is 7,74 km. Map of the rain gauge network in Slovakia containing also climatological and selected hydrological stations is shown in next figure.

Figure 51: Map of SHMÚ rain gauge stations: green – automatic (98), blue – climatological (586), red - hydrological stations in H SAF selected test basins (37)

The instruments

Type of all the automatic rain gauges is tipping bucket (without heating of the funnel). The gauges are able to measure precipitation rates ranging from 0,1 to 200 mm/h at 10 min operational accumulation interval. Shorter accumulation interval of 1 min is also possible which makes the instruments suitable for case studies in the H SAF project.

The data processing

The rain gauge data are not used at SHMÚ directly for the H SAF precipitation validation but they are utilized as the input to the INCA precipitation analysis system which is supposed to become a new validation tool. Prior the INCA analysis the rain gauge data are interpolated onto the regular 1x1 km grid using the inverse-distance-squared (IDS) interpolation method. Only the 8 nearest rain gauge stations are taken into account in the interpolation in order to reduce occurrence of precipitation bull-eyes artifact.

SHMÚ performs the offline automatic and manual quality check of the rain gauge data. In frame of the INCA system a quality control technique called blacklisting has been developed which avoids the data from systematically erroneous rain gauges to enter the analysis. Currently the blacklisting is used in manual mode only.

Radar data

The network

The Slovak meteorological radar network consists of 4 radars (see next figure). One is situated at the top of Maly Javornik hill near city Bratislava, second one is on the top of Kojsovska hola hill close to the city Kosice. The third and fourth radars are installed on Kubinska hola in Orava region and on Spani laz in the south of Central Slovakia. All of them are Doppler, dual-polarization C-band radars of the same type.

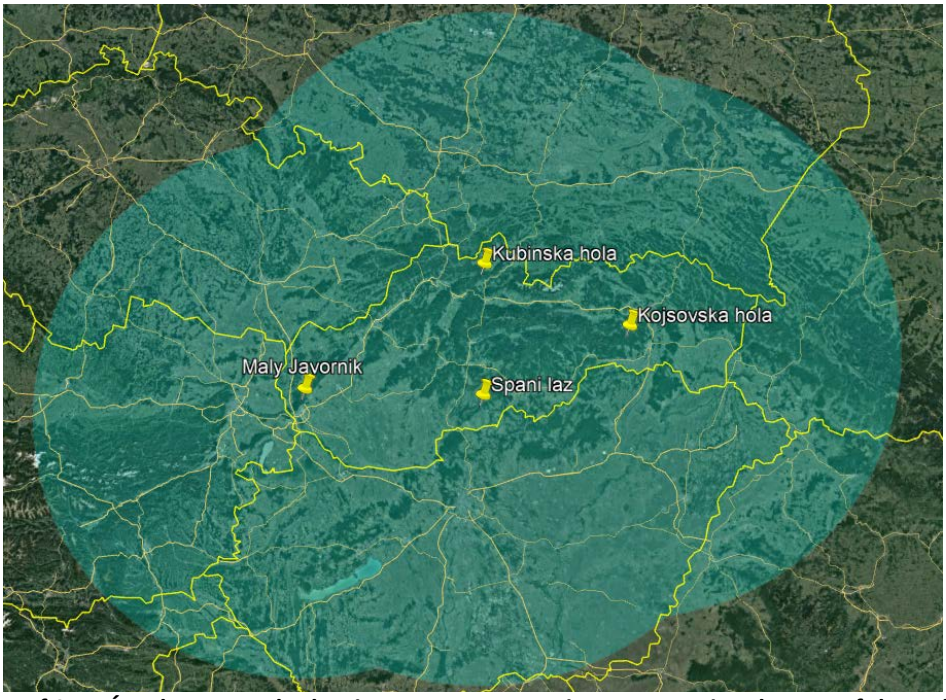

Figure 52: Map of SHMÚ radar network; the rings represent maximum operational range of the radars – 240 km

The instruments

The radars are operated and technically maintained by SHMÚ. Receivers of radars are calibrated regularly by means of internal test signal generator (TSG) every 6 months. The peak power of the transmitted pulses is calibrated with the same periodicity using calibrated power meters.

The basic parameters of SHMÚ radars are summarized in following table.

	Maly Javornik	*Kojsovska hola*	*Kubinska hola*	*Spani laz*
Frequency band	C-Band, Yes 5605 MHz	C-Band, Yes 5645 MHz	C-Band, Yes 5630 MHz	C-Band, Yes 5615 MHz
Polarization (Single/Double)	Double	Double	Double	Double
Doppler capability (Yes/No)	Yes	Yes	Yes	Yes
Scan strategy: scan frequency, elevations, maximum nominal range distance,	*Scan frequency: 5 min* *Elevations (deg): 0.0 0.5*	*Scan frequency: 5 min* *Elevations (deg): 0.0 0.5*	*Scan frequency: 5 min* *Elevations (deg): 0.0 0.5*	*Scan frequency: 5 min* *Elevations (deg): 0.0 0.5*

range resolution	*1.0 1.5 2.0 2.7 3.4 4.4 7.0 11.4 18.3 26.7* *Range: 240 km* *Resolution: 250m*	*1.0 1.5 2.0 2.7 3.4 4.4 7.0 11.4 18.3 26.7* *Range: 240 km* *Resolution: 250m*	*1.0 1.5 2.0 2.7 3.4 4.4 7.0 11.4 18.3 26.7* *Range: 240 km* *Resolution: 250m*	*1.0 1.5 2.0 2.7 3.4 4.4 7.0 11.4 18.3 26.7* *Range: 240 km* *Resolution: 250m*

Table 32: Characteristics of the SHMÚ radars

The data processing

For ground clutter removal the GIP frequency domain filter is used. Isolated bins in the range and azimuth direction are removed by the speckle removal filters. The data with intensities around the noise level and below are eliminated using the LOG threshold.

The measured radar reflectivity is corrected for atmospheric (clear-air) attenuation of the radar beam. RLAN interference is removed using the Interference filter and SQI thresholding in the signal processor. The radar reflectivity is then corrected for attenuation of the radar beam in the precipitation. In the final step, dual-pol filtering of the non-meteorological echoes is applied on the reflectivity data which removes also most of the remaining interference.

Correction for vertical profile of reflectivity (VPR) is not applied at SHMÚ. However beam blocking correction is being used in the quality-checking step for the H SAF validation due to complicated orographical conditions in Slovakia. Software filter for the RLAN interference detected by radars is currently in development at SHMÚ.

Quality-based radar composite CAPPI 2 km products from all radars is used for the H SAF validation. The composition algorithm uses several quality-checking algorithms, where distance from radar, beam-blockage, spike-detection (similarity with neighbor values) and comparison with NWCSAF cloud-type and clout-top-height are considered and evaluated as quality indexes. The resulting value in the overlapping area of several radars is computed as weighted average of values from different radars, where weights are evaluated quality indexes.

Precipitation intensity is derived from radar reflectivity according to the Marshall-Palmer equation ($Z=a*R^b$) with constant coefficients valid for stratiform rain ($a=200$, $b=1.6$).

No raingauge correction of the derived instantaneous precipitation is applied. Effect of elevating radar beam with increasing range and beam attenuation is reduced by limiting the validation area to rain effective range of 120 km for both radars in the composite.

The instantaneous precipitation products are provided in Mercator projection with approximately 1 km resolution. Threshold for precipitation detection is 0,02 mm/h. Time resolution of the current instantaneous products is 5 minutes, for the products prior to April 2010 it was 10 minutes and prior to August 2009 15 minutes.

Precipitation accumulation in case of 3-hourly interval is based on integration of 5 (10 or 15) minutes instantaneous measurements in time period of 3 hours. Accumulated precipitation for intervals of 6, 12 and 24 hours is calculated as a sum of the 3-hourly accumulated precipitation. At least 92% of instantaneous measurements must exist in relevant time period for the 3-hourly accumulated product to be produced.

No rain gauge correction of the accumulated precipitation is applied but the same limitation of validation area is used as for the instantaneous product. Threshold for precipitation detection of the 3-hourly accumulated product is 0,5 mm. Geographical projection and space resolution of the accumulated products are the same as those of instantaneous product (see above).

For validation of H SAF precipitation products it is necessary to know errors distribution of used ground truth data – in case of SHMÚ it is precipitation intensity and accumulated precipitation

measured by Slovak radar network. For this purpose a study called "SHMU study on evaluation of radar measurements quality indicator with regards to terrain visibility" has been elaborated (/hsaf/WP6000/WP6100/precipitation/WG_groups/WG2-radar/WG-2-3_radar quality indication_v1.doc). To find distribution of errors in radar range next steps had to be done:

- simulations of terrain visibility by radar network using 90m digital terrain model
- statistical comparison of radar data against independent rain gauge data measurements
- derivation of dependence (regression equation) describing the errors distribution in radar range with regard to terrain visibility, based on rain gauge and radar data statistical evaluation computation of error distribution maps using regression equation and terrain visibility

Main results of this study are shown in next figure. It is evident that the best visibility of SHMU radars corresponds to the lowest PR-RMSE-RMSE of 60% displayed by light violet colors. PR-RMSE-RMSE is of quite homogeneous distribution with average of 69% in prevalent lowlands of Slovakia displayed by bluish colors. But in central and north-west mountainous areas this error exceeds 100%.

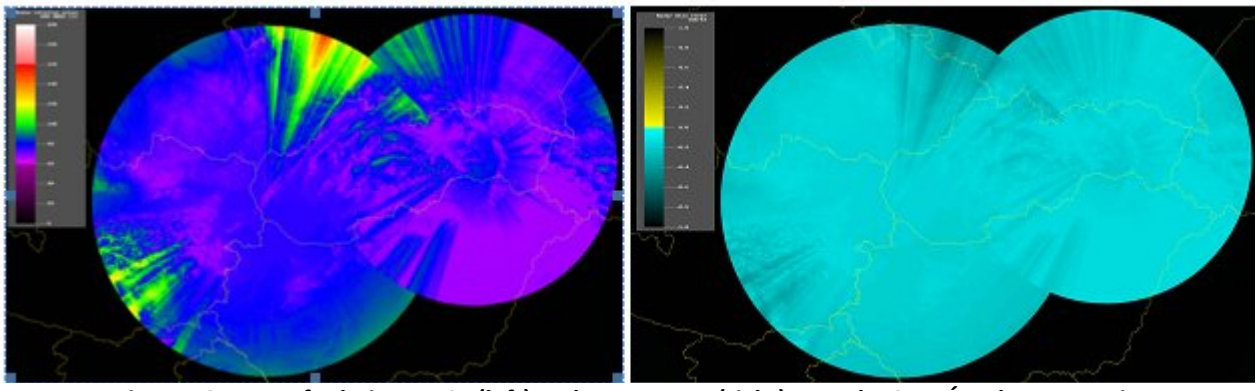

Figure 53: Map of relative RMSE (left) and Mean Error (right) over the SHMÚ radar composite

Similar studies that have been carried out in the PPVG on comparison of radar data with rain gauge data have shown in general that RMSE error associated with radar fields depends considerably on radar minimum visible height above the rain gauge especially in mountainous countries. In lowlands this dependence is not so significant, but no negligible. The reason can be the location of radar sites at the top of hills and impossibility of the lowest elevation to reach the lowland's surface. In case of Slovakia the PR-RMSE error of radar accumulated fields is between 60-90%, with an average PR-RMSE value of 69,3%. Mean Error specified for 24-hours cumulated precipitation is -4,42mm or converted into instantaneous precipitation -0,184 mm/h. RMSE specified for 24-hours cumulated precipitation is 9,48mm or converted into instantaneous precipitation 0,395 mm/h.
Complete SHMU study is available on the H SAF ftp server:
/hsaf/WP6000/WP6100/precipitation/WG_groups/WG2-radar/WG-2-3_radar quality indication_v1.doc

A1.8 Ground Data in Turkey

Rain gauge

The network

356 Automated Weather Observation Station (AWOS) distributed over the country are used for the validation of the satellite precipitation products in the H SAF project. The average distance between the AWOS sites is 40.5 km.

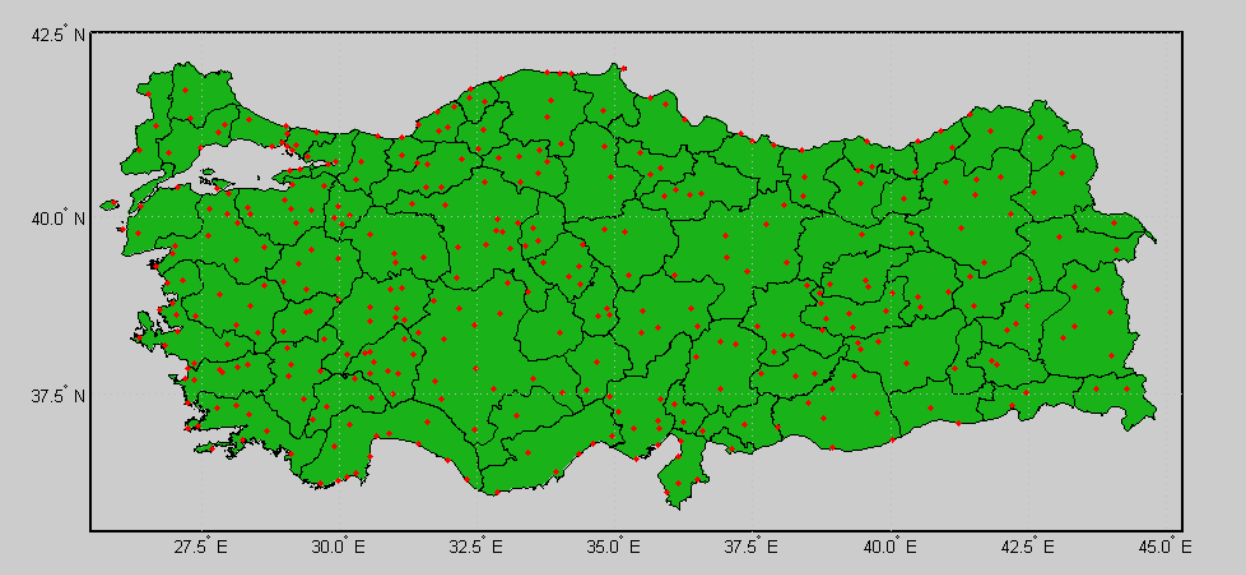

Figure 54: Map Turkish rain gauge stations

The instruments

The gauge type of the network is tipping bucket where each has a heated funnel. The minimum detection capability of the gauge is 0.2 mm per tip. In the maximum capacity of the instrument is 720 mm/h at most. The operational accumulation interval is 1 minute, so that alternative cumulation intervals such as 5, 10, 20, 30 minutes are possible.

Data processing

Quality control

High quality of the ground data is critical for performing the validation of the precipitation products. The validation results or statistics can provide meaningful feedbacks for the product developers and additionally the products can be used reliably only if there is a confidence present about the ground data at a certain level. For this reason, some predefined quality assurance (QA) tests are considered for the precipitation data in order to define the confidence level. First of all, a flagging procedure is defined as described in next table

QA Flag Value	QA Status	Brief Description
0	Good	Datum has passed all QA Test
1	Suspect	There is concern about accuracy of datum
2	Failure	Datum is unstable

Table 33: The precipitation data QA tests are summarized as follows.

Range Test

This test is used to see if any individual precipitation observation falls within the climatological lower and upper limits. The test procedures applied in the study are as follows.

IF $Lim_{Lower} \leq Obser_{j,t} \leq Lim_{Upper}$ **THEN** $Obser_{j,t}$ flag is **'Good'**
IF $Obser_i > Lim_{Upper}$ **OR** $Obser_{j,t} < Lim_{Lower}$ **THEN** $Obser_{j,t}$ flag is **'Failure'**

Lim_{Lower} and Lim_{Upper} thresholds are separately determined for each station on a monthly basis. At any specific site, all the observed monthly data is considered for determination of the upper and lower limits. By applying this test, each observation is flagged either by 'Good' or 'Failure' label depending on the comparison tests mentioned above.

Step Test

It is used to see if increment/decrement between sequential observations in time domain is in acceptable range or not. The applied test procedure is,

IF $|Obser_{j,t}-Obser_{j,t-1}| < Step_j$ **THEN** $Obser_{i,t}$ flag is **'Good'**
IF $|Obser_{j,t}-Obser_{j,t-1}| > Step_j$ **THEN** $Obser_{i,t}$ flag is **'Suspect'**

$Step_j$ threshold is determined again for each site on a monthly basis. For each site, the dataset containing the absolute difference of the sequential observations is determined by considering the observations for the matching month. The 99.9 % cumulative histogram value of the dataset is set as the $Step_j$ threshold for the related site and month.

Persistence Test

Persistence test is used to determine if any group of observations are due to instrument failures. The test procedure applied is defined as,

IF T < Δ THEN Flag for all Obser in T **: 'Good'**
IF T > Δ THEN Flag for **all** Obser in T **: 'Suspect'**

where T is the total number of the sequentially repeating observations forward in time and Δ is the possible maximum number of sequentially repeating observations. As in the other two tests, Δ threshold is determined for each site on a monthly basis. For any site, the data belonging to the same month is taken into account to determine the repeating number of the sequential observations. Then, 99.9 % cumulative histogram value of the repeating number dataset is assigned as the Δ amount for the corresponding site and month. Since there is a high possibility of no-precipitation data (zero), the sequential zero observations are excluded in this test during the determination of the Δ threshold amount and application of the test.

QA Test procedure

By applying the control procedures of the QA test mentioned above, each individual precipitation observation receives three flags referring to the corresponding test. For the corresponding observation if all the test flag is not 'Good' then the observation is excluded from the validation process.

Use of spatialization technique

Due to the time and space structure of precipitation and to the sampling characteristics of both the precipitation products and observations used for validation, care has to be taken to bring data into comparable and acceptable range. At a given place, precipitation occurs intermittently and at highly fluctuating rates. Various maps, time series analysis, statistical and probabilistic methodologies are employed in the validation procedure classically, but some additional new aspects such as the

spatial coverage verification model of point cumulative semivariogram (PCSV) approach (Şen and Habib, 1998) are proposed for usage in this work.

Each precipitation product within the H SAF project represents a foot print geometry. Among these, H01 and H02 products represent an elliptical geometry while H03B and H05 have a rectangular geometry. On the other hand, the ground observation (rain gauge) network consists of point observations. The main problem in the precipitation product cal/val activities occurs in the dimension disagreement between the product space (area) and the ground observation space (point). To be able to compare both cases, either area to point (product to site) or point to area (site to product) procedure has to be defined. However, the first alternative seems easier. The basic assumption in such an approach is that the product value is homogenous within the product footprint. Next figure presents satellite footprint (FOV) centers of the H01 and H02 products, an elliptical footprint for the corresponding center (area within the yellow dots) and Awos ground observation sites. The comparison statistic can be performed by considering just the sites in the footprint area. Although this approach is reasonable on the average but it is less useful in spatial precipitation variability representation. The comparison is not possible when no site is available within the footprint area.

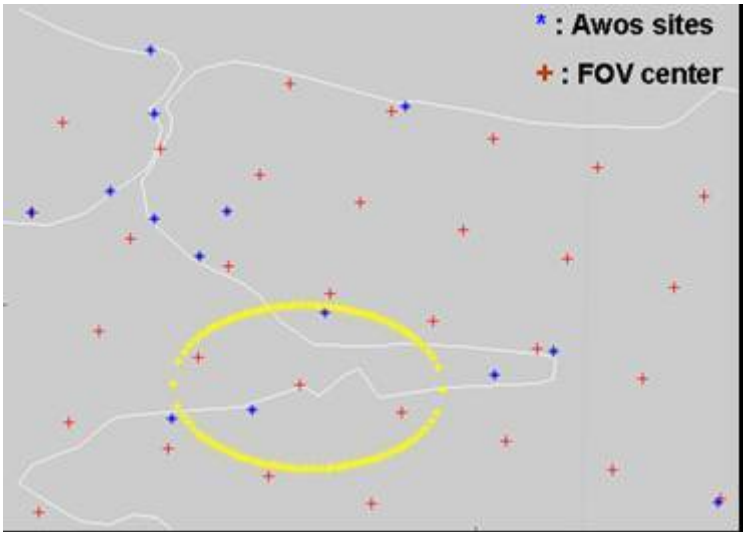

Figure 55: H01 and H02 products footprint centers with a sample footprint area as well as the Awos ground observation sites.

Alternatively, the point to area approach is more appealing for the realistic comparison of the precipitation product and the ground observation. This approach is simply based on the determination of the true precipitation field underneath the product footprint area. To do so, the footprint area is meshed and precipitation amounts are estimated at each grid point by using the precipitation observations at the neighboring Awos sites as shown in Figure 56. A 3x3 km grid spacing is considered for the products with elliptical geometry while 2x2 km spacing is considered for the products with rectangular geometry. For any grid point, Awos sites within the 45 km for the time period of April-September (convective type) and 125km for the rest (stratiform type) are taken into consideration. At each grid point, the precipitation amount is estimated by,

$$Z_m = \frac{\sum_{i=1}^{n} W(r_{i,m}) Z_i}{\sum_{i=1}^{n} W(r_{i,m})} \qquad (4.13.1)$$

where Z_m is the estimated value and $W(r_{i,m})$ is the spatially varying weighting function between the i-th site and the grid point m.

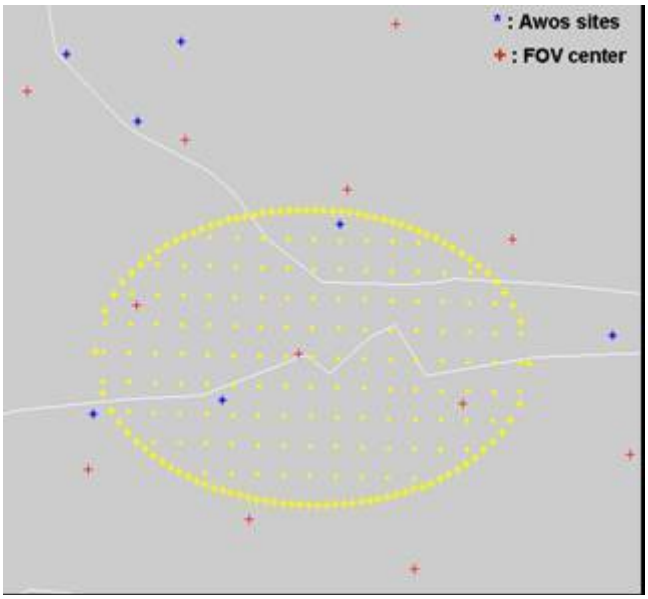

Figure 56: Meshed structure of the sample H01 and H02 products footprint.

Determination of the $W(r_{i,m})$ weighting function in Equation 1 is crucial. In open literature, various approaches are proposed for determining this function. For instance, Thiebaux and Pedder (1987) suggested weightings in general as,

$$W(r_{i,m}) = \begin{cases} \left(\dfrac{R^2 - r_{i,m}^2}{R^2 + r_{i,m}^2} \right)^{\alpha} & \text{for} \quad r_{i,m} \le R \\ 0 & \text{for} \quad r_{i,m} \ge R \end{cases} \qquad (4.13.2)$$

where R is the radius of influence, $r_{i,m}$ is the distance from point i to point m to the point and α is a power parameter that reflects the curvature of the weighting function. Another form of geometrical weighting function was proposed by Barnes (1964) as,

$$W(r_{i,m}) = \exp\left[-4 \left(\frac{r_{i,m}}{R} \right)^{\alpha} \right] \qquad (4.13.3)$$

Unfortunately, none of these functions are observation dependent but suggested on the basis of the logical and geometrical conceptualizations only. They are based only on the configuration, i.e. geometry of the measurement stations and do not take into consideration the natural variability of the meteorological phenomenon concerned. In addition, the weighting functions are always the same from site to site and time to time. However, in reality, it is expected that the weights should reflect to a certain extent the regional and temporal dependence behavior of the phenomenon concerned.

For the validation activities, the point cumulative semi-variogram technique proposed by Şen and Habib (1998) is used to determine the spatially varying weighting functions. In this approach, the weightings not only vary from site to site, but also from time to time since the observed data is used. In this way, the spatial and temporal variability of the parameter is introduced more realistically to the validation activity.

Matching approach

The temporal and spatial matching approaches are applied separately in the validation of the satellite products. As for the temporal matching, the product time is taken into account and 5 minute window (t-2 to t+3) is considered for estimation of the average rainrate for each site.

For the spatial matching, the mesh grid size of 3kmX3km is constructed for each IFOV area. For each grid point, the rainrate is estimated by taking the 5 minute averaged rainrate amounts observed at the nearby AWOS sites within the radius distance of 45 km(for convective type) or 125 km(for stratiform type) considering the weighting of each site with respect to the grid point(Equation 1). The weighting amounts are derived from the spatially varying weighting functions obtained by using the semi-variogram approach (Şen and Habib,1998). Finally, the Gaussian filter is applied to the estimations at the mesh grid of the IFOV area to get the average rainrate. Then, this amount is compared with the satellite precipitation product amount for the validation purposes.

Appendix 3 Continuous statistical scores

H68 vs Grd	RADAR LAND		RADAR SEA		RADAR COAST		GAUGE LAND		OVERALL	
	≥1 mm/h	≥10 mm/h	≥1 mm/h	≥10 mm/h	≥1 mm/h	≥10 mm/h	≥1 mm/h	≥10 mm/h	≥1 mm/h	≥10 mm/h
Nsat	26'078	2'008	10'200	1'642	2'498	635	24'712	1'729	63'488	6'014
Nref	19'335	2'012	12'216	822	3'107	200	13'955	608	48'613	3'642
ME	-0.42	-8.97	0.25	-5.92	0.84	-5.06	1.46	-6.53	0.37	-7.66
SD	5.45	9.14	5.74	11.76	6.16	11.86	4.96	12.10	5.49	10.57
MAE	3.48	9.82	3.51	9.30	3.95	8.99	3.39	8.28	3.49	9.40
MB	0.91	0.47	1.06	0.63	1.22	0.70	1.41	0.56	1.09	0.53
CC	0.37	0.15	0.37	0.09	0.43	0.34	0.22	-0.13	0.33	0.10
RMSE	5.46	12.80	5.74	13.17	6.22	12.89	5.17	13.76	5.51	13.05

Table 34: Continuous statistical scores for H68 vs Ground over European area.

H68 vs DPR	LAND			SEA			COAST			OVERALL		
	≥0 mm/h	≥1 mm/h	≥10 mm/h	≥0 mm/h	≥1 mm/h	≥10 mm/h	≥0 mm/h	≥1 mm/h	≥10 mm/h	≥0 mm/h	≥1 mm/h	≥10 mm/h
Nsat	578'729	16'059	593	1'715'268	33'175	796	53'364	1'244	21	2'541'001	54'030	1'527
Nref	578'729	8'444	282	1'715'268	29'283	1'031	53'364	885	23	2'541'001	41'704	1'446
ME	0.04	-2.87	-16.95	-0.01	-2.96	-17.37	0.00	-2.78	-17.27	0.00	-2.94	-17.27
SD	0.95	3.59	9.17	0.85	3.81	10.08	0.79	3.21	7.25	0.87	3.74	9.72
MAE	0.16	2.97	16.95	0.14	3.02	17.41	0.14	2.85	17.27	0.14	3.01	17.29
MB	1.70	0.04	0.01	0.85	0.03	0.01	1.05	0.03	0.00	1.01	0.03	0.01
CC	0.00	0.01	-0.03	0.01	0.02	-0.03	0.00	0.00	0.50	0.00	0.01	-0.03
RMSE	0.95	4.60	19.27	0.85	4.82	20.08	0.79	4.25	18.73	0.87	4.76	19.82

Table 35: Continuous statistical scores for H68 vs DPR-NS product over the H SAF extended area.

Appendix 4 Multi-categorical statistics

H68 VS Ground		RADAR SEA	RADAR LAND	RADAR COAST	GAUGE LAND	OVERALL
≥0.25 mm/h	POD	0.40	0.48	0.34	0.64	0.49
	FAR	0.15	0.33	0.18	0.33	0.29
	MISS	0.60	0.52	0.66	0.36	0.51
	CSI	0.37	0.39	0.32	0.48	0.41
≥1 mm/h	POD	0.59	0.71	0.54	0.82	0.70
	FAR	0.29	0.47	0.33	0.54	0.46
	MISS	0.41	0.29	0.46	0.18	0.30
	CSI	0.48	0.43	0.43	0.42	0.44

Table 36: Probability Of Detection (POD), False Alarm Ratio (FAR), Missing (MISS) and Critical Success Index (CSI) for H68 vs Radar over Land, Sea, Coast, Gauge over Land and Overall surfaces for different rain rate thresholds over the European area.

Appendix 5 H68 versus DPR maps over FD area

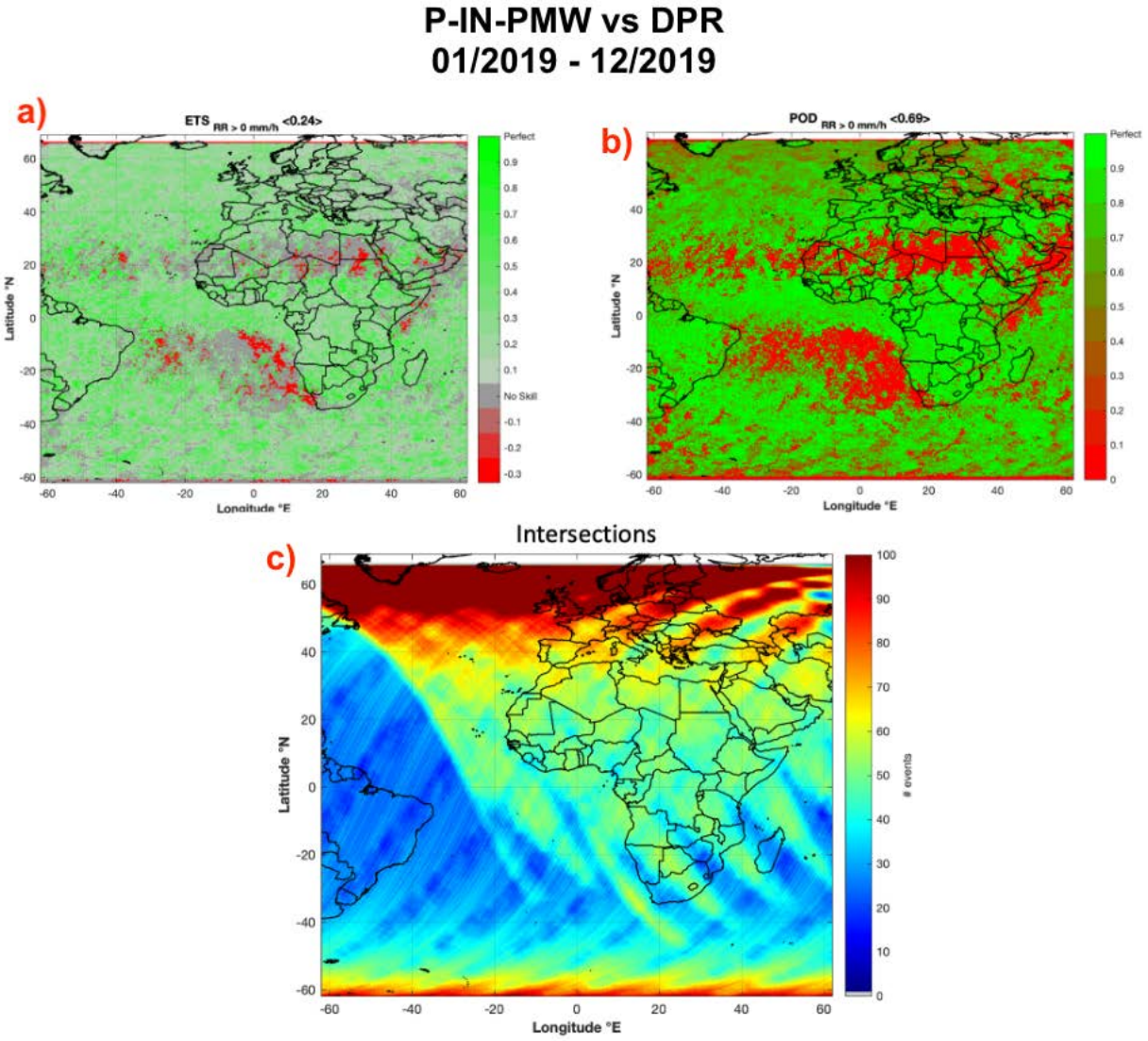

Figure 57: Regular gridded maps (0.5° x 0.5°) of comparison between H68 and DPR-NS products. a) ETS for RR > 0 mm/h. b) POD for RR > 0 mm/h. c) Number of intersections.

Appendix 6 Acronyms

AMSU	Advanced Microwave Sounding Unit
ATMS	Advanced Technology Microwave Sounder
ATS	Automatic Telemetric Station
AWOS	Automated Weather Observation Station
BE	Belgium
BfG	German Federal Institute of Hydrology
CAPPI	Constant altitude plan position indicator
CSI	Critical Success Index
DE	Germany
DPC	Italian Department of Civil Protection
ECMWF	European Centre for Medium-Range Weather Forecasts
EFOV	pixel Extension Field Of View
ENAV	Italian air navigation service provider
EU	European
FAR	False Alarm Ratio
FD	Full Disk
FMI	Finnish Meteorological Institute
GRD	Ground
GRISO	Rainfall Generator of Spatial Interpolation from Observation
HU	Hungary
IFOV	Instantaneous Field Of View
IMWM	Institute of Meteorology and Water Management - Poland
INCA	Integrated Nitrogen model for CAtchments
IRM	Institut Royal Météorologique - Belgium
IT	Italy
ITAF-COMET	ITalian Air Force – Operational Meteorological Center
MAE	Multiplicative Absolute Error
MB	Multiplicative Bias
ME	Mean Error
METOP	Meteorological Operational Satellites
MHS	Microwave Humidity Sounder
MW	MicroWave
NE	North-East
NW	North-West
OMSZ	Hungarian Meteorological Service
PL	Poland
POD	Probability Of Detection
PPVG	Precipitation Product Validation Group
PR	Precipitation Rate
PR-RMSE	Product Requirement Root Mean Square Error
PUM	Product User Manual
PVR	Product Validation Report
RD	Radar
RG	Raingauge
RMSE	Root Mean Square Error

SAF	Satellite Application Facility
SE	South-East
SHMU	Slovak hydrometeorological institute
SK	Slovakia
SRI	Surface Rainfall Intensity
STD	Standard Deviation
SW	South-West
TSMS	Turkish State Meteorological Service
TU	Turkey
UCC	Unique Common Code
WG	Working Group
ZAMG	Zentralanstalt für Meteorologie und Geodynamik